NTNU – Trondheim
Norwegian University of
Science and Technology

Evaluation of fiber for fault detection in a Direct Electrical Heating System

Siri Alsvik Heggdal

NTNU

Norwegian University
of Science and Technology

Department of Energy
and Process Engineering

MASTER THESIS

for

Student Siri Alsvik Heggdal

Spring 2015

Evaluation of fiber for fault detection in a Direct Electrical Heating System

Evaluering av bruk av fiber for brudd deteksjon i røroppvarmingssystem

Background and objective

The formation of wax and hydrates in the subsea production of oil and gas is a well-established problem. Offshore oil and gas industries have highlighted flow assurance as a vital factor when moving towards deeper waters and longer transportation distances. Historically, chemicals (e.g., methanol, MEG) have been used to reduce the critical temperature where wax and hydrates are formed. These additives lead to considerable operational costs, and may also represent a risk to the environment.

An alternative method is to prevent hydrate formation by using direct electrical heating (DEH) in combination with thermal insulation around the production pipe. DEH is an eco-friendly, chemical-free system, which greatly reduces the need for chemicals separation on the platform. DEH systems can be designed having impact protection to withstand e.g. trawl impact. A patented Break Detection system by Nexans can be used as base case for extra security of the pipeline in the DEH systems today. Additionally, measurements of temperature along the pipeline can be made using Distributed Temperature Sensing (DTS), which will indicate/detect operational changes.

The following tasks are to be considered:

1. Perform a literature survey on the limitation of DTS. Emphasis shall be on describing the reliability of DTS measurements and the limiting factors which apply for a subsea system. The results shall be presented and discussed.

2. Conduct DTS measurements using Raman and Brillouin principles to investigate the correlation of distance, accuracy and time lag when applying DTS to a DEH system. Time allowing, the length limitations of Raman DTS measurements shall be investigated experimentally.

3. The experimental setup shall be described, and the results shall be presented, discussed and evaluated.

4. Evaluate and compare Raman, Brillouin and Break Detection for fault detection on a subsea pipeline with DEH.

5. Suggestions for further work shall be made

Within 14 days of receiving the written text on the master thesis, the candidate shall submit a research plan for his project to the department.

When the thesis is evaluated, emphasis is put on processing of the results, and that they are presented in tabular and/or graphic form in a clear manner, and that they are analyzed carefully.

The thesis should be formulated as a research report with summary both in English and Norwegian, conclusion, literature references, table of contents etc. During the preparation of the text, the candidate should make an effort to produce a well-structured and easily readable report. In order to ease the evaluation of the thesis, it is important that the cross-references are correct. In the making of the report, strong emphasis should be placed on both a thorough discussion of the results and an orderly presentation.

The candidate is requested to initiate and keep close contact with his/her academic supervisor(s) throughout the working period. The candidate must follow the rules and regulations of NTNU as well as passive directions given by the Department of Energy and Process Engineering.

Risk assessment of the candidate's work shall be carried out according to the department's procedures. The risk assessment must be documented and included as part of the final report. Events related to the candidate's work adversely affecting the health, safety or security, must be documented and included as part of the final report. If the documentation on risk assessment represents a large number of pages, the full version is to be submitted electronically to the supervisor and an excerpt is included in the report.

Pursuant to "Regulations concerning the supplementary provisions to the technology study program/Master of Science" at NTNU §20, the Department reserves the permission to utilize all the results and data for teaching and research purposes as well as in future publications.

The final report is to be submitted digitally in DAIM. An executive summary of the thesis including title, student's name, supervisor's name, year, department name, and NTNU's logo and name, shall be submitted to the department as a separate pdf file. Based on an agreement with the supervisor, the final report and other material and documents may be given to the supervisor in digital format.

☒ Work to be done in lab (Water power lab, Fluids engineering lab, Thermal engineering lab)
☐ Field work

Department of Energy and Process Engineering, 14. January 2014

Olav Bolland
Department Head

Erling Næss
Academic Supervisor

Research Advisor:
Ph.D Daniel Stanghelle,Nexans AS

Preface

This master thesis was completed in the spring semester of 2015 at the Norwegian University of Science and Technology, at the Department of Energy and Process Engineering. The master thesis is a continuation of the specialization project written during the autumn in 2014.

I would like to thank my research adviser from Nexans, Ph.D. Daniel Stanghelle, for his guidance and support during this research study. His continued encouragement, patient and input have been invaluable in the completion of this project.

I would also like to thank the staff at Nexans who helped me set up and carry out the experimental work.

Siri Alsvik Heggdal

Trondheim, June 9, 2015

Abstract

Direct electrical heating (DEH) is a field proven flow assurance technology which is based on controlling the temperature by electrifying the pipeline and utilizing the pipelines electrical resistance to generate heat.

The main safety principle for a DEH system is to detect any faults in the piggyback cable (PBC) and immediately turn off the power to avoid potential pipeline damages. Break detection using fiber optics (FO) is a qualified fault detection method, patented by Nexans, and is installed in as a base case. Light is continuously going through a looped fiber configuration. In the event of a short circuit, the fiber will instantly burn off and trigger a shutdown of the system. The results from the qualification test concluded that break detection fulfils the safety requirements regardless of the surrounding medium of the pipeline, and fiber location relative to the pipeline and cable fault.

Distributed temperature sensing (DTS) is a method to monitor the temperature profile along a continuous FO element. The measuring principles of Raman and Brillouin are commonly used and verified to be accurate and effective mechanisms to measure the temperature profile of the fiber. The DTS system performance is based on a trade-off between accuracy, measurement time and distance range. This thesis reviews the limiting factors and discusses the reliability of DTS measurements for a DEH system. Raman and Brillouin based DTS systems can be applied for distances up to 40 km and 75 km, respectively, and the literature survey shows that both have a localization accuracy better than 1 m and temperature accuracy within $\pm 1°C$.

The possibility of using DTS for fault detection in DEH systems was explored experimentally by conducting Raman and Brillouin based DTS measurements. The correlation of distance, accuracy and measurement time was investigated. The results indicate that the measurement times for DTS are too long to detect a short circuit situation. The measurement time can be decreased by lowering the accuracy, which also will decrease the ability to detect hot-spots. The measuring units will display an alarm message immediately after a fiber break, which theoretically could be used to switch off the electricity. This would however then be a break detection system and a violation of patent.

Sammendrag

Direkte elektrisk oppvarming (DEH) er en teknologi utviklet for å sikre strømmen av hydrokarboner fra brønn, gjennom rørledning, opp til plattform. Elektrisk vekselstrøm er ledet gjennom DEH-systemet til stålet i produksjonsrøret som varmes opp som følge av sin egen elektriske motstand.

Hovedprinsippet for sikkerheten til DEH systemet er å detektere feil i piggyback-kabelen (PBC) og umiddelbart skru av strømmen for å unngå potensielle skader på produksjonsrøret. Bruddeteksjon ved bruk av fiberoptiske kabler er en kvalifisert feildeteksjonsmetode, patentert av Nexans, og er en del av grunnpakken til DEH-systemet. Et kontinuerlig lyssignal går gjennom en fiberloop. I en kortslutningssituasjon vil fiberen umiddelbart brenne av og slå av det elektriske systemet. Resultatene fra kvalifikasjonstesten beviste at bruddeteksjon oppfyller sikkerhetskravene, uavhengig av plasseringen til fiberen i kabelen, og hvor kabelen er relativ til rørledningen.

Distribuert temperaturmåling (DTS) er en måte å overvåke temperaturprofilen kontinuerlig langs et fiberoptisk element. Måleprinsippene for Raman og Brillouin har vist seg å være nøyaktige og effektive mekanismer for å måle temperaturprofilen. Ytelsen til DTS-systemet er basert på forholdet mellom nøyaktighet, måletid og avstand. Denne avhandlingen beskriver begrensende faktorer og diskuterer påliteligheten av DTS-målinger for DEH-systemer. Raman og Brillouin baserte DTS-systemer kan anvendes for avstander opp til henholdsvis 40 km og 75 km, og har en temperaturnøyaktighet på ±1°C og lokaliseringsnøyaktighet på bedre enn 1 m.

Bruk av DTS for feildeteksjon i DEH-systemer har blitt vurdert eksperimentelt ved gjennomføring av Raman og Brillouin baserte DTS-målinger. Korrelasjonen mellom avstand, nøyaktighet og måletid har blitt undersøkt. Resultatene indikerer at måletiden for DTS er for lang til å detektere en kortslutningssituasjon i et DEH-system. Måletiden kan reduseres ved å senke nøyaktigheten, men dette vil gjøre det vanskeligere å detektere små varmeutviklinger. Måleapparatet viser en alarmmelding umiddelbart etter fiberbruddet, noe som teoretisk sett kan brukes til å skru av strømmen. Dette ville imidlertid da være et bruddeteksjonssystem, og brudd på patent.

Table of content

List of abbreviations

DEH   Direct Electrical Heating.

PBC   Piggyback Cable.

FO   Fiber Optic.

DTS   Distributed Temperature Sensing.

SpBS   Spontaneous Brillouin scattering.

SBS   Stimulated Brillouin Scattering.

AC   Alternating Current.

A/D   Analog to Digital.

OFDR   Optical Frequency Domain Reflectometry.

PEX   Cross-linked polyethylene.

FIMT   Fiber in Metallic Tubes.

List of symbols

n	[-]	Index of refraction.
v	[m/s]	Velocity.
c	[m/s]	Speed of light in vacuum.
L	[m]	Length.
t	[s]	Time.
T	[°K]	Temperature.
T_{ref}	[°K]	Reference temperature.
Δ	[-]	Difference.
α	[m^{-1}]	Attenuation (+/-) of Stokes and anti-Stokes backscatter.
I	[Hz]	Intensity of Stokes (+) and anti-Stokes (-) bands.
C	[-]	Constants (+/-) relating to sensitivity of intensity to temperature.
f_B	[Hz]	Brillouin frequency shift.
V_A	[m/s]	Acoustic velocity.
λ_0	[nm]	Pump wavelength.
L_{max}	[m]	Maximum fiber length.
n_{gr}	[-]	Group index of refraction.
f_p	[Hz]	Light pulse frequency.
ε	[% or με]	Strain.
C_ε	[MHz/με]	Strain coefficient.
C_T	[MHz/°C]	Temperature coefficient.
$z_{sp.res}$	[m]	Spatial resolution.
τ	[s]	Pulse duration.
σ	[°C or Hz]	Standard deviation.
L_0	[m]	Distance at which repeatability is processed.
N	[-]	Number of measurements.
$f_{B,i}(L_0)$	[Hz]	Brillouin frequency profile of measurement i at position L_0.
$\bar{f}_B(L_0)$	[Hz]	Average of the recorded frequency measurements at position L_0.

List of figures

List of tables

1. Introduction

1.1. Background

The exploration and production of oil and gas is gradually moving into ever deeper waters and longer tie-inns, which leads to greater challenges within flow assurance. The subsea environment, which involves low temperature, high pressure and high water cut, constitute ideal conditions for solid depositions such as hydrates and wax to form. To date, chemical injection has been the most common flow assurance strategy. This is however not an environmentally friendly solution, and processing of the chemicals requires great and valuable topside space.

DEH was qualified in 1998 [1], and is now a field proven flow assurance technology. Heat is generated due to an electrical current being passed through the pipeline, maintaining the temperature above the onset of hydrate formation.

Cable faults in the DEH system must quickly be detected and interrupted to prevent potential damage from being caused to the production pipeline. The power cable is equipped with FO cables for safety measures, in terms of break detection and/or DTS. Optical fibers carry information encoded in light signals, and can therefore reach over long distances. DTS can be based on either Raman or Brillouin principles, and their performance depends on the relationship between distance, measurement time and accuracy.

This thesis is a continuation of the work done in the project thesis, where different flow assurance technologies and the working principles of DTS were described in detail.

1.2. Objectives

The aim of this thesis is to evaluate the application of fibers for fault detection in DEH systems. The main objectives have been to:

- o Present the most influential and limiting factors in DTS measurements to evaluate the reliability of DTS for a subsea system. In order to do so, the general working principles of DTS and DEH are described.
- o Conduct laboratory studies using Brillouin and Raman principles. The test selection is based on examining the interdependence between distance, measurement time and

1

accuracy. The experimental setup and approach are described, and the key findings are presented and discussed.

o Discuss the use of DTS and break detection for fault detection in DEH systems. The results are presented in the conclusion, together with recommendations for future work based on results and findings.

1.3. Survey of thesis

Chapter 2 describes the general working principles of DTS. The reliability of DTS measurements is assessed based on limiting factors related to application in DEH systems.

Chapter 3 contains description of the experimental set-up and implementation, in addition to an analysis of the results.

Chapter 4 describes the working principles of break detection technology, and the qualification conducted for DEH application. DTS based on Raman and Brillouin principles, and break detection are compared for DEH fault detection.

Chapter 5 contains the conclusion of the most suited fault detection method on a DEH system based on literature and experimental results, and recommendations for possible future work.

2. Temperature measurements using fiber technology

DTS systems were conceptualized in the 1980s, and the technology has been developed significantly since then [2]. Continuous temperature profiles through the length of the fiber can be created by analysing information extracted from backscattered light. DTS has a wide field of application, including power line integrity, fire detection, building temperature control, subsea flow assurance, pipeline integrity, and oil and gas monitoring [3].

2.1. General working principles for DTS

Temperature is an important and ubiquitous parameter both in research and everyday life. To date, the most applied temperature point sensors are electrical resistance thermometers and thermocouples. Distributed temperature sensors can however provide continuous temperature profiles along the entire fiber length.

2.1.1. Transportation of light

The fiber consists of two dissimilar types of highly pure, solid glass, in addition to three layers of protection, see Figure 1. The inner layer of glass is referred to as the core, and is where the light signal is transported. In order to achieve total internal reflection in the core, the refractive index of the core must be greater than the one of the outer glass layer, the cladding, and the angle of incidence have to be greater than the critical angle. The refractive index, n, is defined as following [4]:
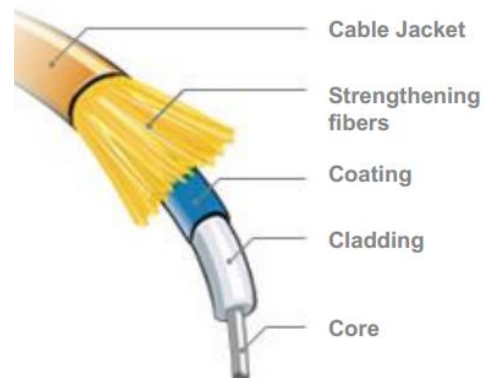
Figure 1: Fiber configuration. [30]

$$n = \frac{Velocity\ of\ light\ in\ vacuum}{Velocity\ of\ light\ in\ a\ given\ material} = \frac{c}{v}$$

Most glass has a refractive index between 1.5 and 1.7 [5]. The speed of the light signal is decreasing with increasing values of the refractive index.

There are two types of optical fibers, single- and multimode. Single-mode fibers are usually applied for longer distances due to no modal dispersion. Modal dispersion occurs when the light signal is spread in time because of various travel paths. In single-mode fibers, the small core size causes the light to travel only one way. Two types of multimode fibers exist, step index and graded index fibers, where core size and light travel path are what separate them. In a multimode fiber the light disperses due to various travel paths for the light and is therefore usually applied for shorter distances [6].

Figure 2 shows the relativ thickness of the fiber core to caldding and light travel paths for single- and multimode fibers. The change in input signal is illustrated on the right hand side in the figure.
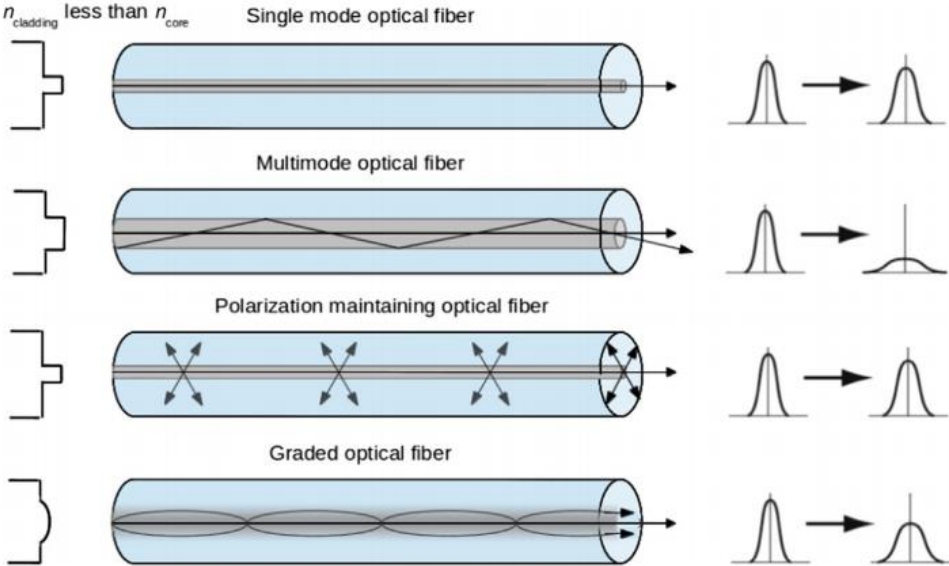
Figure 2: Single- and multimode fibers, including dispersions of input signal. [7]

Short laser light pulses, or a continous light, are sent into the fiber core, and transmits through the length of the fiber due to total internal reflection. As the light propagates, various interaction mecanisms with the fiber glass cause what is referred to as backscattered light. The backscattered light is traveling in the oposite direction of the launched light pulse, and is recorded by a monitoring unit at the beginning of the fiber. A continous temperature profile along the fiber length can be created by continously monitoring the backscattered light [5].

The three main spectral components in the backscattered light are Rayleigh, Brillouin and Raman bands, see Figure 3.
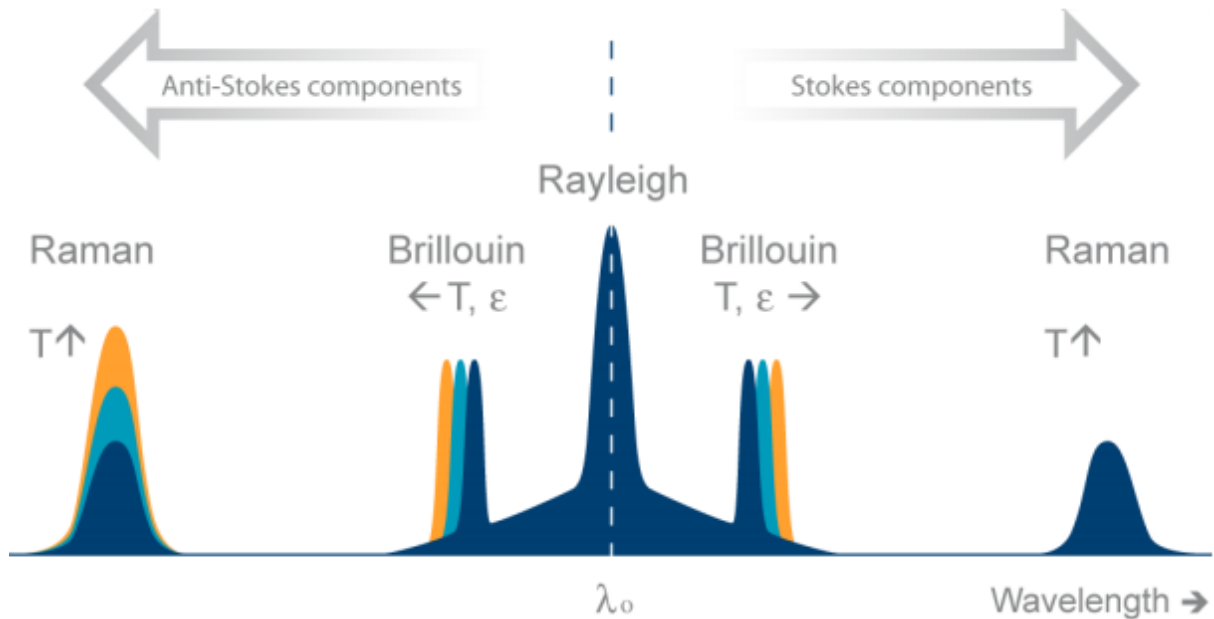
Figure 3: Scattering effects in fiber optic sensors caused by temperature and strain. [6]

The components vary in strength and wavelength, and their values can be applied to determine the temperature profile.

Rayleigh, Brillouin and Raman scattering are caused by density and composition changes in the fiber glass, bulk vibrations, and molecular vibrations, respetively.

The difference in wavelength between the scattered and incident light, reflects an increase or reduction in energy in the scattered photon [7].

To link a temperature value to a location on the fiber cable, the origin of the backscattered light needs to be pinpointed. The backscatter light has to travel in the opposite way, towards the launched light, over a distance from the point in which the backscatter occurs. The velocity can be determined by the refractive index of the fiber. Finally, by recording the backscattered light in time sequences, t, and applying the following equation, the origin of the backscatter can be determined [5].

$$L = \frac{t * v}{2}$$

Both Brillouin and Raman scattering are established measuring principles used for DTS.

2.1.2. Raman

Temperature is affecting the degree of molecular vibration, which also applies to the Raman scattering signal. Most DTS systems based on Raman scattering compare the intensity of the Stokes to the anti-Stokes signal to find the temperature value [7]. Higher temperature leads to higher intensity at the point where the backscattered light originated.

A simplification of the temperature calculation based on the ratio of anti-Stokes to Stokes signals is given by the following equation [5]:

$$T = T_{ref}\left(1 + \frac{\Delta\alpha}{\ln\left(\frac{C+}{C-}\right)} + \frac{\ln\left(\frac{I+}{I-}\right)}{\ln\left(\frac{C+}{C-}\right)}\right)$$
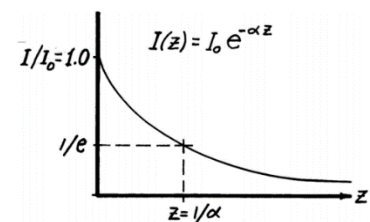
Figure 4: Attenuation in a fiber. [5]

The equation is a linear combination of the three terms, offset, differential attenuation and temperature measured from the anti-Stokes to Stokes ratio, from left to right. The light is exponentially attenuated in a fiber, as illustrated in Figure 4, where $\Delta\alpha$ is highly dependent of position, and C+ and C- are constants. The intensity ratio, I+/I-, is the energy of the Stokes to the anti-Stokes band and is a function of attenuation and local temperature conditions. The calculated temperature can be applied to show how the instrumentation is calibrated for linear attenuation through the fiber. A typical calibration curve is presented in Figure 5, which shows the backscatter power plotted against temperature. [5].
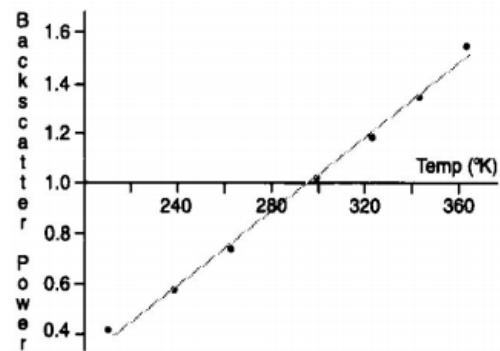
Figure 5: Raman calibration curve. [5]

Figure 6 illustrates the general working principles for a Raman based DTS system. The system is single-ended, in which all the light is emitted into and received from the same end of the fiber.
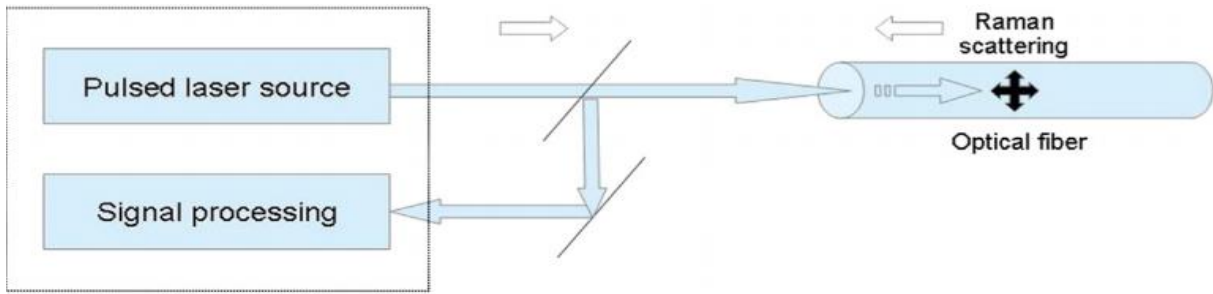
Figure 6: Raman based DTS system. [7]

2.1.3. Brillouin

Brillouin scattering is caused by interaction between the launched light pulse and bulk vibrations in the fiber. The wavelength of the Brillouin backscattered light will be higher or lower compared to the launched light pulse depending on whether the vibration waves emit or receive energy from the glass. Both Stokes and anti-Stokes bands are temperature and strain dependent. [7].

As opposed to Raman systems which are intensity based, the Brillouin systems are related to frequency shifts, see Figure 3.

The Brillouin scattering undergoes a Doppler frequency shift, f_B, which is proportional to the acoustic velocity, V_a, of the fiber material. The frequency shift is given by the following equation [6]:

$$f_B = \frac{2nV_a}{\lambda_0}$$

Both the refractive index and the wavelength of the pump are nearly constant, so the acoustic velocity is what mainly influences the frequency shift. The acoustic velocity is directly linked to the density of the fiberglass, which is temperature and strain dependent. [6].

The frequency shift can be conveted into a temperature using a calibration curve as the one presented in Figure 7.
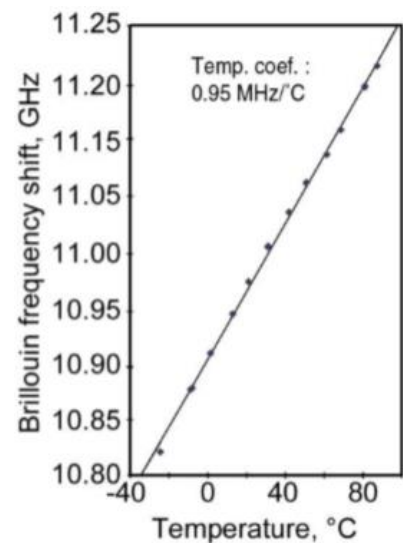
Figure 7: Typical temperature calibration curve for Brillouin system. [6]

Systems based on Brillouin scattering, applies standard low-loss single-mode optical fibers [8].

There are two types of Brillouin-based DTS, spontaneous Brillouin scattering (SpBS) and stimulated Brillouin scattering (SBS). To date, SpBS has been the preferred method for DTS [7], and is a single-ended fiber system. In SBS on the other hand, the backscattered signal is amplified due to counter propagating light signals in a looped fiber configuration. SBS can therefore be used for even greater distances, currently up to 75km [9].

2.1.4. Application of DTS in DEH systems

DEH is a field proven flow assurance technology developed to prevent the formation of hydrates and wax in subsea pipelines. DEH is designed to keep the temperature in the pipeline above the onset of hydrate formation during shutdown or low production rates. The working principle of DEH is to send electrical AC current through the steel in the production pipeline, which is heated due to the electrical resistance.

When the system is turned on, the current flows down the riser, through the feeder and PBC into the far end of the pipeline. Most of the current will return back through the pipeline into the feeder cable in the near end, and back up the riser cable. Figure 8 presents an overview of a DEH system. [10]
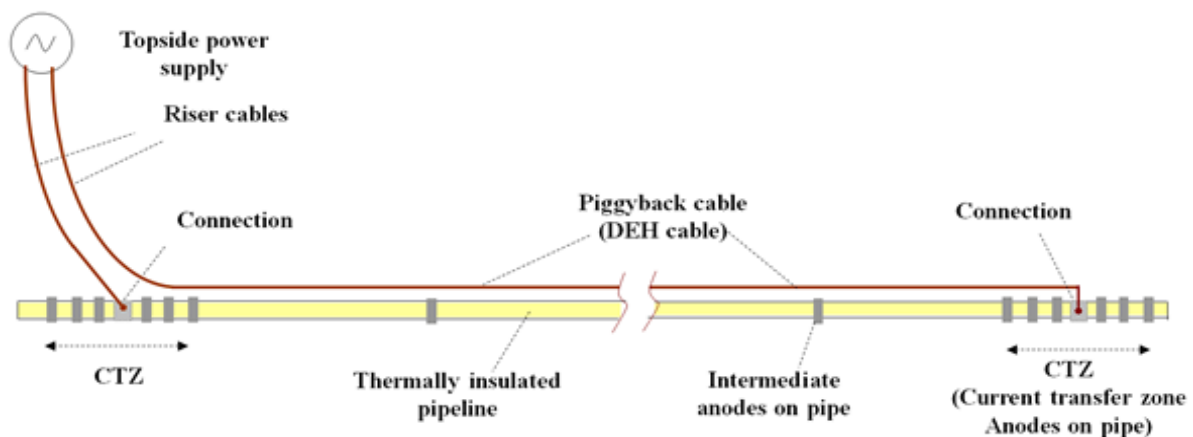
Figure 8: Overview of the DEH system. [31]

The main safety principle for a DEH system is to detect and turn off the power before the current leak escalates and causes damage to the pipeline. The DEH system is therefore designed with FO cables for either break detection and/or DTS. The working principles for break detection are described in section 4.1.2.

Figure 9 shows where the fibers are located in the different sections of a DEH system.
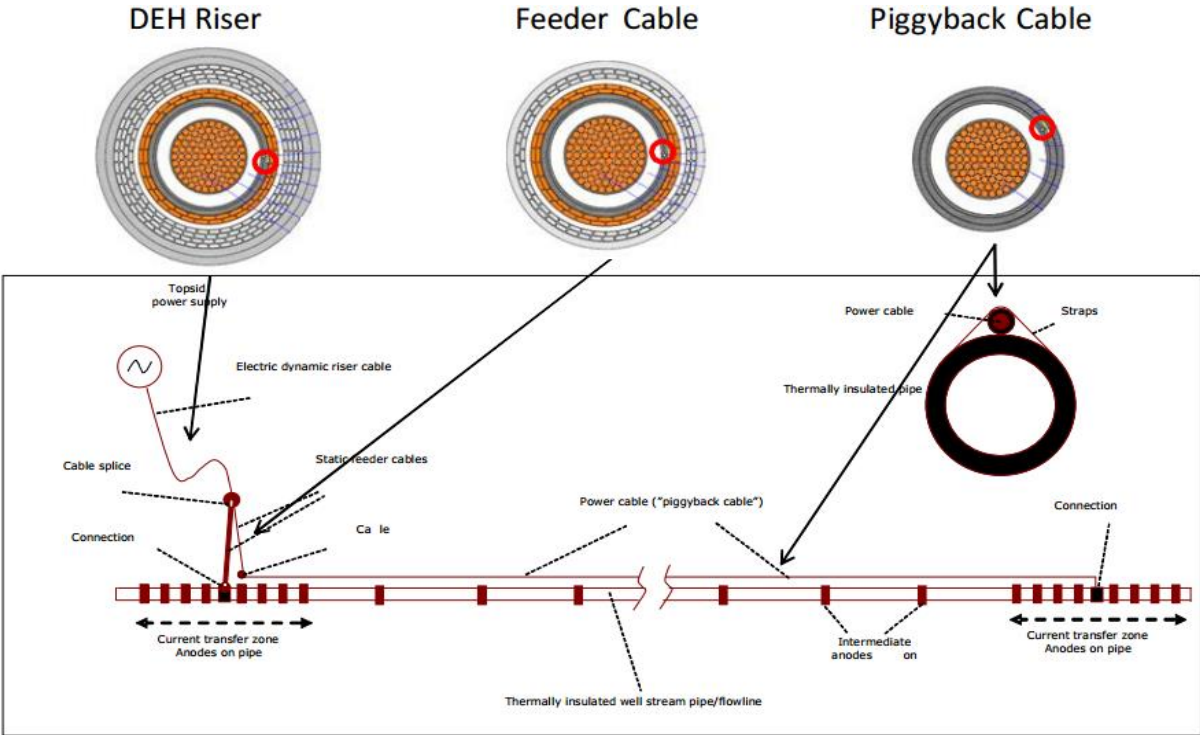
Figure 9: Position of the fiber in different parts of the DEH system. [17]

2.2. Limiting factors of DTS measurements

Both Raman and Brillouin based DTS systems can be useful tools in temperature surveillance for subsea installations. Due to different behaviour and drawbacks, they may have different field of application. As indicated in Figure 10, there is a trade-off in the DTS systems between distance, accuracy and measurement time. Understanding this trade-off is a necessity when evaluating Raman, Brillouin and Break Detection for DEH.
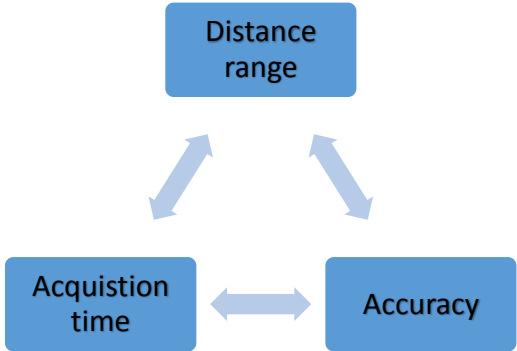
Figure 10: Trade-off in DTS measurements.

2.2.1. Distance

Distance range is defined as the maximum fiber length that can be measured with stated performance when applying a specified measurement configuration. The fiber distance range is mainly defined by spatial resolution, required accuracy, measurement time and type of scattering mechanism. [6].

The intensity of the Raman backscattered light is fairly low. High numerical aperture multimode fibers are therefore preferable in order to take full advantage of the backscattered light. Modal dispersion will occur due to the light having different travel paths through the fiber core, causing limited fiber bandwidth [6]. The substantial weakening of the signal leads to fiber length restrictions. Maximum length with multimode Raman fibers is currently approximately 30 km, and single-mode fibers can be applied up to 40 km [11]. The maximum fiber length, L_{max}, for Raman systems, assuming measurements are made within the stated accuracy, can be estimated by applying the following equation [12]:

$$L_{max} = \frac{c}{2n_{gr}f_p}$$

The speed of light in vacuum is constant, and the group refractive index, n_{gr}, of the core will also remain virtually constant. The laser pulse frequency, f_p, is therefore primarily what determines the maximum fiber length. Inaccuracies in the specified values for the pulse frequency and group refractive index result in an error of the estimated maximum length of about ±1.14% [12].

The SBS systems are configured in loops, where the pump pulse interacts with the counter-propagating probe signal, see Figure 11. This process causes the backscattered light signal to amplify, which enables the sensing fiber to reach over greater distances. Brillouin based systems usually consist of low-loss single-mode optical fibers [13]. To date, the longest DTS fiber is 75 km, but the next generation reaching even higher distance ranges is currently under development [9].
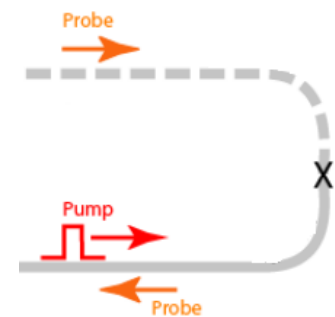
Figure 11: SBS system. [6]

Distance precision is related to the accuracy of the position where the backscattered light originates. There are several factors affecting this precision, including acquisition time, accuracy of stated index of refraction, and knowledge and control of the fiber lay-loss. Maintaining the precision becomes more difficult as the distance increases. [14].

2.2.2. Strain effects

Strain, caused by tension to the fiber, is a measure of deformation of the fiber material. In this context, strain, ε, is normally defined as the ratio of total deformation, ΔL, to initial conditions, L, see equation below [6]:

$$\varepsilon = \frac{\Delta L}{L}$$

Strain is usually given in percentage or micro-strain. Extension and compression gives positive and negative fiber strain, respectively. A typical strain range for a SBS based DTS measuring unit is ±3% of total length [6]. The frequency shift can be conveted into a strain percentage by using a calibration curve as the one presented in Figure 12.

Measurements of strain can be useful in a wide field of applications, anything from evaluation of strain in the fiber itself, to complex structural monitoring. [6]. In DTS systems the temperature is the main parameter and, if applicable, should strain be avoided if it affects the measurement result.

Figure 12: Typical strain calibration curve. [6]

Raman based systems are not tension sensitive, which eliminates the possibility for strain induced inaccuracies. Brillouin on the other hand is sensitive to both temperature and strain, and the cross-sensitivity can lead to large deviations in the measured temperature. The relationship between strain and temperature can be expressed linearly as shown in the following equation [15]:

$$\Delta f_B = C_\varepsilon \Delta\varepsilon + C_T \Delta T$$

Where the temperature and strain coefficients can be determined by using Yamauchi's method [15]. Typical values for the coefficients are C_T=1 MHz/°C and C_ε=0.05 MHz/$\mu\varepsilon$ [16]. The temperature calibration curve in Figure 7 shows that a 0.95 MHz frequency shift corresponds to a temperature change of 1°C. Furthermore, a 1% strain in the fiber corresponds to a 505.5 MHz frequency shift, see Figure 12. The frequency shift related to strain is almost an order of 3 greater than the one related to temperature changes. Strain will therefore have significantly impact on the detected frequency shift when tension is present.

The effects of temperature and strain could theoretically be separated by conducting measurements using both Raman and Brillouin principles at the same time [16]. The temperature would then be measured with Raman, and compared to the results achieved in the Brillouin measurements to separate out the stain contribution. However, this would increase the costs and is not practical for the industry.

Effects of strain can be limited by adding some excess fiber length. The fibers are bundled in metallic tubes, and often laid in a zigzag pattern. One critical parameter is the estimation of the excess fiber length to achieve a strain-free fiber over the lifetime of the cable. The additional fiber length is given as a percentage, and has to be considered when determining the position along a cable. [6].

The DEH systems are designed with FO cables for safety measures. DTS technology can be used to measure the temperature in the fiber, which is placed in the PBC along the production pipeline. The location of the fibers in a PBC is shown in Figure 13. When electricity is applied to the pipeline, it will expand
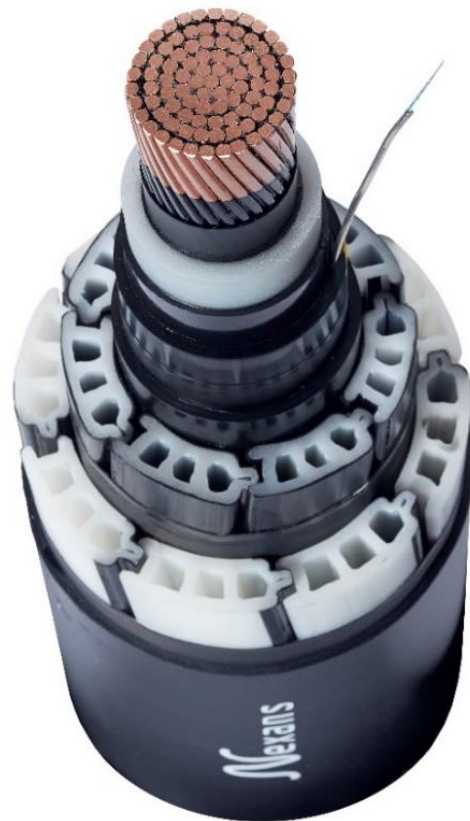
Figure 13: Optical fiber integrated in a PBC. [28]

due to temperature increase. The PBC is mechanically anchored to the pipeline, and is therefore exposed to the expansion-induced strains from the pipeline. The elongation of the pipeline is typically in the order of 0.1-0.2%, which corresponds to an axial load to the PBC and terminations of more than 10 tons [17]. This will affect the detected backscattered signal in a Brillouin-based DTS system due to the temperature/strain cross-sensitivity.

2.2.3. Time lag

Information transmitted in the fiber is encoded in light signals, which travel with speed of light. Despite the low transportation time, a delay to some extent is inevitable. Measurement time is defined as the necessary time to create a temperature profile along the fiber with a certain resolution of the sensor. It comprises detection and processing of the backscattered light signal [12].

Thermal response time for a sensing fiber is strictly dependent on the cladding, cabling arrangement and the degree of thermal contact between the fiber and the measured item. This item can for instance be a power cable, and the thermal response time is generally less than 0.5 s in the fiber when the conductor is being measured [12]. The fiber is typically placed in the centre of the power cable, between three conductors. The location of the fibers in a PBC is shown in Figure 13, and the thermal response time in a DEH system also partly depends on operational conditions, which is described in section 2.3.4.

Due to the low intensity of the Raman backscattered signal, it may take several minutes to determine the actual temperature at a point along the sensing fiber. Enough signals have to be processed and compared to create a reliable curve. This means DTS based on Raman scattering is convenient to apply in situations where the temperature is changing relatively slowly. [7].

The measurement time for SBS systems might vary significantly depending on the resolution, typically between 20 s and 10 min [6].

Acquisition time can vary greatly, everything from seconds to hours, depending on field of application [18]. One of the main concerns associated with applying electricity to heat

production pipelines is the potentially fatal consequences if a failure occurs. A failure in the power cable, due to a trawl impact or dropped object, must be detected and located quickly to avoid short circuiting of the cable and possible damage on the production pipeline. Application of DTS may according to existing literature not be suitable for fault detection on a PBC due to relatively long acquisition times.

There is a clear link between measurement accuracy and measurement time. Increased accuracy can be achieved by increasing the measurement time [13]. Increasing the resolution with a factor of one or two, would quadruple the sampling time [5]. Reduction in number of averages or increase in spatial resolution, which worsens the temperature and localization accuracy, respectively, are ways to reduce the measurement time.

2.2.4.   Accuracy

Accuracy refers to how close the reading of an instrument is to the true value being measured. The producers of a measuring unit usually state a value for the accuracy, and it is often expressed as a percentage of full-scale output or reading. For instrumentation, the given value for accuracy generally includes hysteresis, non-linearity and non-repeatability. [19].

Temperature and distance are the main parameters of interest when considering the accuracy of a DTS system. A system based on SBS technology, can offer a resolution better than 20 $\mu\varepsilon$ and 1°C for a DEH system reaching over lengths up to 75 km. In addition, the localization accuracy can be as good as a meter. [17].

A standard Distributed Anti-Stokes Raman Thermometer, based on spontaneous Raman scattering, can operate over tens of kilometres with 1°C temperature resolution and 1 m spatial resolution [20].

Table 1 shows an example of measurement performance parameters, including temperature and spatial resolution, for a DEH system [17]. Both the temperature and spatial resolution are as indicated here better in the riser than the remaining cable system.

Sensor Name	Spatial Resolution	Temperature Resolution	Length
DEH Riser	1 m	< 0.5K	2 km
DEH Cable System	3 m	≈ 1 K	45 km

Table 1: Temperature resolution for different parts of the DEH system. [17]

Spatial resolution is a measure of the localization accuracy along the fiber. The spatial resolution is defined as the smallest length of an event that can be measured with the stated accuracy [6]. In cases where the temperature change happens in a region smaller than the spatial resolution, the detected temperature will be smaller than the actual temperature by a ratio of temperature variation distance/spatial resolution [12]. The spatial resolution can be calculated using the following equation [12]:

$$z_{sp.res} = \frac{c\tau}{2n_{gr}}$$

The speed of light in vacuum and the group refractive index are constants, so the pulse duration, τ, is the parameter that determines the spatial resolution.

Temperature resolution is the smallest temperature difference the measuring unit can detect, and is therefore a measure of temperature accuracy [12].

2.2.5. Costs

Both CAPEX and OPEX related to application of DTS in a subsea oil and gas field are small in the big picture. The topside measuring unit and the fiber have negligible costs compared to the pipeline. The cost driver will be in cases where the DEH cable is damaged and not is detected instantly, which in worst case might lead to damage of the production pipeline, or other equipment. [11].

2.3. Reliability of DTS measurements

The limiting factors related to application of DTS are also linked to the reliability of the system. Errors emerge from different sources, and can be constant and repeatable or vary randomly.

2.3.1. Error

"Difference between the value indicated by the measurement system and the true value of the measurand being sensed" [19].

Uncertainty intervals are estimated errors for a measurement unit or system where the level of accuracy depends on the complexity. Narrow intervals can be achieved by applying calibrated, high quality measuring systems.

There are primarily two types of errors in the context of DTS measurements, random and systematic errors. Random errors are caused by unknown or uncontrollable factors that influence the measurement, and are consequently not repeatable. The occurrence of these errors can be due to the measuring or the system itself, or from the surrounding environment. Random errors are defined as the difference between a single reading and the average of all readings *[19]*.

$$Random\ error = reading - average\ of\ readings$$

A systematic error is consistent, repeatable and independent of replication. The main sources of this error come from imprecise calibration of the measurement system, changes in the measurand when inserting the measuring device, or from influence by other variables than the measurand. Systematic errors are given by the difference between the true value and the average of a large number of readings *[19]*.

$$Systematic\ error = average\ of\ readings - true\ value$$

The difference between systematic and random errors is presented graphically in Figure 14.
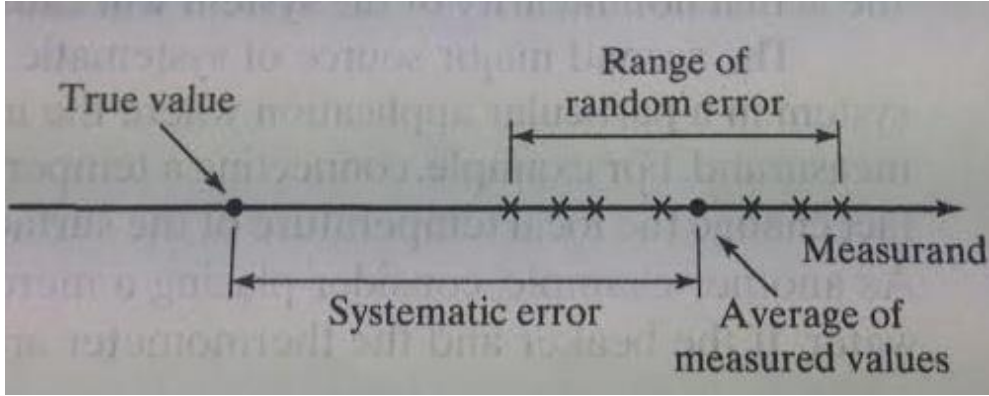
Figure 14: Systematic versus random error. [19]

Small errors arise from various sources in DTS systems, including the instrumentation, the fiber, the laser wavelength applied, and the nature and age of the installation. These errors can appear as depth discrepancies, temperature errors or poor resolution. *[5]*. Measuring units based on both Raman and Brillouin principles typically state an error of less than ±1°C, as described in section 2.2.4 above.

2.3.2. Repeatability

"Repeatability is an instrument's ability to produce the same output repeatedly under identical conditions" [19].

Repeatability, also referred to as measurement resolution, is random fluctuations in measured temperature values between successive measured profiles [6]. The repeatability can be expressed as twice the standard deviation of the measurement:

$$Repeatability\ (L_0) = 2\sigma$$

Where standard deviation is given by:

$$\sigma = \sqrt{\frac{1}{N}\sum_{i=1}^{N}(\Delta f_{B,i}(L) - \overline{\Delta f_B}(L_0))^2}$$

When a number of measurements are recorded sequentially in identical conditions, the difference between each measurement and the average of the measurements can be processed. The repeatability is then calculated from the average of the standard deviation at each distance. Finally, the results are compared with some acceptance values given for the measuring unit in order to evaluate the repeatability. Table 2 presents some repeatability acceptance values for various fiber lengths when conducting SBS based DTS measurements.

	Test distance range		
Repeatability	5 km to 25 km	30 km	50 km
0 km	0.70	0.50	0.50
5 km	0.71	0.50	0.50
10 km	0.72	0.55	0.60
15 km	0.92	0.60	0.80
20 km	1.19	0.75	0.90
25 km	1.40	0.80	1.00
30 km	x	1.00	1.20
35 km	x	x	1.40
40 km	x	x	1.70
45 km	x	x	1.90
50 km	x	x	2.20

Table 2: Repeatability acceptance values. [30]

Figure 15 illustrates a typical repeatability curve for a fiber sensor. The standard deviation is increasing with distance, mainly due to exposure of more noise.
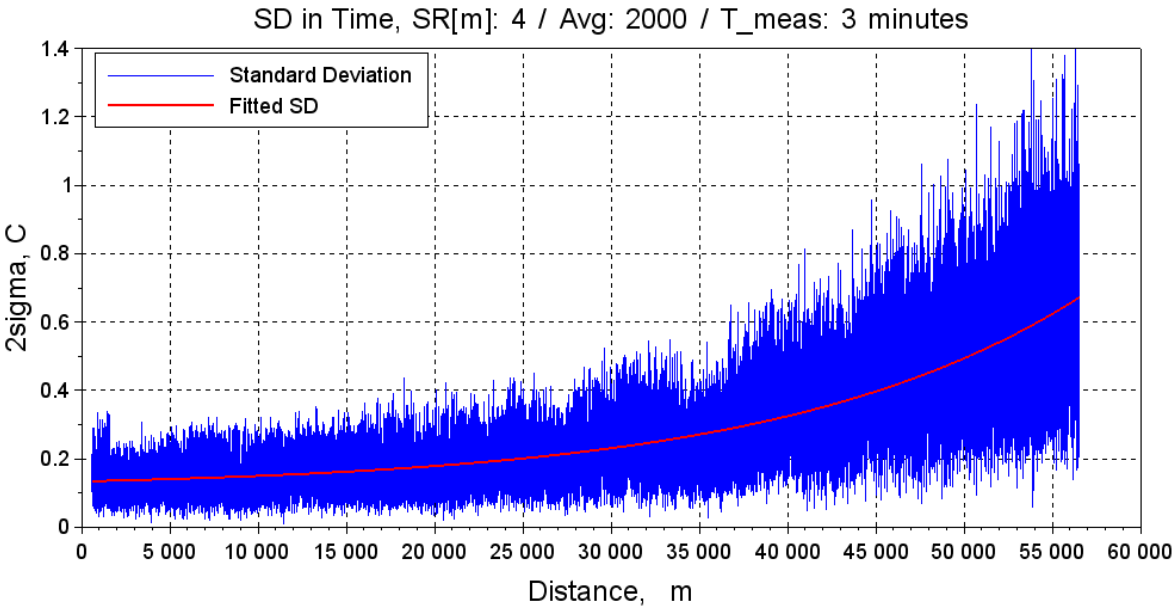
Figure 15: Typical repeatability distribution along a 57km long fiber. [30]

Measurements can have poor accuracy, but still have high level of repeatability. In such cases, an error of approximately same magnitude would occur in all measurements. The more launched light pulses, the longer measurement time, but the better repeatability. The effect of random errors is then limited. [5].

2.3.3. Experimental uncertainty analysis

An uncertainty analysis can be carried out in order to combine uncertainties from all sources into the total uncertainty of a measurement. The analysis is commonly performed during design phase when determining measurement methods and devices. In addition, the analysis might be repeated after completion to confirm the validity of the results.

The uncertainty of most measurands can usually be predicted. The estimates should have same level of confidence, typically 95% or 99%. [19].

2.3.4. Operational conditions

The operating conditions for a DEH system in a subsea environment are highly complex. Changing temperatures, heat from the pipeline, possible impact loads from dropped objects or trawl impact, and strain in the cable due to thermal expansion in the production pipe are a few of the challenges [17]. In addition will ocean currents and circulation of seabed sediments cause the pipeline to move. Sections of the PBC and/or pipeline might be partly or completely buried into the seabed, in which the seabed will act as an insulating layer and elevate the temperatures significantly during operation.

In this complex environment, the temperature in the PEX layer of the cable should ideally not exceed 90°C [17]. If a DTS system is operating during start-up of the DEH system, the interpretation of the measured values will be changed. Detected elevated differences in temperature or hot-spots might be due to cable burial or caused by a cable fault. Misinterpretation of the measurements might be costly or in worst case be fatale for the production pipeline. The temperature will reach a steady state value at some point in time, but due to the uncertainty of the conditions, the DTS measuring would probably not detect a cable fault until damage were done to the pipeline.

The PBC is mechanically anchored to the pipeline and will therefore experience elongation and strain due to thermal expansion of the pipeline. To protect the PBC from dropped objects and trawl impact, the PBC is equipped with either a integrated or mechanical protection system [1].

The formation of solid depositions such as hydrates and wax depend on many factors, including hydrocarbon composition, water production, temperature and pressure. The system is dynamic, meaning that the conditions will change throughout the lifetime of the field. The need for flow assurance will therefore vary. Each DEH system is custom engineered to accommodate the specific field. Most DEH systems are designed to be used during shutdowns and for continuous use during the tail end production of the field. [10].

2.4. Summary

DTS can be applied in subsea systems for temperature surveillance. The fibers can reach great distances and information travels through them with the speed of the light signals. Despite the many advantages of optic fibers, DTS has some limitations. The Brillouin scattering is affected by both temperature and strain. Strain effects lead to inaccurate temperature measurements, for example when DEH is applied to a pipeline which is expanding due to a temperature increase. DTS based on Raman is independent of strain, but has length limitations. Maximum length with Raman fibers is currently around 40 km, while SBS systems have been installed for fibers up to 75 km.

The DTS system performance is a trade-off between accuracy, measurement time and distance range as illustrated in Figure 10.
A longer acquisition time gives higher measurement resolution or better measurement repeatability [6]. In certain situations, such as in fault detection for electrical systems, short acquisition time is crucial to avoid damages. DTS based on Raman scattering is convenient to apply in situations where the temperature is changing relatively slowly, not in a short circuit situation. Brillouin systems can have comparatively shorter acquisition times, but can normally not go below 20 s in order to maintain a required accuracy.

Figure 16 shows an example of calculated precision for a 50 km long Brillouin based fiber, given in temperature and strain units by applying a calibration curve. The longer acquisition time, the better precision and the more even resolution distributions throughout the fiber length. [14].
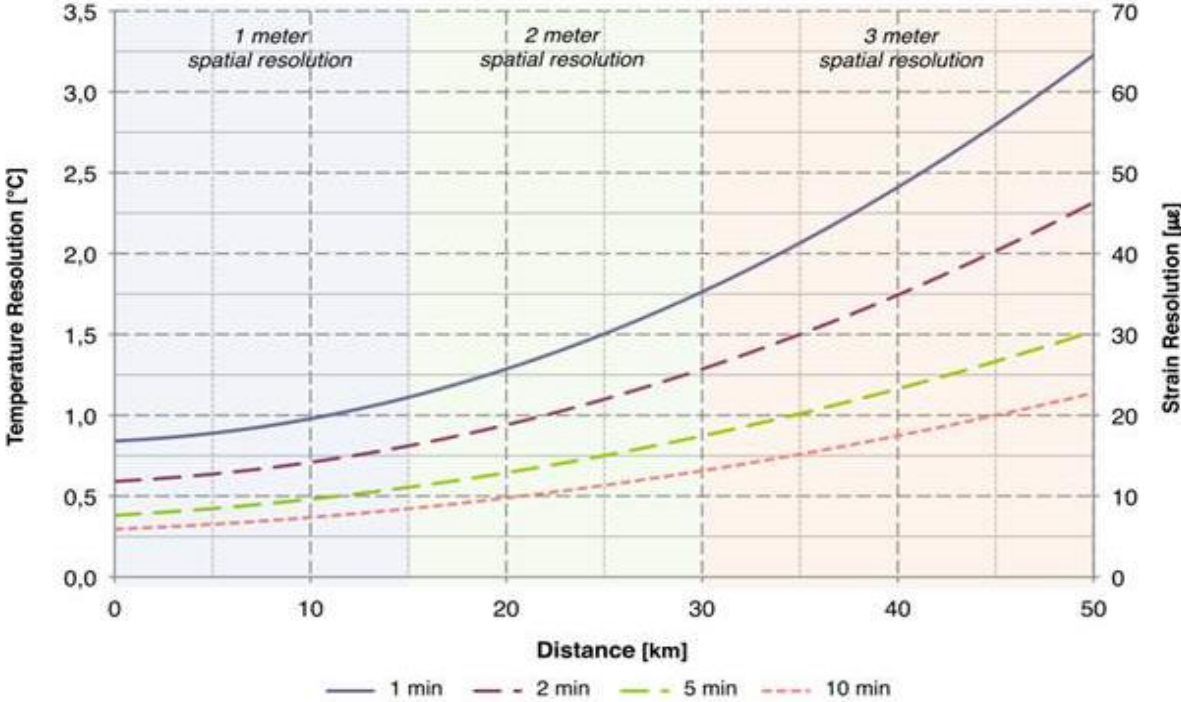
Figure 16: Relationship between performance parameters for a SBS system. [30]

The spatial resolution is determined by the laser pulse duration or width, which also indicates the amount of energy in the light signal. Smaller spatial resolutions means less energy, causing the signal to reach over limited distances. [21].

A specific measurement time or accuracy is often required in a measurement, and therefore needs to be defined during configuration phase. When one parameter is manually set, the remaining ones will be adjusted to achieve the best results. In cases where the fiber length is given and it is preferable to achieve an overall optimal performance, the automatic configuration tools usually can be applied.

Table 3 presents an example of optimal measurement configuration values for different fiber lengths when using a SBS based measuring unit.

	Optimization			
	Standard (5 / 10 / 15 / 25 km)	Long distance (30 km)	Long distance (50 km)	High optical budget (< 1km)
Spatial resolution	1.5m (15ns pulse width)	3.0m (30ns pulse width)	3.0m (30ns pulse width)	1.0m (10 ns pulse width)
Sampling interval	0.5m	1m	1m	0.4m
Frequency steps	1 MHz	1 MHz	1 MHz	1 MHz
Averaging	1000	1000	2000	1000
Measurement time	<5 min	<5 min	<10 min	<5 min

Table 3: Optimal measurement configuration for varying fiber lengths. [30]

Figure 17 shows typical performance values for the relationship between accuracy, distance and measurement time for a Raman system [22]. The temperature resolution improves with longer measurement times, and is progressively worsening with distance.
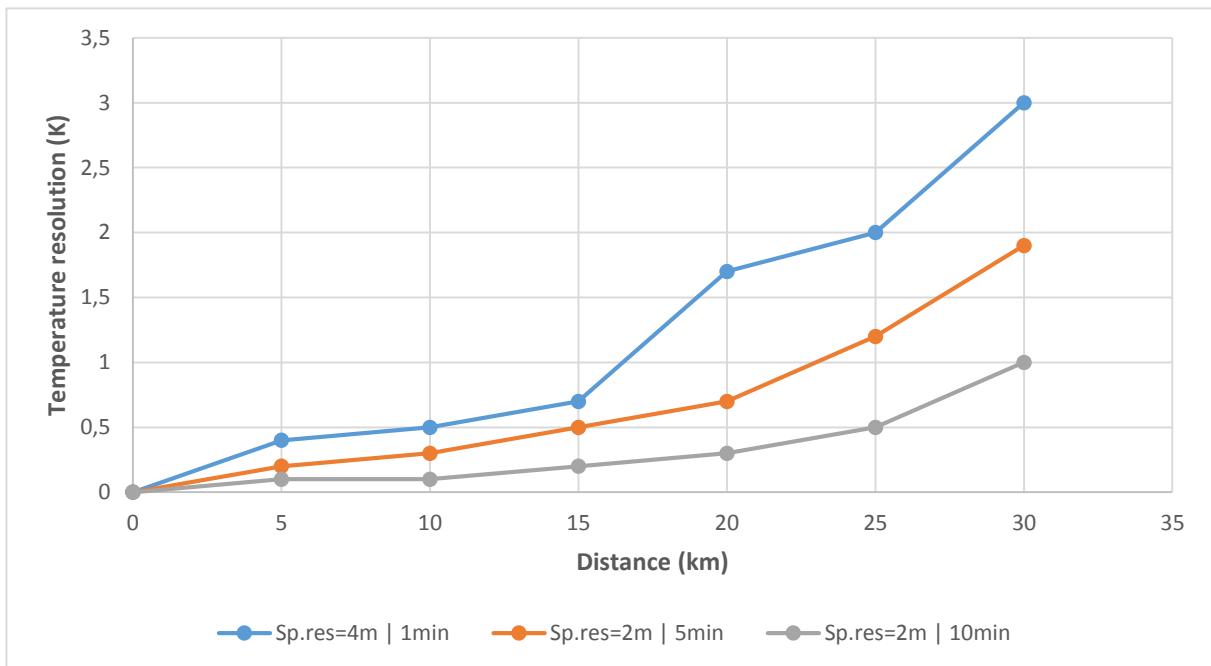
Figure 17: Typical temperature resolutions for a Raman based system.

3. DTS measurements for DEH systems

3.1. Introduction

The DTS system performance is usually a trade-off between accuracy, measurement time and fiber length, as described above. The purpose of the experimental work was to investigate and document the correlation between the limiting factors of DTS. The suitability of DTS in DEH systems was evaluated based on the conducted measurements applying both Brillouin and Raman principles.

3.2. Brillouin experiment

This experiment was performed in collaborations with Nexans Norway, located in Oslo. Guidance and supervision mainly by Guillen Lopez, product engineer at Nexans.

The monitoring unit used in the experiment is called DITEST STA-R, and is based on SBS technology, see Figure 18.

Figure 18: DTS monitoring unit based on SBS technology. [30]

3.2.1. Experimental setup

The sensing fiber had a length of approximately 37.5km, meaning a 75km loop. The main part of the fiber was wrapped around three spools. The single-mode optical fibers were connected to each other either by splicing or connectors, see photos in appendix A2. The fibers are joint together in order to create a continuous optical waveguide [6].

The fiber loop was connected to the monitoring unit via two terminals. The sensing fiber was connected to "Channel 1- To", and the return fiber to "Channel 1- From".

Figure 19 illustrates the overall experimental setup conducted with the measuring unit DITEST.
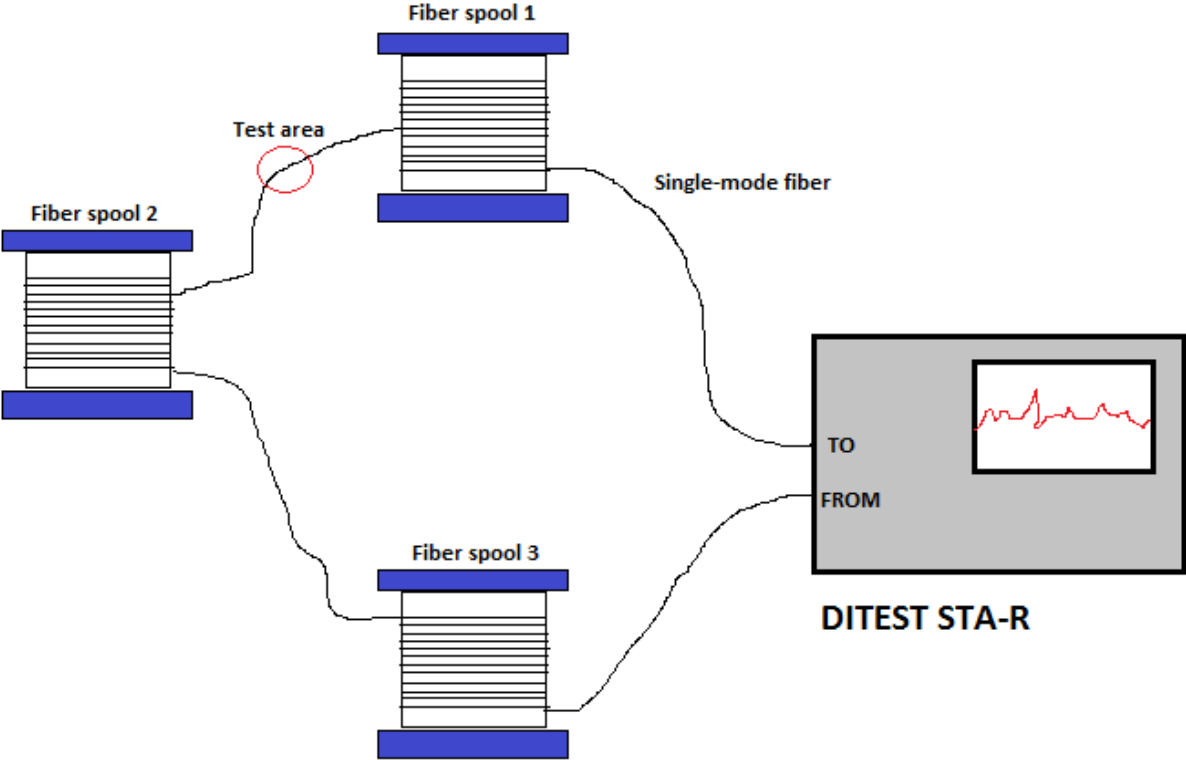
Figure 19: Experimental setup, including the measurement unit and three fiber spools.

3.2.2. DITEST STA-R

The monitoring unit, DITEST STA-R, is produced by Omnisens, see Figure 20. The unit is based on SBS technology, which sends out and receives light signals. The pump and probe signals are generated from the same laser source in the DITEST and the backscattered signal is detected and recorded.

The instrument can be used for manual or long-term automatic unattended measurements, where the results automatically are recorded and stored. This unit is limited to
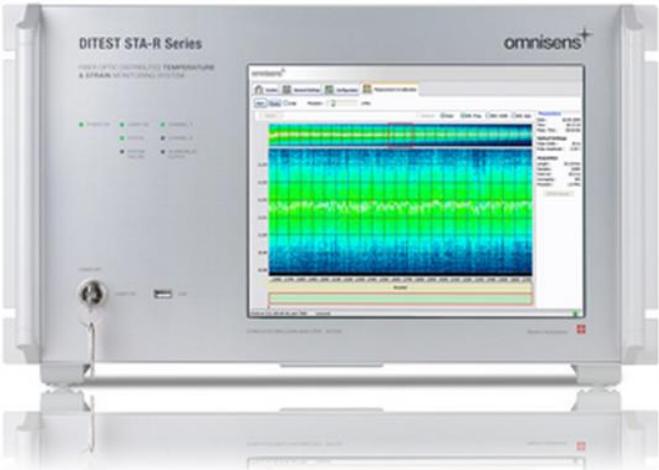
Figure 20: DITEST STA-R monitoring unit. [6]

single-mode fibers and 50 km is maximum length according to the rated performance. See Table A.1 in appendix for more performance and technical specifications.

The DITEST integrator contain the following electro-optic components, visually shown in Figure 21:

- o A laser with a wavelength of 1550 nm.
- o Electro-optic signal processing module to create the pump and probe signals.
- o Wavelength DeMultiplexing, filtering and routing to separate the pump and probe signals.
- o 1x2 switch devices to manage the two channels.
- o Photo detector for detection of probe signal intensity as a function of time.
- o Fast A/D and digital processing to digitalize and process the results from the photo detector.

[6]
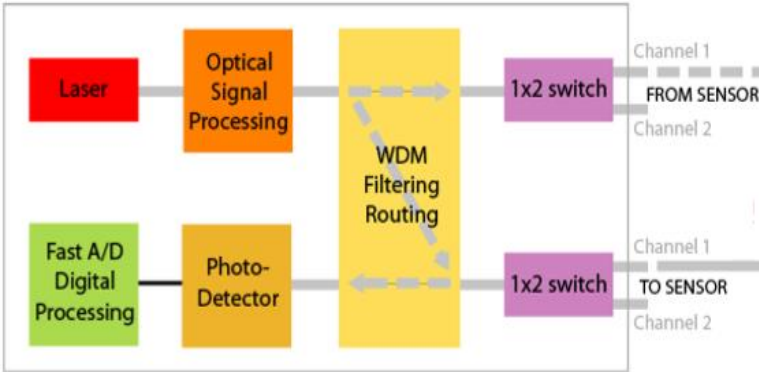
Figure 21: Electro-optic components. [6]

3.2.3. Test matrix

The table below presents an overview of the performed tests, including the main measurement specifications.

Test no.	Explanation	Fiber length (km)	Condition	Spatial resolution	Averaging	Parameter of interest
1	Accuracy vs. distance	37.36	Ambient	1	1000	Frequency and time
2	Spatial resolution vs. time lag	37.36	Ambient	10	1000	Frequency and time
3	Spatial resolution vs. time lag	37.36	Ambient	5	1000	Frequency and time

4	Spatial resolution vs. time lag	37.36	Ambient	3	1000	Frequency and time
5	Time lag vs. distance	30	Ambient	1	1000	Time
6	Time lag vs. distance	20	Ambient	1	1000	Time
7	Time lag vs. distance	10	Ambient	1	1000	Time
8	Time lag vs. distance	7	Ambient	1	1000	Time
9	Time lag vs. averaging	37.36	Ambient	3	100	Time
10	Time lag vs. averaging	37.36	Ambient	3	200	Time
11	Time lag vs. averaging	37.36	Ambient	3	500	Time
12	Time lag vs. averaging	37.36	Ambient	3	2000	Time
13	Cross-sensitivity	37.36	Ambient	3	1000	Location and frequency
14	Hot-spot detection	37.36	Heater (140 °C)	1	1000	Location and frequency
15	Hot-spot detection	37.36	Heater (140 °C)	3	1000	Location and frequency
16	Hot-spot detection	37.36	Heater (140 °C)	5	1000	Location and frequency
17	Hot-spot detection	37.36	Heater (140 °C)	10	1000	Location and frequency
18	Fiber break evaluation	Irrelevant	Ambient	1	1000	Location and frequency

Table 4: Test matrix for a Brillouin based DTS experiment performed with a DITEST.

3.2.4. Methodology

All measurements were repeated minimum three times to limit the effect of random errors. The fiber was placed in a stable environment for most experiments, with ambient temperature of approximately 20°C.

For each test, all parameters except one were fixed. The sensor length, spatial resolution and averaging can be regulated on the DITEST, as shown on the right hand side in Figure 22.
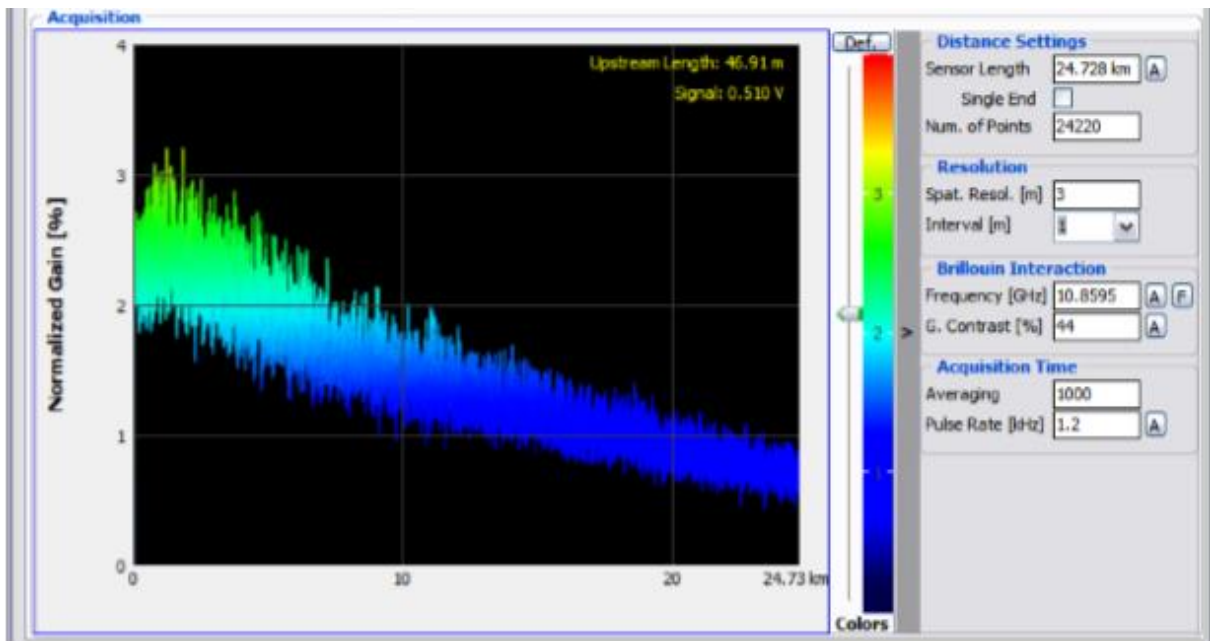
Figure 22: DITEST configuration. [6]

In order to create a hot-spot situation, a hot air gun was used, see Figure A.5. The hot air gun was set to 140°C, and held approximately 10 cm over a small fiber area. The fiber was cooled down to ambient temperature before the same measurements were repeated for a different spatial resolution.

In test 13, strain was applied to a fiber length of approximately 10 cm. The endpoints of this section were manually pulled in opposite directions to create strain. In between each series of strain measurements, a strain-free measurement were conducted to ensure that the fiber was complete, with no internal defects.

A complete fiber break was created in test 18, using a scissor to cut of the fiber at one point.

All measurements were automatically logged, including test names, time, duration and location. The measurement time was hence found by taking the average of the time between the recorded measurements.

The logged measurements were then extracted via Data Viewer. Data Viewer is a part of the DITEST Configuration Interface, and can be used to view, analyse and manage recorded data [6]. Figure 23 shows how Data Viewer interface looks, including frequency response and measurement information.

27
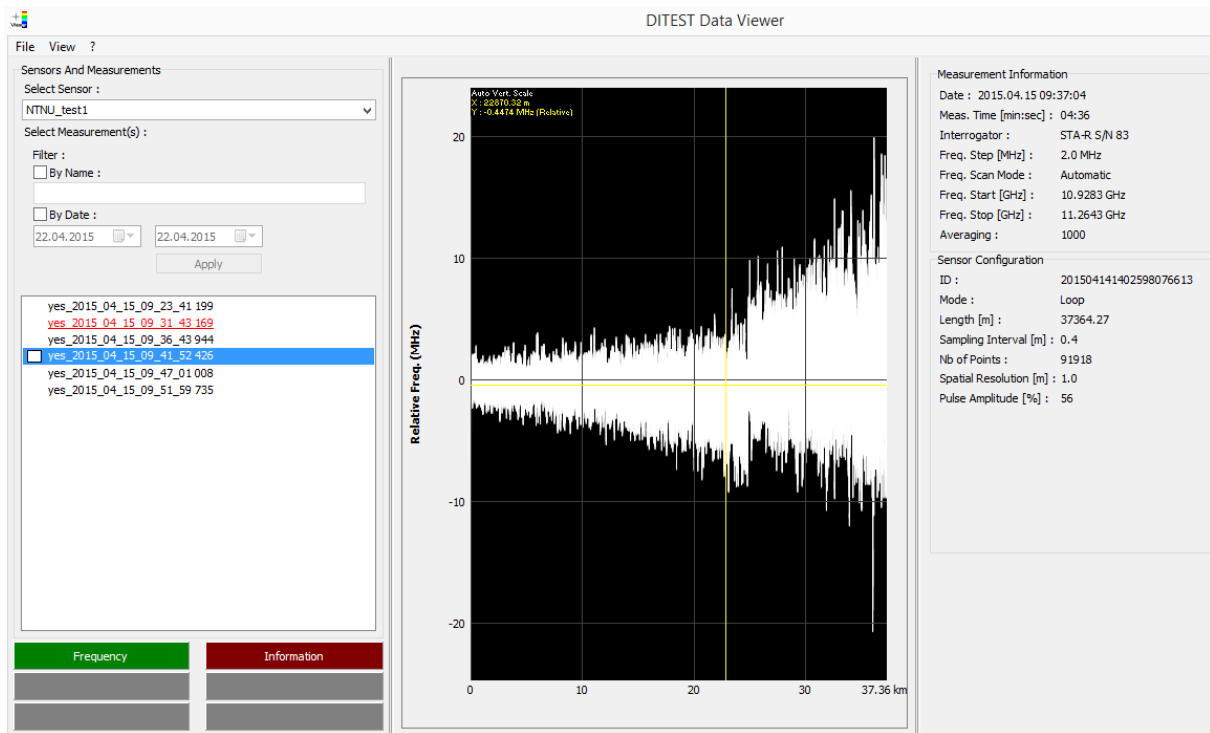
Figure 23: Measurement analysis in Data Viewer.

The results are presented as screenshots from Data Viewer, in addition to some Excel plots.

3.2.5. Results

The key findings from the experiment are presented in table 5.

Test no.	Key findings
1	o Increased distance → lower accuracy o Higher spatial resolution → higher accuracy
2-4	o Higher spatial resolution → shorter measurement time
5-8	o Increased distance → longer measurement time o Approximately linear relationship between distance and measurement time
9-12	o Higher number of averages → longer measurement time
13	o Applied stain → detectable frequency response o False fiber break alarm message
14-17	o Higher spatial resolution → smaller frequency response due to hot-spot o Hot-spot not detected for spatial resolution = 1 m
18	o Fiber break alarm message

Table 5: Key findings in Brillouin experiment.

28

All test results are detailed in appendix A3, including measurement specifications of each individual test. The results are presented as frequency responses (MHz), relative to a baseline, along the fiber length (km), see Figure 24 for an example.
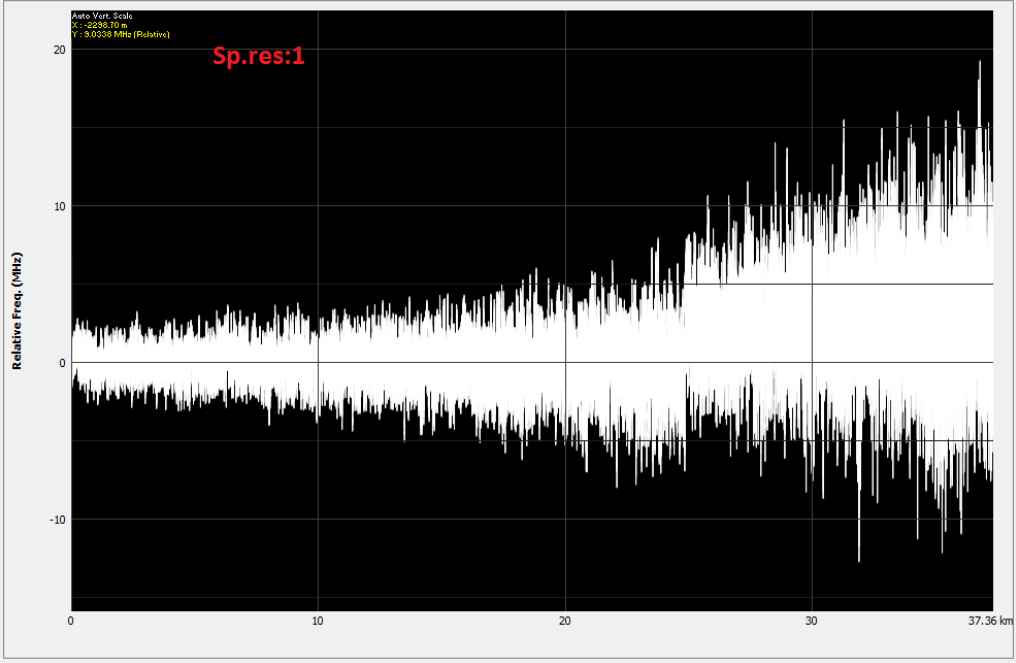
Figure 24: Relative frequency profile along fiber length.

3.2.6.   Summary of laboratory studies based on Brillouin principles

The Figures A.6-A.9 indicate that the accuracy is varying throughout the fiber length, but the degree of change is strictly dependent on spatial resolution. Higher spatial resolution results in better accuracy. With spatial resolution equal to 1 m, the relative frequency is almost 20 MHz, while it is less than 1 MHz for a spatial resolution of 10 m. The spatial resolution should not be less than 3 m when using this test equipment. If the spatial resolution is too low, the light pulse will not have enough energy, and the gain in the signal will therefore not be sufficiently big [21]. This causes instabilities and poor measurement repeatability. From the calibration curve, see Figure 7, it is stated that 1 MHz approximately corresponds to 1°C. The measurements with spatial resolution of 1 m are consequently varying with up to 20°C.

In Figure 16, it is stated that a spatial resolution of 1 m only is applicable for fiber lengths up to 15 km when applying the DITEST. This matches the results presented in Figure A.6, where the deviation is relatively small and constant up to a fiber length of 20 km, and increases substantially over the remaining length. A 37.5 km long fiber should have a spatial resolution

29

of at least 3 m to ensure that the signal has enough energy and that the accuracy is varying within acceptable limits [21]. Figure 25 shows how measurement time varies with spatial resolution, and confirms the statement that spatial resolution should be at least 3 m. The measurement time is almost tripled going from 3 m to 1 m in spatial resolution, which is a substantial increase considering it goes from 100 s to 300 s. The higher spatial resolution, the lower measurement time. There is however a relatively small time difference, approximately 5 s, between a 5 m and 10 m spatial resolution. The results are exponentially distributed.
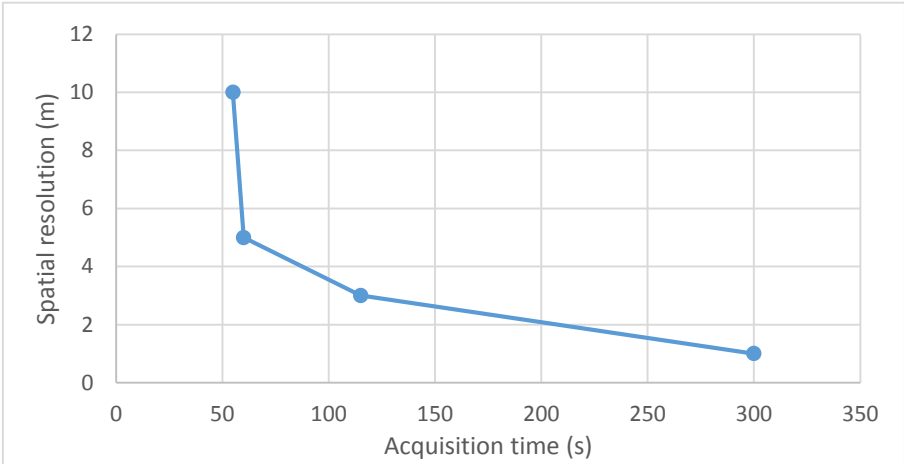
Figure 25: Measurement time for different spatial resolutions.
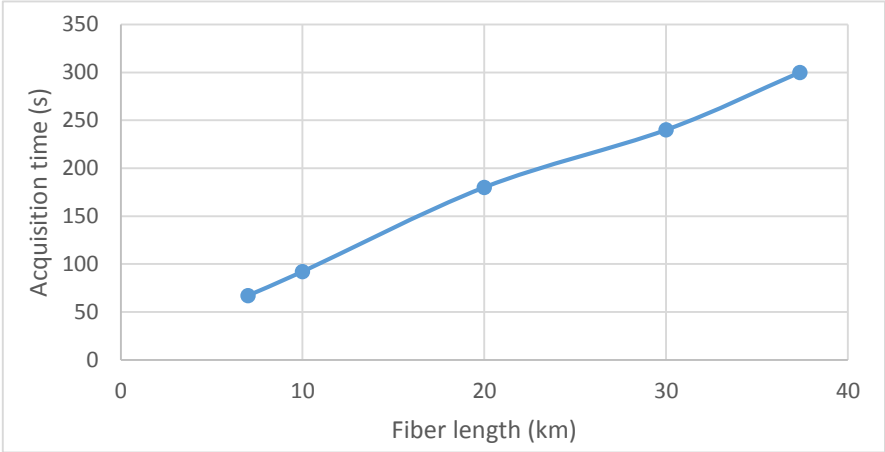
Figure 26: Measurement time for various fiber lengths

Acquisition time depends on several factors, including spatial resolution, fiber distance, and averaging. Figure 26 shows that measurement time is approximately linearly distributed with fiber length. By applying one of the integrated functions in Excel, a linear trend line can be created, also providing the accompanying equation.

The following equation represents the linear relationship between acquisition time and fiber length:

$$y = 7.58x + 17.66$$

And by assuming that the graph intersects at the origin:

$$y = 8.22x$$

Where x and y represent fiber length (km) and acquisition time (s), respectively.
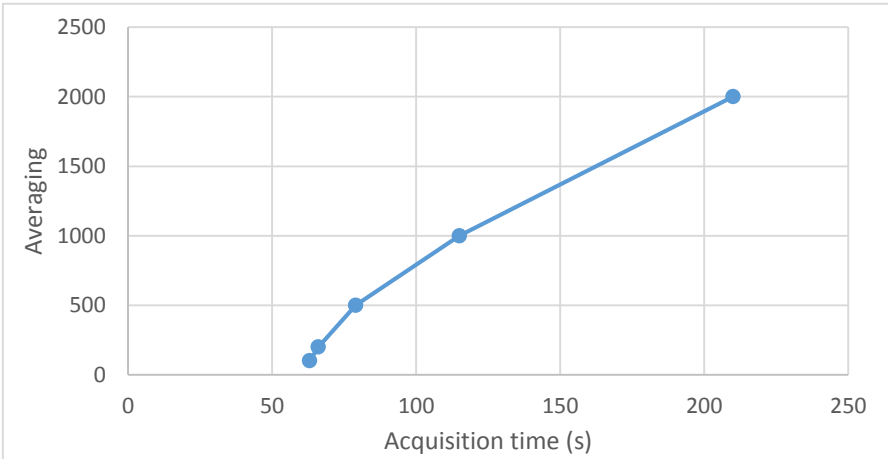
Figure 27: Measurement time for various number of averages.

A high number of averages provides good accuracy, but increases the acquisition time significantly. Averaging values ranging from 100 to 2000 were tested, with resulting acquisition times from approximately 60 s to 210 s, see Figure 27. The relationship between averaging and acquisition time is not quite linearly distributed, the slope is steeper in the beginning than in the end section. In order to achieve sufficient accuracy, number of averaging should be around 2000 for a fiber of this length [21]. In the optimization table, see section 2.4, it is given that optimal measurement condition for a 30 km and 50 km long fiber includes averaging values of 1000 and 2000, respectively. If time is the limiting factor, going from 1000 to 2000 in averaging increases the measurement time with approximately 100 s.

The applied strain has a clear impact on the frequency distribution at a point 25 km along the fiber, see Figure A.13 and A.16. The first measurement series was interrupted by an alarm message displaying "Fiber broken or disconnected. Channel: 1", shown in Figure A.14. A measurement with no strain was then conducted to ensure that the fiber still was intact. As indicated in Figure A.15, the fiber appears to be complete considering the similarity to the measurement conducted under identical conditions shown in Figure A.7. The DITEST is giving a fiber break alarm although that is not the case. This raises question to the reliability of the measuring unit in situations where tension is present. Figure A.13 and A.16 have slightly different frequency distributions, most likely due to the difficulty of controlling the degree of strain created by hand. The frequency response from the point where strain was applied until the fiber end appears to be affected. The relative frequency is fairly low and stable up until this point, where it expands and remains high. This might indicate that the measurements are quite inaccurate, up to 10 MHz in this case, in whole sections rather than just in the area where strain is applied.

The created hot-spot is not detected with a spatial resolution of 1 m. As shown in Figure A.17, there is no clear frequency change at any position, indicating that spatial resolution of 1 m is too small for a fiber of this length. The red circles marked in Figure A.18-A.20, illustrate a frequency step caused by the applied heat. The most evident peaks are for spatial resolutions of 3 m and 5 m, with relative frequencies of 5 MHz and 3.5 MHz, respectively. There is a frequency peak at the same location for 10 m spatial resolution, but only with a magnitude of approximately 1 MHz. The peak is so small it could be mistaken for random fluctuations. The temperature change occurs in a relatively small region compared to the spatial resolutions, so the detected temperature is smaller than actual temperature.

In cases where the fiber is cut off, the DITEST is not providing any information, except an alarm message, see Figure A.21. Neither frequency distribution or fiber break location are given. The alarm was displayed immediately after the measurement was tried started.

3.3. Raman experiment

The original plan was to conduct the measurements in collaborations with Lios, one of the leading producers of Raman based DTS systems, in Germany. Due to time constraints, another experiment was conducted with Nexans in Oslo.

The applied measuring unit is produced by Lios, and is a part of their OTS generation 2 series. The measuring unit allows a fiber length of maximum 4 km, but has the same working principles as the ones reaching over tens of kilometres. The length limitations of Raman DTS measurements could therefore not be investigated and tested as intended in this experiment.

A fiber of approximately 3.5 km was first tested, but could not be applied due to problems associated with configuration of the measuring unit. The DTS expert in Nexans could not interpret the error messages or understand why the unit did not accept a fiber of this length. It was believed there were some license based problems. The alternative was a fiber of less than 1 km, making the study of how measurement parameters vary with distance less representative for Raman systems as a whole.

3.3.1. Experimental setup

The applied multimode fiber had a length of just under 700 m, where the main part was wrapped around a spool. Figure 28 presents an overview of the experimental setup.
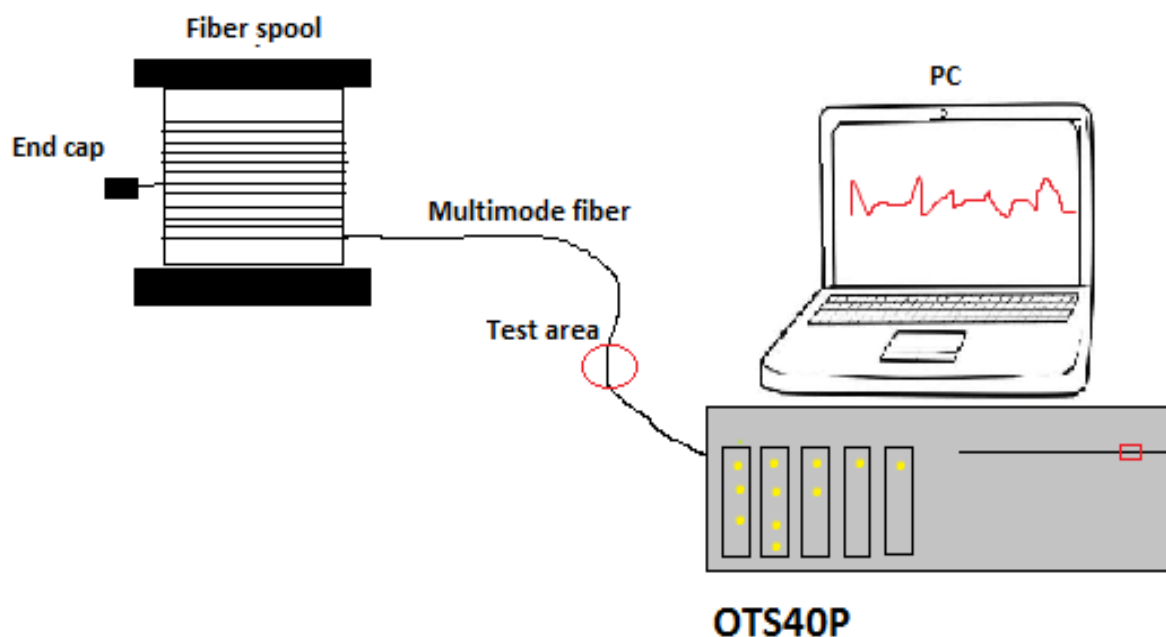
Figure 28: Experimental setup, including measuring unit and fiber spool.

The measuring unit does not have an integrated screen, so it was connected to an external computer. This computer had the parameterization and visual display software "Charon_02" already installed.

The fiber was connected to the monitoring unit through one of the four terminals at the back. All terminals were tested, but "SENSOR CABLE- Ch.1" was applied during the experiment, see Figure B.2 in appendix. This is a single ended system, so the far end of the fiber was connected to an endcap to stop the light path.

The fiber length included one fiber splice, joining the first 5 m of fiber with the remaining length, see fiber splice in Figure B.3.

3.3.2.   OTS40P

The measuring unit applied in this experiment is called OTS40P, and is a part of the OTS product series produced by Lios.

The measuring principle is based on Optical Frequency Domain Reflectometry (OFDR) technology. A continuous temperature profile along the fiber is provided, but only once the backscattered signal from the whole measurement period has been measured in terms of frequency and then Fourier transformed. Compared to most Raman based DTS systems, which sends out laser pulses, the OFDR monitoring unit sends out a continuous wave. The continuous backscattered signal is filtered and converted into electrical signals, amplified and mixed into the low frequency spectral range. The Fourier transform of the averaged frequency signals provides the Stokes and anti-Stokes curves in the time domain. The amplitudes of these curves are proportional to the intensity of the Raman scattering, and the temperature is given from the relationship between the Stokes and anti-Stokes amplitudes. [23].

The schematic design of the OFDR Raman DTS system is shown in Figure 29.
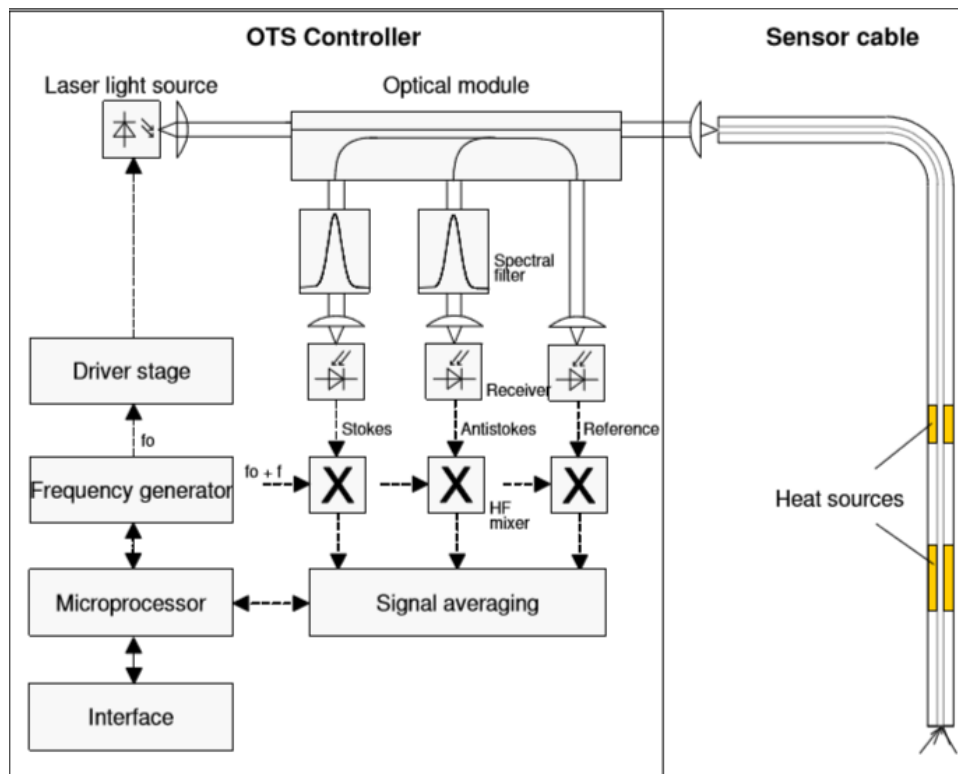
Figure 29: DTS based on OFDR principle. [32]

The fiber sensor can be divided into zones, where each zone can have different alarm triggering parameters. The zones can for instance be divided with regard to great depth variations or partly buried cables. An alarm is triggered if one of the alarm criteria in a zone is exceeded.

The front of the monitoring unit is shown in Figure 30. The five columns represent operation, communication, switching contacts, alarms and explosion protection, from left to right.
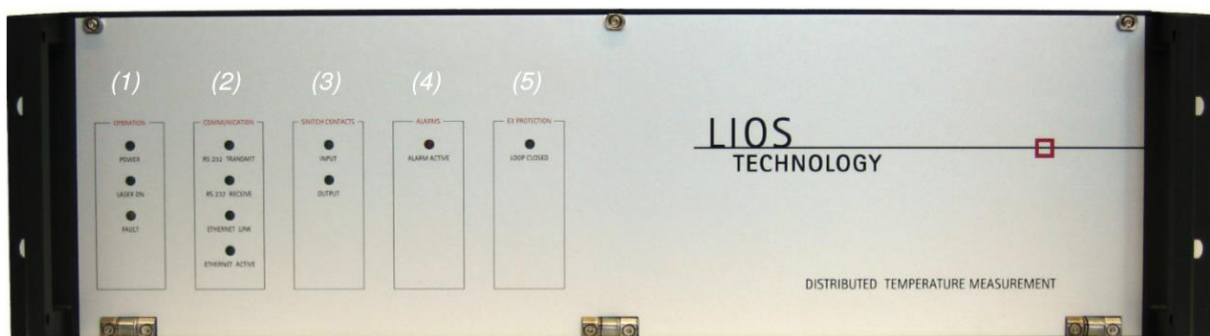
Figure 30: OTS40P, view from front. [29]

The OTS controller includes the following modules:

- o Transmitter module, containing the laser and its control.
- o Receiver module, including the entire optical design.
- o Digital module, controlling the overall operation of the Controller and temperature measurement process.
- o Power supply module, supplying all the OTS Controller components with the necessary operating voltage.

[24]

See Table B.1 in the appendix for technical data for the OTS40P.

3.3.3.   Test matrix

The test matrix below shows an overview of the tests that have been carried out, including the key measurement specifications.

Test no.	Explanation	Measurement time (s)	Fiber length (m)	Condition	Spatial resolution	Averages (time domain)	Parameter of interest
1	Accuracy vs. distance	9	665	Ambient	1	2	Temperature
2	Accuracy vs. spatial resolution	9	665	Ambient	0.87	2	Temperature
3	Accuracy vs. spatial resolution	9	665	Ambient	2	2	Temperature
4	Accuracy vs. spatial resolution	9	665	Ambient	3	2	Temperature
5	Accuracy vs. time	49	665	Ambient	1	2	Temperature
6	Accuracy vs. fiber length	9	500	Ambient	1	2	Temperature
7	Accuracy vs. fiber length	9	300	Ambient	1	2	Temperature
8	Accuracy vs. fiber length	9	100	Ambient	1	2	Temperature
9	Accuracy vs. averages	9	665	Ambient	1	1	Temperature
10	Accuracy vs. averages	9	665	Ambient	1	3	Temperature
11	Accuracy vs. averages	9	665	Ambient	1	5	Temperature

12	Accuracy vs. averages	9	665	Ambient	1	10	Temperature
13	Hot-spot detection	9	665	Heater (140 °C)	1	2	Location and temperature
14	Hot-spot detection	9	665	Heater (140 °C)	1.5	2	Location and temperature
15	Hot-spot detection	9	665	Heater (140 °C)	2	2	Location and temperature
16	Hot-spot detection	9	665	Heater (140 °C)	3	2	Location and temperature
17	Fiber break evaluation	9	Irrelevant	Ambient	1	2	Location and temperature

Table 6: Test matrix for a Raman based DTS experiment performed with OTS40P.

3.3.4. Methodology

All measurements were repeated at least three times to limit the effect of random errors.

The fiber was kept in a stable environment for the main part of the experiment, with an ambient temperature between 20°C and 25°C.

The measurement parameters were set in Charon_02, as a part of the configuration of the OTS Controller. The spatial resolution, measurement time and number of averages were manually set as shown in Figure 31.
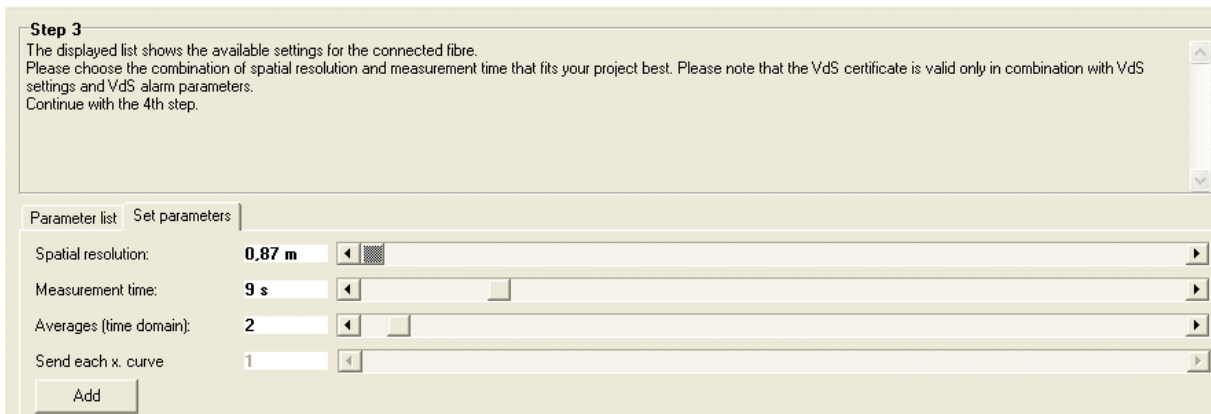
Figure 31: OTS40P configuration.

The measurement time was held constant at 9 s through all measurements. The number was set relatively low due to the short fiber that was used. One measurement with long measurement time, 50 s, was conducted to check whether it had a substantial impact on the temperature profile.

As for the Brillouin experiment, a hot-spot was created using a hot air gun. It was set to 140°C, and held less than 10 cm above the fiber. The fiber was cooled down to ambient temperature before the same measurements were repeated for a new spatial resolution. Approximately 1 m of the fiber was coiled up, and heated with the same hot air gun, see Figure B.4. This was done to evaluate the temperature profile when a larger area was exposed to the heat.

The fiber break situation was created by breaking off the fiber by hand, while light signals still were sent into the fiber.

The Charon_02 displayed frequency, backscatter and temperature profiles along the measured fiber length, see Figure 32. The temperature profiles of interest were screenshotted and saved for further analysis.

Figure 32: Frequency, backscatter and temperature profiles displayed in Charon_02. [29]

3.3.5. Results

The key findings from the experiment are summarized in Table 7.

Test no.	Key findings
1-4	o Increased distance → lower accuracy o Higher spatial resolution → higher accuracy
5	o Longer measurement time → unchanged accuracy
6-8	o Increased distance → lower accuracy
9-12	o Higher number of averages → unchanged accuracy
13-16	o Higher spatial resolution → smaller response in temperature profile due to hot-spot o Greater fiber length being exposed to heat → greater response in temperature profile
17	o Fiber break alarm message o Fiber break location is provided

Table 7: Key findings in Raman experiment.

All experimental results, including measurement specifications, from the measurements conducted with Raman principles are listed in appendix B3. The results are presented as temperature (°C) profiles along the fiber length (m) as illustrated in Figure 33.

Figure 33: Temperature profile along fiber length.

3.3.6. Summary of laboratory studies based on Raman principles

The temperature accuracy is changing throughout the fiber length, where the temperature variations are relatively small and stable up to 450 m, a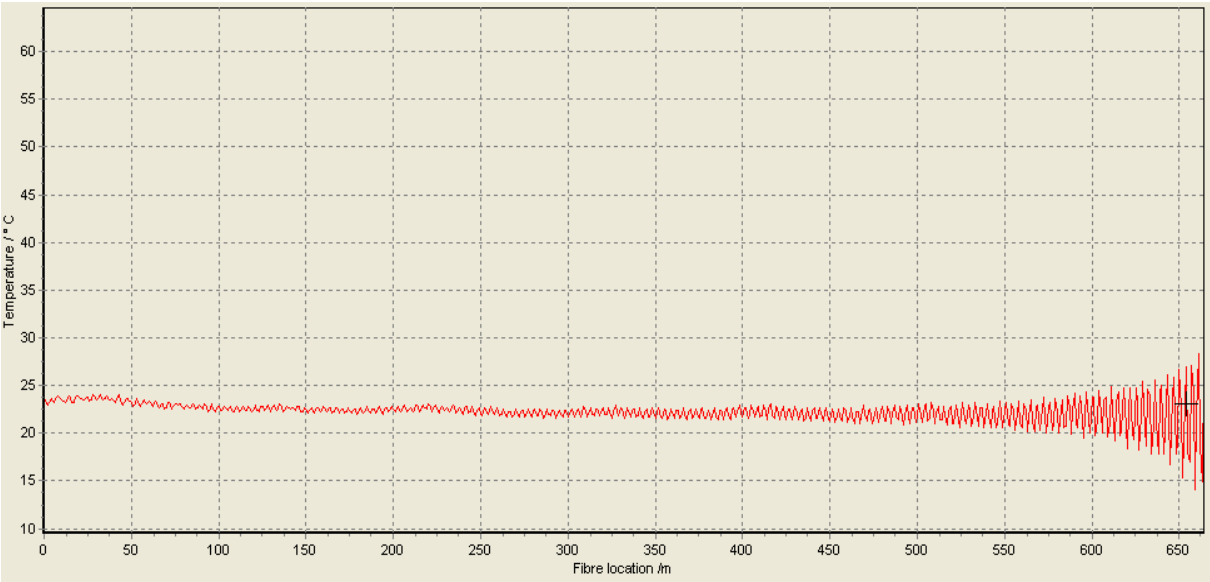nd increasing with distance the remaining part. As indicated in Figure B.5-B.8, the accuracy is better at higher spatial resolutions. At a point 600 m from the fiber start, the temperature is varying with approximately 5°C, 4°C and 2°C for a spatial resolution of 1 m, 2 m and 3 m, respectively. Fiber length should theoretically not have a substantial impact on the temperature resolution due to the relatively short fiber.

The temperature resolution for fiber lengths ranging from 100 m to 670 m were examined, see Figure B.10-B.13. It seems like the OTS40P always is measuring the entire length, but only displaying the temperature profile for the defined fiber length. This allegation is based on the fact that the temperature profiles are unaffected towards the fiber end for lengths shorter than full length. It would appear that the accuracy is getting worse towards the fiber end due to some effects from the endcap.

Number of averages does not have a significant effect on the temperature accuracy in the performed tests with spatial resolution of 1 m, see Figure B.14-B.17. The measurement time is constant for all measurements, so by increasing the number of averages, the accuracy theoretically should improve. The fiber might be too short, or the measurement time set too low, for the number of averages to have an impact on the temperature profile.

A fivefold increase in the measurement time, from 9 s to 50 s, does not affect the temperature profile noteworthy, see Figure B.9. The fiber is most likely too short for the acquisition time to have a noticeable impact on the accuracy.

The created hot-spots do not constitute significant peaks in the temperature profiles. There is a 4°C peak with spatial resolution of 1 m, and it is smaller for higher spatial resolutions. This verifies the theory claiming that the temperature response is smaller with lower hot-spot fiber length/spatial resolution ratio. In order to confirm this allegation, a greater fiber length, approximately 1 m, was exposed to the heat. For a spatial resolution of 1 m and 2 m, the temperature peak constituted around 17°C and 12°C, respectively. The amplitude of these peaks are approximately tripled compared to when a smaller area was heated. These results

indicate that the greater continuous fiber length being exposed to the heat, at least up to the spatial resolution, the more substantial the temperature response is. A fiber has poor heat conductivity itself, but heat would for example spread in a PBC in case of an electrical fault. A fault in the cable can be very small, but the heat development can still be quick. In such cases when applying the OTS40P, the question of interest would be whether the heat spreads over a sufficiently large area to be detected before damage is caused to the equipment.

An alarm message, including fiber break location, is displayed immediately after the fiber is cut off. The message claims that the fiber break is at 8 m, which seems reasonable after doing a quick visual estimate. As indicated in Figure B.24, a temperature profile is not provided after the break, only a caution triangle at the relevant position.

4. DTS and break detection for fault detection

The essential safety requirement for cable fault protection is the ability to detect potential faults before the pipeline gets damaged. The power supply must be switched off in time to avoid a short circuit between the PBC and the steel pipe.

Fibers can be applied to detect and localize faults in DEH systems. DTS based on Raman and Brillouin, in addition to a technology referred to as break detection, will in the following chapter be evaluated and compared for this purpose.

4.1. Fault development study

SINTEF, Nexans and Statoil have carried out a fault development study for a DEH system in a Joint Industry Project. The aim was to investigate and document the fault development in the PBC for varying fault sizes and start currents. A summary of the test procedure and results will be presented here. The full report, "Safe Fault Detection on Direct Electrical Heating Piggyback Cables", is a public document, see references for more details [25].

4.1.1. Electrical measurements

Topside in-feed current or impedance measurements have traditionally been the main methods for cable protection. The power supply is shut off if the in-feed current is measured to be outside normal operating conditions.
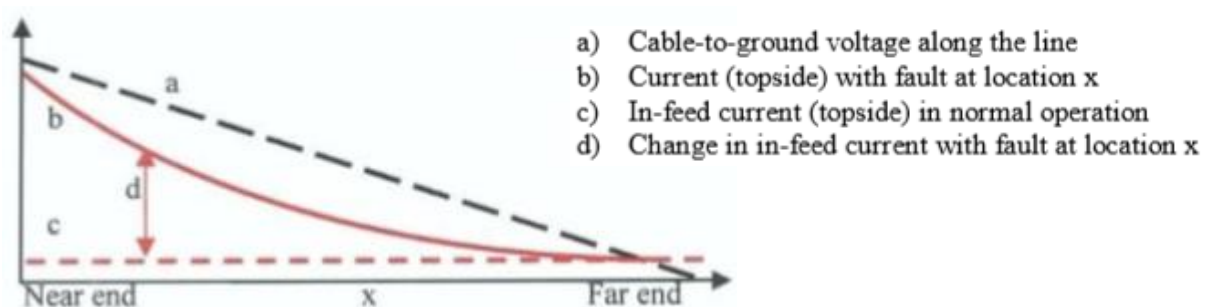
Figure 34: Change in in-feed current vs. fault location. [17]

Figure 34 shows the relationship between measured in-feed current and fault location.

Electrical measurements can provide sufficient protection for the main part of the pipe, but if the cable fault is located in the far end of the pipeline, the in-feed current will remain the same. This scenario is presented in the figure, where the solid and dotted red lines overlap.

Insulation faults of different sizes were applied to the PBC test sample placed on the seabed. An example of the Large fault, 25 cm^2, is shown in Figure 36. The choice of fault current levels were based on calculations performed to predict faults in the far end of the PBC in Tyrihans.

A common outcome for all test settings was a decreasing current, which stabilized after some days, see Figure 35 for one example.

Based on the findings in this experiment, it was concluded that minor fault currents at the far end of the PBC can not be detected, and will cause serious damage to the cable, see Figure 37.
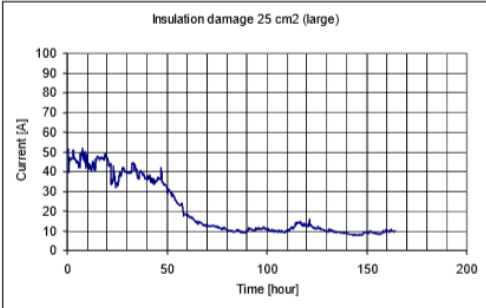
Figure 35: Change in current over time. [25]

Figure 36: Large fault, 25cm^2. [25]

Figure 37: Test object after test period. [25]

Other evaluated fault detection methods in this study are differential current measurements, screen current measurements, FO temperature monitoring, FO break monitoring and current fast Fourier transform analysis.

4.1.2. FO break detection

Fault detection based singly on electrical measurements does not fulfil the safety requirements in the far end region. FO break detection was therefore suggested as a complementary detection method.

Nexans has patented break detection by fiber optics in DEH systems [26]. The main principle is to produce the DEH cables with fiber in metallic tubes (FIMT). The fibers are looped and a light is continuously going through the fibers in the cables. There is no practical length limitation for this fault detection method. In the event of trawl impact or dropped item damage on the cable, to the extent it creates a short circuit, the FIMT will instantly burn off. The light will then not go through the fiber and triggers a shutdown of the system. The monitoring system is digital in terms of having only two potential outcomes, a complete or broken fiber. The shutdown happens immediately, eliminating the possibility of damaging the production pipe. [10].

Single mode fibers are applied in break detection, mainly due to the low modal dispersion and ability to reach over great distances. The fiber is installed in all parts of the DEH cable system, including riser, feeder and piggyback cable. [17].

4.1.3. Qualification of FO break detection for DEH

Further in the fault development study, an electrical qualification test based on break detection was carried out.

FO elements were integrated in a full-scale Tyrihans prototype PBC and tested to ensure that the fiber element would break before damage was caused to the production pipeline. The cable was strapped on top of a pipeline segment, and placed in a vessel filled with seawater and pressurized to 30 bar, see

Figure 38: Pressure vessel applied during testing. [25]

Figure 38. The correlation between depth and pressure is approximately 1 bar per 10 m [27], so 30 bar is equivalent to a depth of around 300 m.

Tests were conducted with the insulation fault at different places relative to the fiber element.

All tests are listed in the Table 8.

Test No.	Fault size	Fault position	Surrounding medium	Current [A]
I	Large	Close to FO	Seawater	68
II	Medium	Opposite FO	Seawater	30
III	Medium	Opposite FO	Clay	24
IV	Small	Opposite FO	Seawater	10

Table 8: Test matrix for FO break detection technology. [25]

The results, including minutes before fiber break and severity of cable damage, are listed in Table 9.
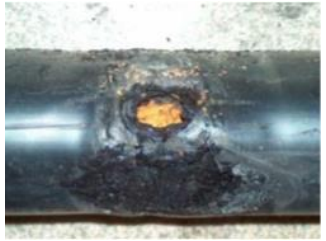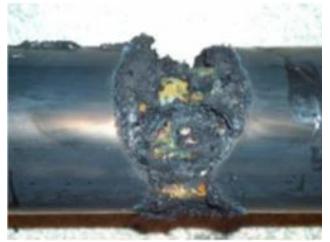
Test No.	Minutes before fiber break	Picture of cable damage	Picture of cable damage when outer sheath was removed
I	26		
II	60		
III	300	Damage to cable similar to Test II.	---
IV	25		

Table 9: Results from fiber break detection qualification test. All photos: [25]

Based on the results from this experiment, it was concluded that application of break detection fulfills the safety requirements for cable fault protection in a DEH system. The fiber broke before damage was caused to the pipeline, also when the fault was facing the pipe and the fiber was placed on opposite side. Nor varying surrounding mediums seem to have a substantial negative effect on the fiber break ability.

4.2. Comparison of Raman, Brillouin and break detection

Break detection is already installed for fault detection in many DEH systems operating today, while DTS measurements currently only are conducted for the purpose of temperature surveillance.

4.2.1. Time lag

The fault development in a PBC depends on fault size and current levels, as described in section 4.1. When running the qualification test on break detection for DEH, it took between 25 and 300 minutes before the FO element broke. The damages on the cable were minor, and the pipeline was unaffected. This indicates that the thermal response time in the cable is good, and that the fiber is conveniently located so that it breaks before severe damage is caused to the surrounding cable. Once the light is stopped at the break point, it instantaneously triggers a shutdown of the system.

There are several ways to lower the measurement time in DTS measurements due to the interrelation between accuracy and time. By lowering the localization accuracy, i.e. increasing the spatial resolution, the measurement time is reduced. The measurement time was almost six times smaller with spatial resolution of 5 m compared to 1m, in the Brillouin experiment. Correspondingly, the measurement time was more than halved when going from 2000 to 500 number of averages. The shortest acquisition time achieved during the testing was around 50 s. The performance data claims it can be as low as 20 s, see appendix A1.

The relationship between measurement time and accuracy was not detectable in the Raman experiment, most likely due to the short fiber length that was tested. All tests were performed with acquisition time of 9 s. The minimum measurement time for this specific measuring unit is 5 s.

In cases where the cable fault is small and develops relatively slowly, minutes or hours, the DTS measuring units theoretically should be able to detect the temperature changes in time to shut down the system.

Time is the limiting factor in a short circuit situation, the level of accuracy in the temperature measurements is somewhat irrelevant. There is not time to process the backscattered signals to create a complete temperature profile. An alarm message was displayed immediately after the induced fiber break in both the Raman and Brillouin experiment. This alarm message should ideally trigger the electricity to be switched off, but then it is practically a break detection system and violations of patent [28].

4.2.2. Distance

Break detection systems applies single-mode fibers to limit the modal dispersion, and can therefore reach over long distances. The fiber fault location does not have a big impact on the performance of the break detection system since the information is traveling with the speed of the light signals. The fiber break will be detected within a fraction of a second regardless of fault location. The light can for instance travel 100 km, with a refractive index of 1.5, in one millisecond. This was calculated by applying the equations for refractive index and distance in section 2.1.1.

The Brillouin systems based on SBS technology can reach over distances up to 75 km, due to amplification of the light signal. The measurement accuracy is strictly dependent on fiber length, as illustrated in the results from Test 1. The accuracy is getting progressively worse with distance. The measurement time is approximately linearly distributed with fiber distance. The time also depends on number of averages and spatial resolution, but for a spatial resolution of 1 m and averages equal to 1000, it took around 75 s to detect and process signals from 10 km fiber, see Figure 26.

Raman based DTS systems usually apply multimode fibers to achieve higher light-gathering capacities due to the relatively low signals, and can reach up to 30 km. Maximum length for single-mode fibers is defined to be 40 km with the current DTS systems. [11]. The fiber applied in the Raman experiment was less than 700 m, so the fiber length did therefore not affect the temperature accuracy or measurement time noticeably. The results are hence not

representable for how Raman based DTS systems, with fibers reaching over longer distances, generally work. The temperature resolution is quite good and stable up to 500 m, where it gets progressively worse towards the fiber end. This variation is likely due to some instabilities caused by the end-cap which stops the light, rather than a response because the fiber is too long.

To date, the longest DEH cable is 43 km, delivered to the Lianzi project in Congo and Angola [1]. DTS measurements based on Raman principles are hence excluded as an alternative in such systems due to the length limitations.

4.2.3. Accuracy

Monitoring performed with fiber break detection has two possible outcomes, normal operation with a complete fiber, or cable fault indicated by a fiber break. The accuracy of the monitoring is hence related to the ability to correctly detect and localize the fault. Break detection technology has been qualified for use in DEH systems. The fiber broke in time to prevent damage on the pipeline, regardless of fiber location relative to cable fault and type of medium surrounding the cable. The fault location can be determined the same way as for DTS measurements, which is described in section 2.1.1.

The accuracy term in DTS context applies to the ability to localize and quantify faults in the subsea DEH system. Both the Raman and Brillouin based DTS systems claim to have localization accuracy better than 1 m and temperature accuracy within $\pm 1°C$.

Heat was applied to a relatively short fiber length, approximately 10 cm, during the hot-spot experiments. The frequency or temperature responses, from the Brillouin and Raman experiments respectively, do not indicate that the hot air gun was set to 140°C. Maximum response in the Brillouin experiment was 5 MHz, which corresponds to approximately 5°C, and around 4°C in the one based on Raman principles. The response is decreasing with increasing spatial resolution. This matches the theory claiming that the detected temperature is smaller than actual temperature by a ratio of fiber length where temperature change occurs to spatial resolution. A fault can be very small and yet cause great damage, so it is therefore crucial to have a spatial resolution small enough to detect the abnormalities.

The spatial resolution is determined primarily by the pulse duration, which also indicates the amount of energy in the signal. The measurement accuracy is progressively getting worse throughout the fiber length, but high spatial resolution contributes to an overall better accuracy due to higher energy levels. The Brillouin measurements conducted with spatial resolution of 1 m and fiber length of less than 40 km, resulted in measurements that were highly inaccurate. This is likely caused by insufficient energy in the pulse signal, not providing enough gain in the signal. A fiber of more than 30 km should at least have 3 m spatial resolution, but this could however cause the detected response from a small hot-spot to mistakenly be ignored. Figure 16 and 17 illustrate the relationship between the performance parameters for a Brillouin and Raman DTS system. The frequency response in the Brillouin hot-spot experiment with spatial resolution of 10 m is visible, but still small enough to be a random fluctuation, see Figure A.20. Correspondingly, for the Raman experiment with a spatial resolution of 3 m, the small temperature response is illustrated in Figure B.21.

4.2.4. Uncertainties

The fibers used in the experiments are mainly wrapped around spools, which causes the fiber to be under tension. This leads to noise, i.e. inaccuracies, in the Brillouin measurements due to the temperature/strain cross-sensitivity [21]. The results from the cross-sensitivity experiment indicates that the frequency response from the point where strain was applied until the fiber end was affected, see Figure A.16. Information about the proportion of fiber under tension is therefore not provided. A false fiber break alarm appeared during the same experiment. It seems like a certain amount of strain is perceived as a fiber break by the Brillouin measuring unit. The amount of strain created by hand is difficult to control and maintain constant during the test period.

A PBC will be affected by strain due to expansion in the pipeline when heat is applied, which must be taken into consideration when applying Brillouin for DTS. Tension will also occur when the pipeline is moved or twisted as a result of sea currents and movement of seabed sediments. These movements can cause some sections of the PBC to be completely or partly buried into the seabed, which may appear as hot-spots when DTS measurements are conducted during start-up of the DEH.

The location of the fiber relative to the pipeline affects the thermal response time. Worst-case scenario is with the cable fault facing the pipeline, and the FO element located on the opposite side of the PBC.

The fiber applied in the Raman experiment was relatively short, 670 m, so distance should theoretically not have a substantial impact on the temperature accuracy. The detected temperature profile is however varying with up to 5°C the last 100 m, which possibly is caused by effects from the fiber endcap.

5. Conclusions and further work

5.1. Conclusion

The work described in this thesis has been focused on evaluation of fibers for fault detection on subsea pipelines with DEH. The overall safety requirement for DEH is that faults in the PBC are detected before the integrity of the pipeline is threatened.

The DTS system performance is based on a trade-off between accuracy, measurement time and distance range. The correlation of these parameters have been investigated for Raman and Brillouin based DTS systems in experimental studies and a literature survey. Time is the parameter that primarily limits the suitability of DTS for fault detection. The measurement time increases with distance and level of accuracy. Localization and temperature accuracy are determined by spatial resolution and number of averages, respectively. Small hot-spots are not detectable if the spatial resolution is set too big, but a lower spatial resolution is equivalent with longer measurement time.

The Brillouin experiment was conducted with a 37.5 km long single-mode fiber. Acquisition time proved to be approximately linearly distributed with fiber length. The measurement time increases with 75 s for every 10 km fiber, using a spatial resolution of 1 m. By decreasing the number of averages to 100, compared to 1000-2000 which is recommended, the acquisition time is still around 60 s for 3 m spatial resolution. The measurement specification states that the acquisition time can go down to 20 s.

The results from the Raman experiment do not reveal the full potential of this measurement technique. The applied fiber was less than 700 m, so the change in measurement parameters had small, or no, impact on the system performance. Maximum measuring length of Raman based DTS with single-mode fiber is claimed to be 40 km.

Break detection is an existing fault detection method in DEH systems. In a short circuit situation, the fiber will burn off and immediately trigger a shutdown of the system. In the qualification test of break detection for DEH, it was found that the fiber breaks before damage is caused to the pipeline regardless of fault size and fault current levels. It took between 25 and 60 minutes before the fiber broke for different fault sizes, with seawater surrounding the cable. The heat development in the cable is slower with clay relative to seawater as surrounding medium.

Due to the relatively long acquisition time in DTS measurements, the fiber is likely to break before a temperature profile is created in a short circuit situation. When a fiber break is created, an alarm message is displayed on the DTS measuring units. The fault is hence not detected by temperature measurements, but by the fiber break alarm, which in theory is a break detection system.

DTS and break detection are both useful tools for surveillance and control of subsea pipelines with DEH, but appear to have different field of application. DTS measurements can be conducted to monitor the temperature continuously, such as to detect slowly developing hot-spots and to indicate cable burials. Break detection remains the preferred fault detection method, mainly due to the immediate response and its high reliability regardless of distance, influence of strain and operational conditions of the DEH. The ideal solution would be to combine DTS and fiber break detection into one fiber and measuring unit, but this is currently not possible due to violations of patent.

5.2. Suggestions for future work

Due to the limited scope of this thesis, there are several aspects that should be investigate further to create a more complete picture of the application of DTS.

Firstly, the length limitations of Raman based DTS measurements were not investigated experimentally as intended. Fiber lengths of minimum 40 km should be used to check whether a temperature profile could be created based on the backscattered signal.

Secondly, the possibility of stimulated Raman scattering should be looked into. If the Raman signal could be amplified and therefore applied over longer distances, it would be the preferred option over Brillouin due to no cross-sensitivity.

Thirdly, more extreme values of the DTS performance parameters should be tested with the aim to minimize the measurement time.

Lastly, the effect of fiber location relative to cable fault and pipeline should be investigated by conducting DTS measurements in a full-scale DEH system.

References

[1] Nexans, "Direct Electrical Heating (DEH) technology keeps subsea flowlines flowing as oil and gas projects go deeper and longer," Nexans, 6 May 2015. [Online]. Available: http://www.nexans.us/Corporate/2015/1505-Nexans-DEH_at_OTC2015_GB.pdf. [Accessed 26 May 2015].

[2] A. Ukil, H. Braendle and P. Krippner, "IEEE Xplore," May 2012. [Online]. Available: http://ieeexplore.ieee.org/stamp/stamp.jsp?tp=&arnumber=5955066. [Accessed 3 February 2015].

[3] FOSTA, "Distributed Temperature and Strain Sensing (DTS &DTSS) Systems," [Online]. Available: http://www.fos-ta.com/brochuresE/5-Distributed-Temp-n-Strain-System-DTS-DTSS.pdf.

[4] R. Tricker, "2 Theory," in *Optoelectronics and Fiber Optic Technology*, Newnes, 2002, pp. 36-75.

[5] J. J. Smolen and A. Van der Spek, "Distributed Temperature Sensing: A DTS primer for Oil and Gas Production," Shell, 2003.

[6] Omnisens, *DITEST STA-R Fiber Optic Distributed Temperature and Strain Analyzer,* Omnisens, 2013.

[7] Y. Bai and Q. Bai, "Fiber Optic monitoring System," in *Subsea Pipeline Integrity and Risk Management*, Gulf Professional Publishing, 2014, pp. 145-164.

[8] L. Thèvenaz, "Brillouin distributed time-domain sensing in optical fibers: state of the art and perspectives," 22 January 2010. [Online]. Available: http://link.springer.com/article/10.1007/s12200-009-0086-9.

[9] N. Primerov, Interviewee, *Fiber technology.* [Interview]. 20 November 2014.

[10] D. Stanghelle, Interviewee, *DEH.* [Interview]. 16 October 2014.

[11] G. Lopez, Interviewee, *DTS working prinsiples.* [Interview]. 17 April 2015.

[12] G. Yilmaz and S. E. Karlik, "A distributed optical fiber sensor for temperature detection in power cables," 18 August 2005. [Online]. Available: http://ac.els-cdn.com/S0924424705003766/1-s2.0-S0924424705003766-main.pdf?_tid=e6fdda34-b750-11e4-905c-00000aab0f02&acdnat=1424252062_4bafa535542386d8e50f2e96d68458f7. [Accessed 18 February 2015].

[13] M. Nikles and F. Briffod, "Greaty extended distance pipeline monitoring using fiber optis," June 17 2005. [Online]. Available: http://proceedings.asmedigitalcollection.asme.org/proceeding.aspx?articleid=1575805. [Accessed 23 February 2015].

[14] M. Niklès, "Fiber Optic Distributed Scattering Sencing System: Perspective and Challenges for High Performance Applications," [Online]. Available: http://www.micronoptics.com.cn/pdfs/nikles.pdf. [Accessed 3 March 2015].

[15] K. Kishida, Y. Yamauchi and A. Guzik, "Study of Optical Fibers Strain-Temperature Sensitivities Using Hybrid Brillouin-Rayleigh System," 11 January 2014. [Online].

Available: http://link.springer.com/article/10.1007%2Fs13320-013-0136-1. [Accessed 10 February 2015].

[16] V. Lanticq, R. Gabet, F. Taillade and S. Delepine-Lesoille, "Distributed Optical Fibre Sensors for Structural Healt Monitoring: Upcoming Challenges," in *Optical Fibre, New Developments*, InTech, 2009, pp. 178-200.

[17] F. Ravet, A. Børnes, C. Borda, E. Tjåland, H. Hilde and M. Niklès, "DEH CABLE SYSTEM PREVENTIVE PROTECTION WITH DISTRIBUTED TEMPERATURE AND STRAIN SENSORS," 28 September 2012. [Online]. Available: http://proceedings.asmedigitalcollection.asme.org/proceeding.aspx?articleid=1721535. [Accessed 12 March 015].

[18] D. Peck and D. P. Seebacher, "Distributed Temperature Sensing using Fibre-Optics (DTS Systems)," 17 June 2000. [Online]. Available: http://www.engcom.com.au/publications/eea2000_dts.pdf. [Accessed 26 February 2015].

[19] A. J. Wheeler and A. R. Ganji, Introduction to Engineering Experimentation, Third Edition, Pearson, 2010.

[20] K. Grattan and D. T. Sun, "Fiber optic sensor technology: an overview," 1 November 1999. [Online]. Available: http://ac.els-cdn.com/S0924424799003684/1-s2.0-S0924424799003684-main.pdf?_tid=e9be3cba-d220-11e4-94ac-00000aacb362&acdnat=1427200133_8edb988328b7c011a85154f9d89d020a. [Accessed 24 March 2015].

[21] C. Borda, Interviewee, *DITEST working principles.* [Interview]. 17 April 2015.

[22] Lios Technology, "Distributed Temperature Sensing Systems: Controllers OTS200P-SM / OTS300P-SM Single-Mode," 2008. [Online]. Available: http://ctemps.org/files/ctemps/lios_datasheet_ots200p-sm_ots300p-sm_10_2008.pdf. [Accessed 16 May 2015].

[23] Lios, "Distributed Temperature Sensing Systems- Controllers OTS20P to OTS40P," [Online]. Available: http://ctemps.org/files/ctemps/lios_datasheet_ots20p_ots40p_10_2008.pdf. [Accessed 11 May 2015].

[24] Protectowire, "Protectowire FiberSystem 4000 OTS Series Controllers," 2011. [Online]. Available: http://protectowire.com/documents/ds-9203.pdf. [Accessed 11 May 2015].

[25] A. Bruaset, J. J. Bremnes and A. H. Børnes, "Safe Fault Detection on Direct Electrical Heating Piggyback Cables," 2006. [Online]. Available: https://www.onepetro.org/download/conference-paper/ISOPE-I-06-177?id=conference-paper%2FISOPE-I-06-177. [Accessed 28 Apil 2015].

[26] Nexans.Norway Patent 324585, 2006.

[27] The Engineering ToolBox, "Hydrostatic Pressure," [Online]. Available: http://www.engineeringtoolbox.com/hydrostatic-pressure-water-d_1632.html. [Accessed 29 April 2015].

[28] D. Stanghelle, *DTS information and pictures,* Oslo: Nexans, 2015.

[29] Lios, "OTS Generation 2 Distributed Temperature Measurement System," LIOS Technology, Köln, 2006.

[30] N. Primerov, Writer, *Omnisens Technology and DITEST*. [Performance]. Omnisens, 2014.

[31] Nexans, "Nexans' answers," Nexans, [Online]. Available: http://www.nexans.com/eservice/Corporate-en/navigate_276719_-3973_20_9024/Nexans_answers.html. [Accessed 16 May 2015].

[32] Lios Technology, "CHARON_02," Lios, Köln, 2004.

Appendix

Appendix A: Brillouin experiment

File including all measurements based on Brillouin principles can be handed out on request.

A1. Technical data for the DITEST

Performance	Number of channels	2 independent and selectable channels (standard) Compatible with up to 20 channel external switches - model SO-N (option)		
	Sensor configuration	Loop configuration (requires two fibers)		
	Sensing fiber	Standard single mode fibers		
	Distance range	50 km		
	Spatial resolution * *Typical*	0.5 to 20 m (by increment of 0.1 m) *1 m at 20 km / 2 m at 30 km / 3 m at 50 km*		
	Distance resolution	0.1 m		
	Number of distance points	100'000		
	Optical Budget	Standard configuration: 10 dB sensing (22 dB total loop) High optical budget upon request: 20 dB sensing (25 dB total loop)		
	Measured variables	Strain, Brillouin Frequency shift, Brillouin gain and width		
		Brillouin Freq. Shift	Temperature	Strain
	Resolution	0.1 MHz	0.1°C	2 $\mu\varepsilon$
	Range	10 GHz to 13 GHz	-273°C to 700°C (limited by optical fiber)	-3 % compression to 3 % elongation
	Acquisition time	>20 seconds 1-2 minutes typical 5-10 minutes for high resolution measurements		
Technical Data	Graphical interface	SVGA 300 mm (12") color screen (1024x768)		
	Communication and Connectors	Ethernet port, USB, RS232, SPST output relays (alarm and system status, Max 250VAC and 1 Amp)		
	Data storage	Internal hard disk (160 GB or more)		
	Data format	Database, text files (tab delimited text),		
	Optical connectors	E-2000 / APC		
	Dimensions (W x D x H)	449 x 500 x 266 mm (19" rack)		
	Weight	21 kg		
	Power supply	100-240 VAC / 47-63Hz / <200 VA		
Features	Measurement modes	Manual or automatic unattended measurements		
	Configuration	Automatic measurement configuration (self-adjusting to varying conditions)		
	Data analysis	Off-line data viewer software for measurement analysis, multiple trace comparison with respect to selectable baseline, measurement trends and time evolution, analysis at fixed distances, ...		
	Self-Diagnosis	Long term operation 24/7 guaranteed by automatic recovery and continuous system monitoring including system status, measurement quality and fiber break detection		
	Laser safety	Omnisens DITEST products emit invisible infra-red radiation in the 1550 nm wavelength range classified to EN 60825-1(2001-03) as Class 1M laser products.		
Environmental Specifications	Operating temperature	0°C to 40°C		
	Storage temperature	-10°C to 60°C		
	Relative Humidity	Max 90% non-condensing		
	Altitude	< 2000 m (6560 ft)		
	Protection rating	IP20 (indoor use)		
	Pollution protection	Pollution degree 2		

Table A. 1: DITEST performance, technical specifications and features. [6]

A2. Equipment and setup

Figure A. 1: Experimental setup.

Figure A. 3: Fiber splice for single-mode fiber.

Figure A. 4: Fiber connector.

Figure A. 2: DITEST connection terminals.

Figure A. 5: Hot air gun applied to create a hot-spot.

A3. Experimental results

The results from the performed experiments are presented in the following section. The test number in the headlines correspond to the number given in the test matrix.

TEST 1: Accuracy vs. distance

The following graphs are showing the frequency distribution relative to a baseline measurement conducted under the same conditions. The x-axis represents the sensing fiber length (km) and the y-axis is relative frequency (MHz). The accompanying measurement specifications, including spatial resolution, are given in the table on the left hand side.

Measurement Information	
Date :	2015.04.15 09:42:29
Meas. Time [min:sec] :	04:21
Interrogator :	STA-R S/N 83
Freq. Step [MHz] :	2.0 MHz
Freq. Scan Mode :	Automatic
Freq. Start [GHz] :	10.9283 GHz
Freq. Stop [GHz] :	11.2963 GHz
Averaging :	1000
Sensor Configuration	
ID :	201504141402598076613
Mode :	Loop
Length [m] :	37364.27
Sampling Interval [m] :	0.4
Nb of Points :	91918
Spatial Resolution [m] :	1.0
Pulse Amplitude [%] :	56
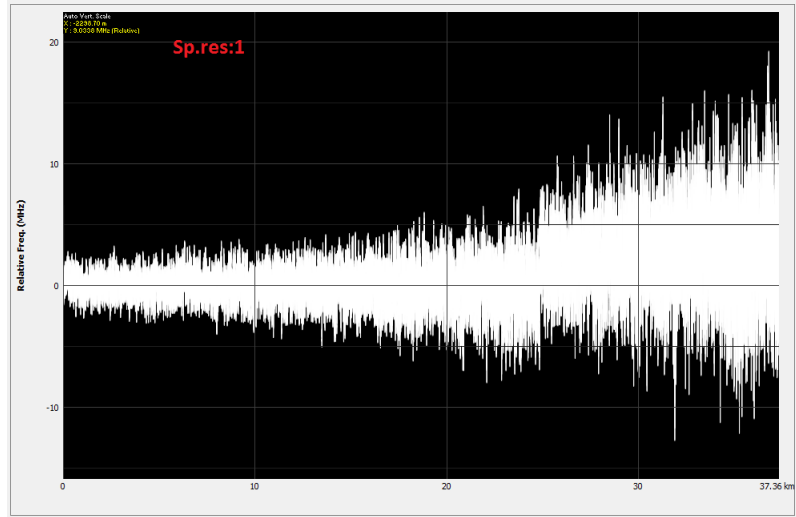
Table A. 2: Measurement specifications Test 1a

Figure A. 6: Accuracy vs. distance for spatial resolution=1 m.

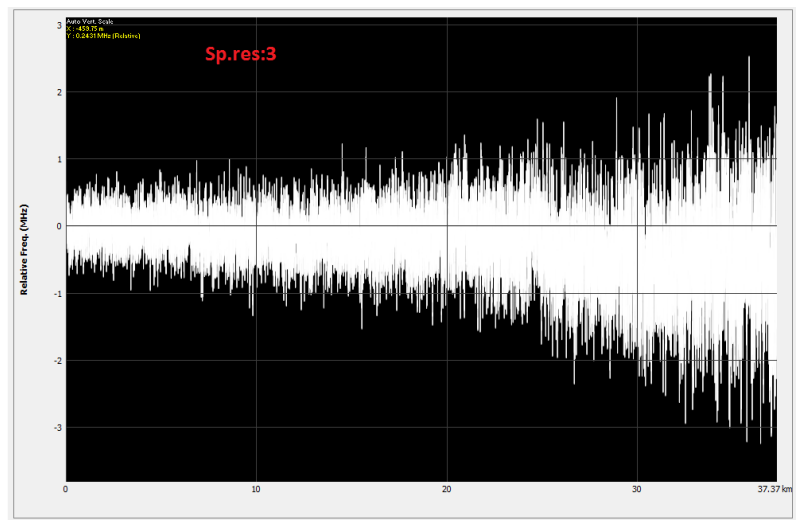| Measurement Information	
Date :	2015.04.16 08:58:44
Meas. Time [min:sec] :	01:33
Interrogator :	STA-R S/N 83
Freq. Step [MHz] :	2.0 MHz
Freq. Scan Mode :	Automatic
Freq. Start [GHz] :	11.0413 GHz
Freq. Stop [GHz] :	11.1533 GHz
Averaging :	1000
Sensor Configuration	
ID :	201504160841511095497
Mode :	Loop
Length [m] :	37365.07
Sampling Interval [m] :	1.0
Nb of Points :	36948
Spatial Resolution [m] :	3.0
Pulse Amplitude [%] :	67

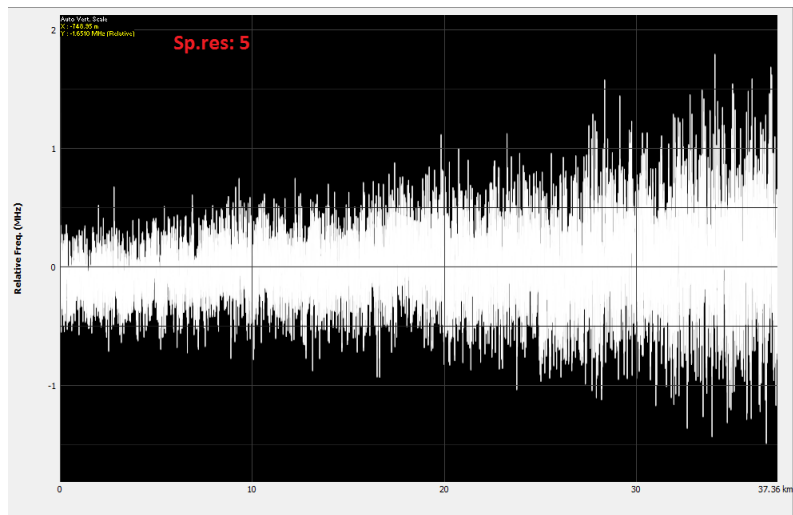*Table A. 3: Measurement specifications Test 1b.*

Figure A. 7: Accuracy vs. distance for spatial resolution=3 m.

Measurement Information

Date : 2015.04.15 10:20:56
Meas. Time [min:sec] : 00:44
Interrogator : STA-R S/N 83
Freq. Step [MHz] : 2.0 MHz
Freq. Scan Mode : Automatic
Freq. Start [GHz] : 11.0563 GHz
Freq. Stop [GHz] : 11.1523 GHz
Averaging : 1000

Sensor Configuration

ID : 201504141402598076613
Mode : Loop
Length [m] : 37364.27
Sampling Interval [m] : 2.0
Nb of Points : 18624
Spatial Resolution [m] : 5.0
Pulse Amplitude [%] : 56

Table A. 4: Measurement specifications Test 1c.

Figure A. 8: Accuracy vs. distance for spatial resolution=5 m.

Measurement Information

Date : 2015.04.15 10:08:01
Meas. Time [min:sec] : 00:40
Interrogator : STA-R S/N 83
Freq. Step [MHz] : 2.0 MHz
Freq. Scan Mode : Automatic
Freq. Start [GHz] : 11.0563 GHz
Freq. Stop [GHz] : 11.1523 GHz
Averaging : 1000

Sensor Configuration

ID : 201504141402598076613
Mode : Loop
Length [m] : 37364.27
Sampling Interval [m] : 4.1
Nb of Points : 9461
Spatial Resolution [m] : 10.0
Pulse Amplitude [%] : 56

Table A. 5: Measurement specifications Test 1d.
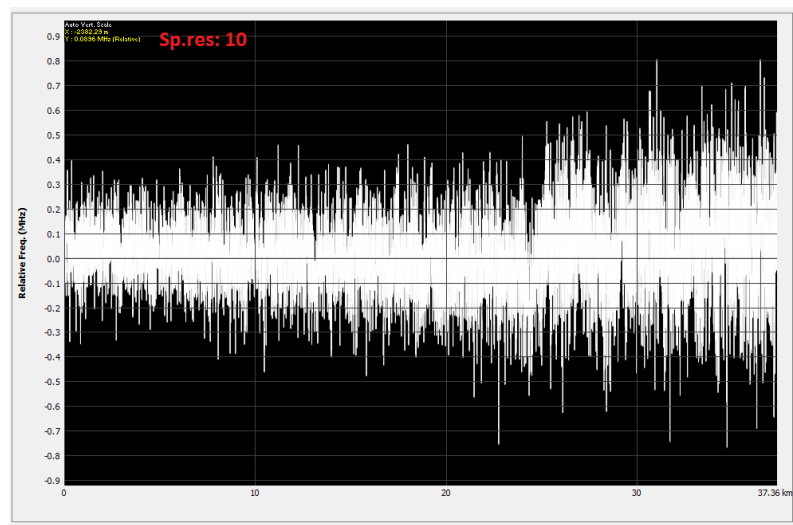
Figure A. 9: Accuracy vs. distance for spatial resolution=10 m.

TEST 2-4: Spatial resolution vs. time lag

Figure A.10 illustrates how acquisition time is varying with spatial resolution. The main measurement specifications are given in Table A.6.

Fiber length (km)	37.36
Averaging	1000
Frequency step (MHz)	2
Conditions	Ambient

Table A. 6: Measurement specifications Test 2-4.
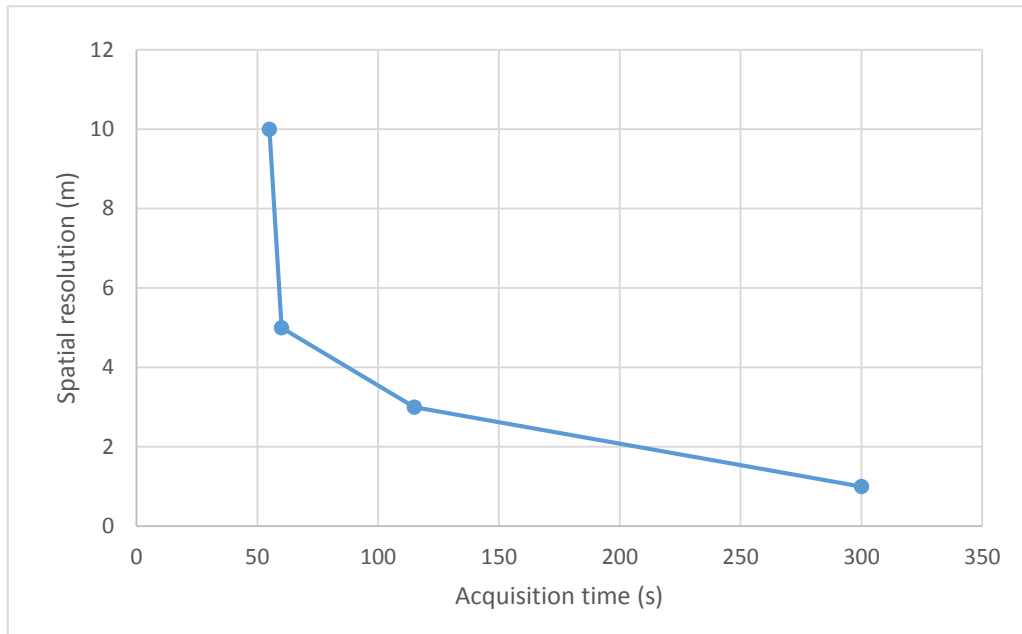
Figure A. 10: Time lag vs. spatial resolution.

TEST 5-8: Distance vs. time lag

Figure A.11 shows how acquisition time depends on fiber length. The main measurement specifications are given in Table A.7.

Spatial resolution (m)	1
Averaging	1000
Frequency step (MHz)	2
Conditions	Ambient

Table A. 7: Measurement specifications Test 5-8.
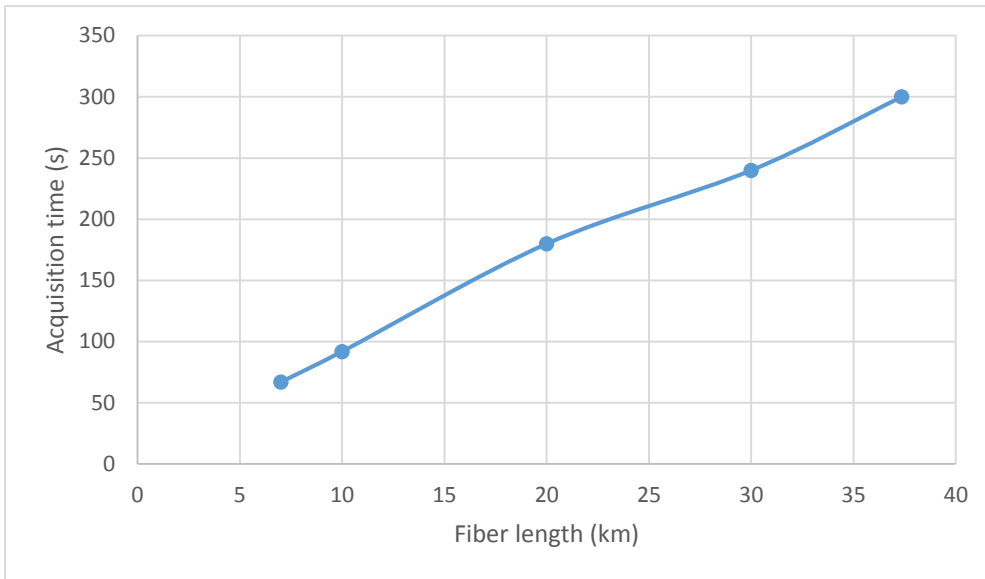
Figure A. 11: Time lag vs. distance.

TEST 9-12: Averaging vs. time lag

Figure A.12 presents the relationship between acquisition time and number of measurements being averaged. The most relevant measurement specifications are given in Table A.8.

Fiber length (km)	37.36
Spatial resolution (m)	3
Frequency step (MHz)	2
Conditions	Ambient

Table A. 8: Measurement specifications Test 9-12.
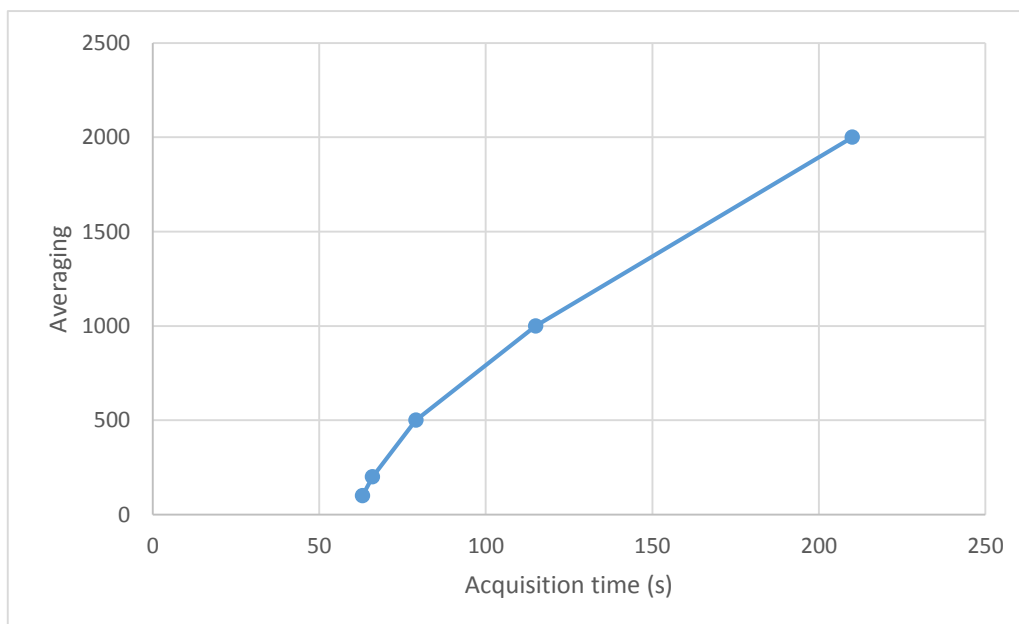
Figure A. 12: Time lag vs. averaging.

TEST 13: Cross sensitivity

The following graphs are showing the frequency response when strain is applied to the fiber, relative to a baseline measurement conducted under the same conditions with no strain. The x-axis represents the sensing fiber length (km) and the y-axis is relative frequency (MHz). The accompanying measurement specifications are given in the tables on the left hand side.

Measurement Information
Date : 2015.04.17 11:54:46
Meas. Time [min:sec] : 02:26
Interrogator : STA-R S/N 83
Freq. Step [MHz] : 2.0 MHz
Freq. Scan Mode : Automatic
Freq. Start [GHz] : 10.9783 GHz
Freq. Stop [GHz] : 11.2343 GHz
Averaging : 1000

Sensor Configuration
ID : 201504170937517894363
Mode : Loop
Length [m] : 37364.27
Sampling Interval [m] : 1.0
Nb of Points : 36947
Spatial Resolution [m] : 3.0
Pulse Amplitude [%] : 61
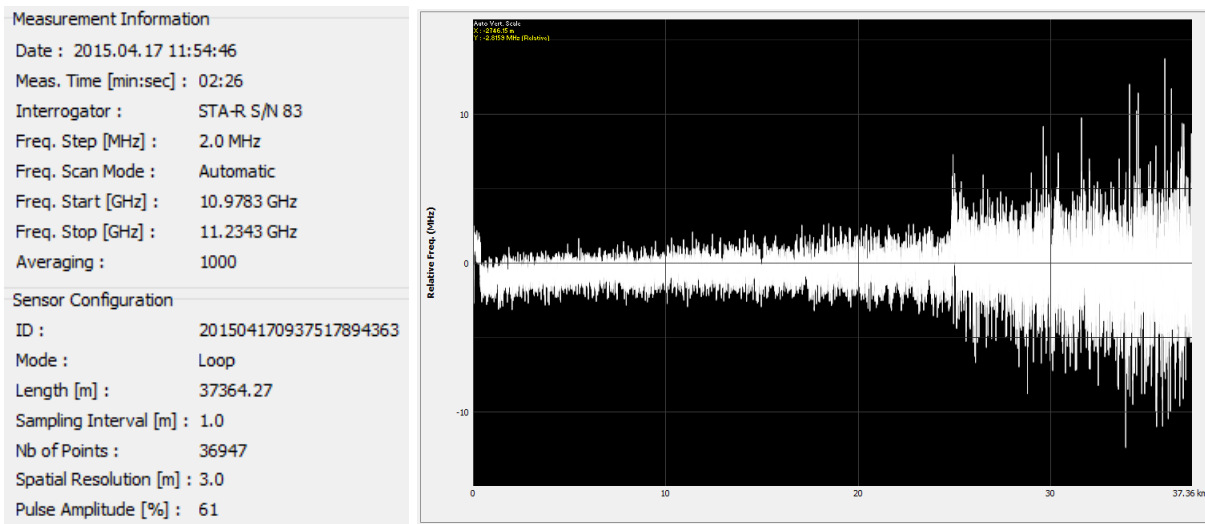
Table A. 9: Measurement specifications Test 13a.

Figure A. 13: Frequency response when strain was applied I.
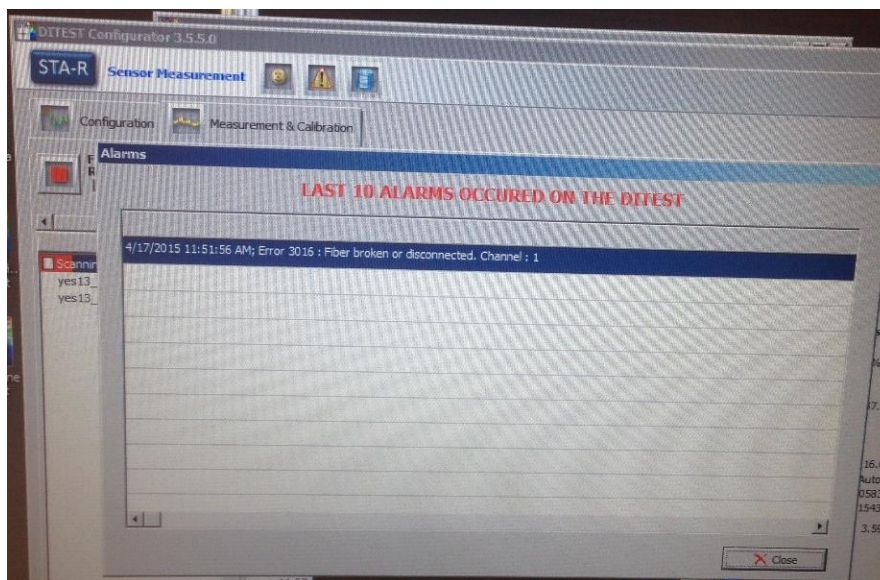
Figure A. 14: False fiber break alarm.

Measurement Information	
Date :	2015.04.17 11:58:00
Meas. Time [min:sec] :	01:38
Interrogator :	STA-R S/N 83
Freq. Step [MHz] :	2.0 MHz
Freq. Scan Mode :	Automatic
Freq. Start [GHz] :	11.0263 GHz
Freq. Stop [GHz] :	11.1543 GHz
Averaging :	1000
Sensor Configuration	
ID :	201504170937517894363
Mode :	Loop
Length [m] :	37364.27
Sampling Interval [m] :	1.0
Nb of Points :	36947
Spatial Resolution [m] :	3.0
Pulse Amplitude [%] :	61
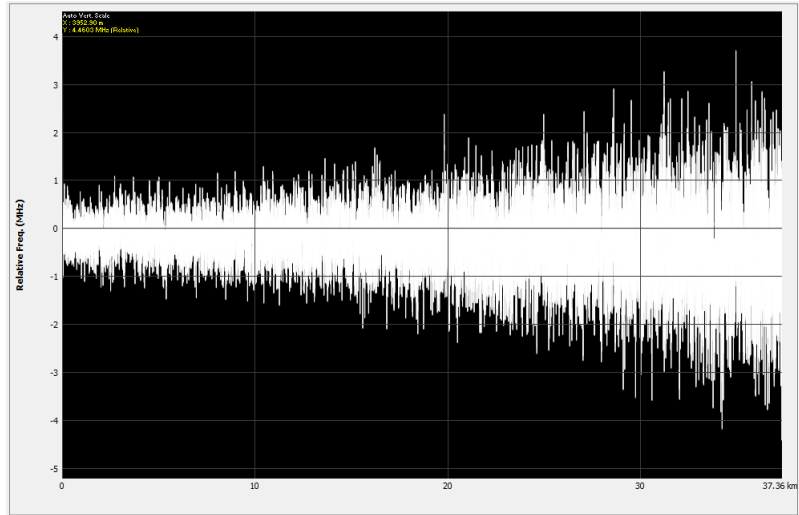
Table A. 10: Measurement specifications Test 13b.

Figure A. 15: Frequency response when strain not was applied.

Measurement Information	
Date :	2015.04.17 12:00:37
Meas. Time [min:sec] :	02:39
Interrogator :	STA-R S/N 83
Freq. Step [MHz] :	2.0 MHz
Freq. Scan Mode :	Automatic
Freq. Start [GHz] :	10.9943 GHz
Freq. Stop [GHz] :	11.1703 GHz
Averaging :	1000
Sensor Configuration	
ID :	201504170937517894363
Mode :	Loop
Length [m] :	37364.27
Sampling Interval [m] :	1.0
Nb of Points :	36947
Spatial Resolution [m] :	3.0
Pulse Amplitude [%] :	61
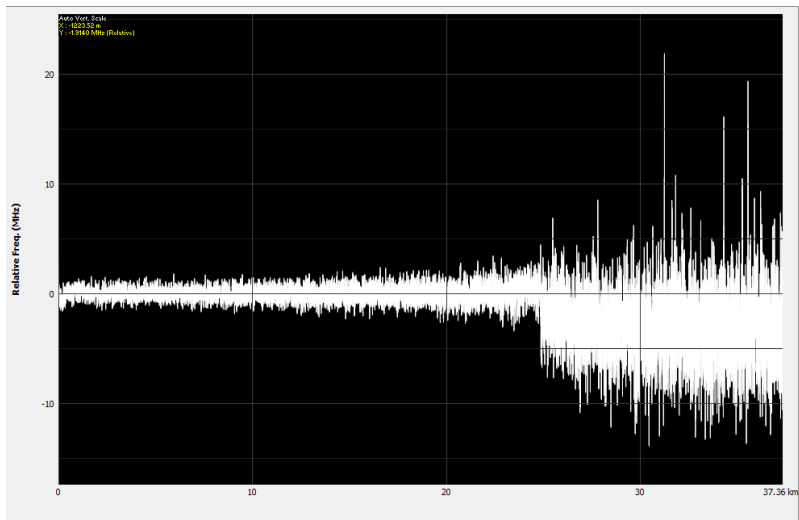
Table A. 11: Measurement specifications Test 13c.

Figure A. 16: Frequency response when strain was applied II.

TEST 14-17: Hot-spot detection

The ability to detect hot-spots for varying spatial resolutions is illustrated in the following. The graphs are showing the frequency response when heat is applied to the fiber, relative to a baseline measurement preformed with no heat. The x-axis represents the sensing fiber length (km) and the y-axis is relative frequency (MHz). The complementary measurement specifications are given in the tables on the left hand side.

Measurement Information	
Date :	2015.04.16 13:11:04
Meas. Time [min:sec] :	08:05
Interrogator :	STA-R S/N 83
Freq. Step [MHz] :	2.0 MHz
Freq. Scan Mode :	Automatic
Freq. Start [GHz] :	10.7573 GHz
Freq. Stop [GHz] :	11.4133 GHz
Averaging :	1000
Sensor Configuration	
ID :	2015041610403689000309
Mode :	Loop
Length [m] :	37364.67
Sampling Interval [m] :	0.4
Nb of Points :	91919
Spatial Resolution [m] :	1.0
Pulse Amplitude [%] :	56
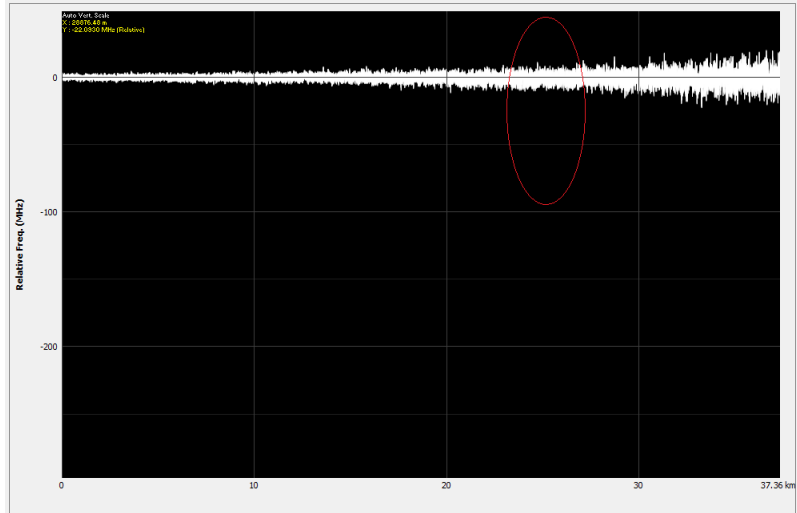
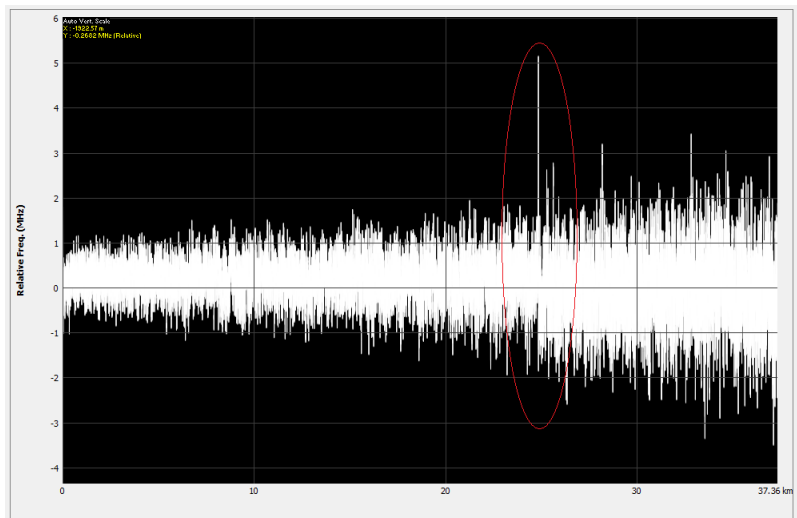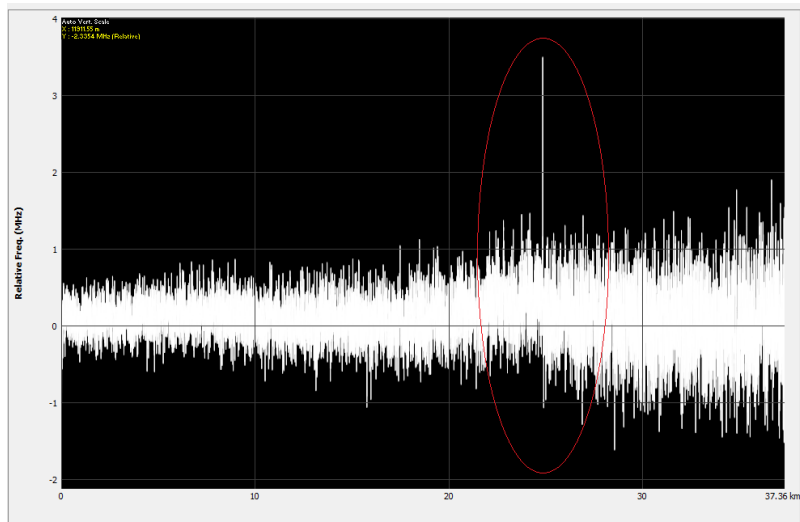*Table A. 12: Measurement specifications Test 14.*

Figure A. 17: Hot-spot detection with spatial resolution=1 m.

Measurement Information	
Date :	2015.04.16 11:25:28
Meas. Time [min:sec] :	01:42
Interrogator :	STA-R S/N 83
Freq. Step [MHz] :	2.0 MHz
Freq. Scan Mode :	Automatic
Freq. Start [GHz] :	11.0293 GHz
Freq. Stop [GHz] :	11.1573 GHz
Averaging :	1000
Sensor Configuration	
ID :	2015041610403689000309
Mode :	Loop
Length [m] :	37364.67
Sampling Interval [m] :	1.0
Nb of Points :	36948
Spatial Resolution [m] :	3.0
Pulse Amplitude [%] :	56

Table A. 13: Measurement specifications Test 15.

Figure A. 18: Hot-spot detection with spatial resolution=3 m.

64

Measurement Information	
Date : 2015.04.16 11:14:26	
Meas. Time [min:sec] :	00:48
Interrogator :	STA-R S/N 83
Freq. Step [MHz] :	2.0 MHz
Freq. Scan Mode :	Automatic
Freq. Start [GHz] :	11.0453 GHz
Freq. Stop [GHz] :	11.1573 GHz
Averaging :	1000
Sensor Configuration	
ID :	20150416 1040368900309
Mode :	Loop
Length [m] :	37364.67
Sampling Interval [m] :	2.0
Nb of Points :	18624
Spatial Resolution [m] :	5.0
Pulse Amplitude [%] :	56

Table A. 14: Measurement specifications Test 16.

Figure A. 19: Hot-spot detection with spatial resolution=5 m.

Measurement Information	
Date : 2015.04.16 11:05:26	
Meas. Time [min:sec] :	00:40
Interrogator :	STA-R S/N 83
Freq. Step [MHz] :	2.0 MHz
Freq. Scan Mode :	Automatic
Freq. Start [GHz] :	11.0613 GHz
Freq. Stop [GHz] :	11.1493 GHz
Averaging :	1000
Sensor Configuration	
ID :	20150416 1040368900309
Mode :	Loop
Length [m] :	37364.67
Sampling Interval [m] :	4.1
Nb of Points :	9461
Spatial Resolution [m] :	10.0
Pulse Amplitude [%] :	56
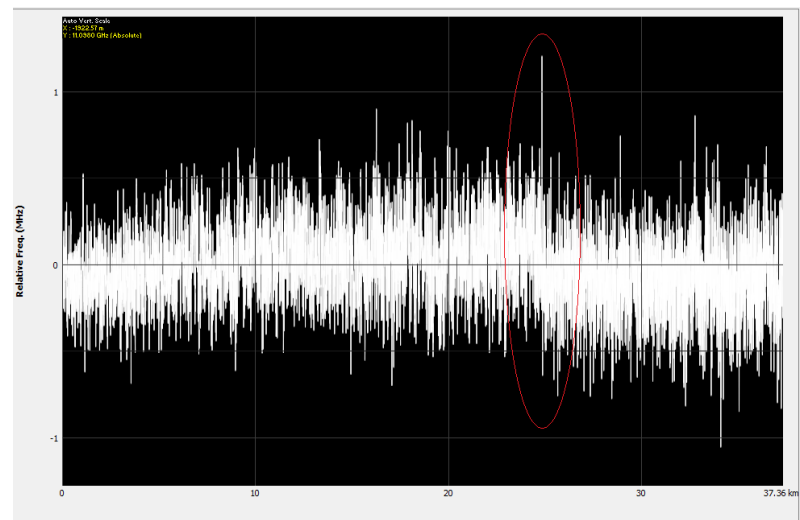
Table A. 15: Measurement specifications Test 17.

Figure A. 20: Hot-spot detection with spatial resolution=10 m.

TEST 18: Fiber break evaluation

The following meassage appeared when measurements were tried continued after a complete fiber break.
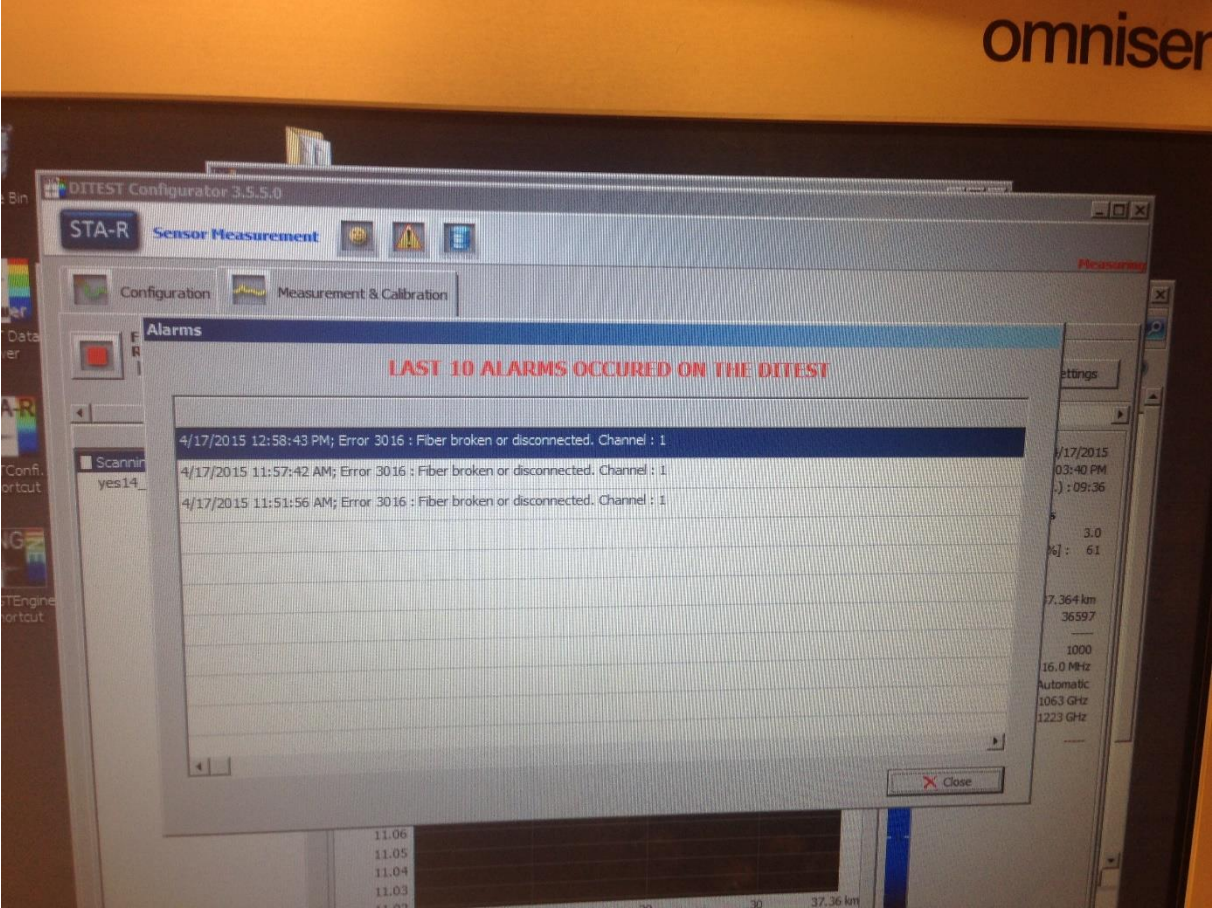
Figure A. 21: Fiber break alarm.

Appendix B: Raman experiment

B1. Technical data for the OTS40P

Sensor Specification	
Range	OTS20P: 2km OTS40P: 4km
Spatial resolution	3m; 1.5m (standard), 1m; 0.5m (option) Adjustable during commissioning.
Optical	
Fibre and electric connectors	on the rear side
Optical connector	E2000 – angle 8° High laser safety: enhanced connector with immediate laser shut-down if pigtail removed.
Laser classification	OTS evaluation unit : Class 1 product to EN60825-1:2001-11 System including sensor fibre: Class 3B product to EN60825-1:2001-11 Fibre Output $P_0 = 110$ mW, $\lambda = 976$ nm
Measurement set-up	Single end measurement / 1 channel (standard) No.of measurement channels: 2, 3, 6, 8 (option)
Fibre specification Type	GI 62.5/125 μm alternatively GI 50/125 μm (please specify at order)
Bandwidth	440 MHz km @ 850nm
Attenuation	≤ 2.7dB/km @850nm/ GI62.5/125 μm ≤ 2.4 dB/km @850nm/ GI50/125 μm
EX loop (option)	Socket E2000/duplex/compact Fibre multimode graded index
Power supply	
DC power supply	20..30 V DC, nominal 24 V DC
Power consumption	Max. 50 W @ 24V DC
Accumulator loading voltage	30 V DC
Accumulator discharge voltage	Down to 20 V DC
Socket	SUB-D 3W3, 3pin
Alternatively: AC power supply	85 – 264 V AC, 47 – 63 Hz nom. 115 VAC, resp. 230VAC
Input current	0.95 A typ. @115 V AC 0.45 A typ. @230 V AC
Socket	IEC320C13 inlet
Communication	
Data formats	Temperature profiles, zone maximum and average values, zone alarms, alarm locations, error messages and notes available by public protocols designed for transmissions to third party systems as well as to LIOS software CHARON_02. Backscattering and frequency raw data graphical displays provided by CHARON_02 only.
Interface RS232	Socket SUB-D 9 pin male
Interface Ethernet (option)	TCP/IP, Socket RJ45
Inputs	4 programmable logical inputs, Socket SUB-D 9 pin female Input trigger logic configurable.

Outputs	10 or 20 programmable outputs, event notification, direct interface with third party supervisory systems, Socket SUB-D 25 pin female resp. SUB-HD 44 Output trigger logic configurable.
Display (option)	10.6 cm x 5.6 cm size front touch screen offers several display modes in order to display status data or event lists.
Event memory	Battery backed event list includes all alarms, events, fault messages and measurement statistics, retrievable by CHARON_02 or via display.
Key switch	Reset of relay outputs, accessible from front side
Zone and event processing	
Maximum number of zones	128
Maximum number of sub zones (option)	640
Alarm actuation	Based on individual, customized alarm parameter sets per zone
Operation condition	
Temperature	0°C – 40 °C
Relative humidity	Up to 95% (non condensing)
Deployable in areas endangered by explosions	EX up to ATEX zone "zero" (option)
Fan filters	exchangeable
Compliance	
EMC	EN 61000-6-2:2001 (Immunity for industrial environments) EN 61326:1997 +A1:1998 +A2:2001 EN 61000-3-2:2000 Further observed regulations in separate certificate.
Security of laser facilities	EN 60825-1:2001-11 EN 60825-2:2000
ATEX EX	94/9/EG DMT 01 ATEX E 146 X Further observed regulations in separate certificate.

Table B. 1: Technical data for OTS40P. [23]

B2. Equipment and setup
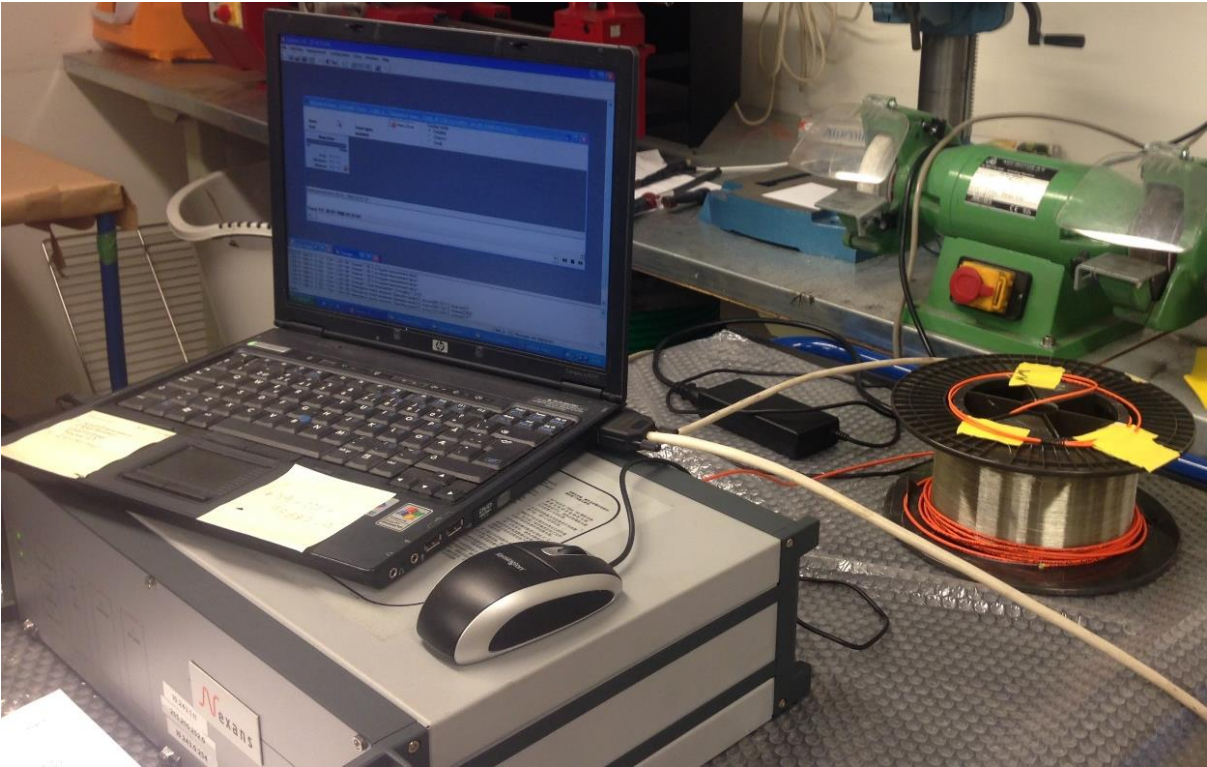
Figure B. 1: Experimental setup, including measuring unit, PC and fiber spool.

Figure B. 2: OTS40P connection terminals.

Figure B. 4: 1 m of fiber exposed to heat.

Figure B. 3: Fiber splice for multimode fiber.

B3. Experimental results

The measurement results are presented in the following section. The test number given in the headlines are related to the number specified in the test matrix. The main measurement specifications are presented in a table for each measurement.

TEST 1-4: Accuracy vs. distance and spatial resolution

The following graphs presents the temperature (°C) profile along the fiber length (m) for various spatial resolutions.

Spatial resolution (m)	0.87
Averages (time domain)	2
Conditions	Ambient

Table B. 2: Measurement specification Test 2.
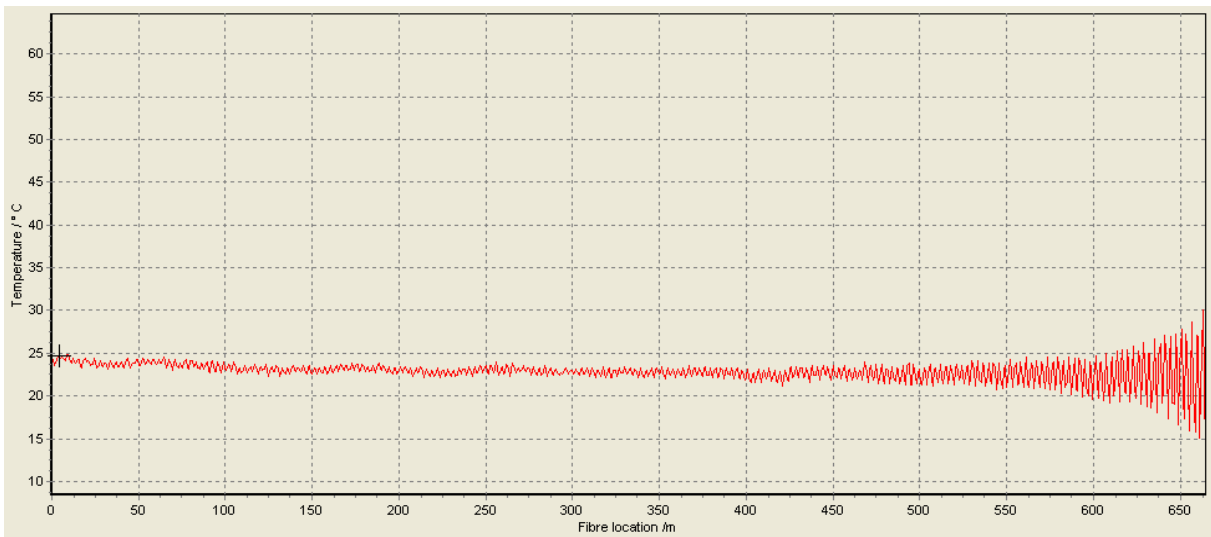
Figure B. 5: Temperature distribution along fiber for spatial resolution=0.87 m.

Spatial resolution (m)	1
Averages (time domain)	2
Conditions	Ambient

Table B. 3: Measurement specification Test 1.
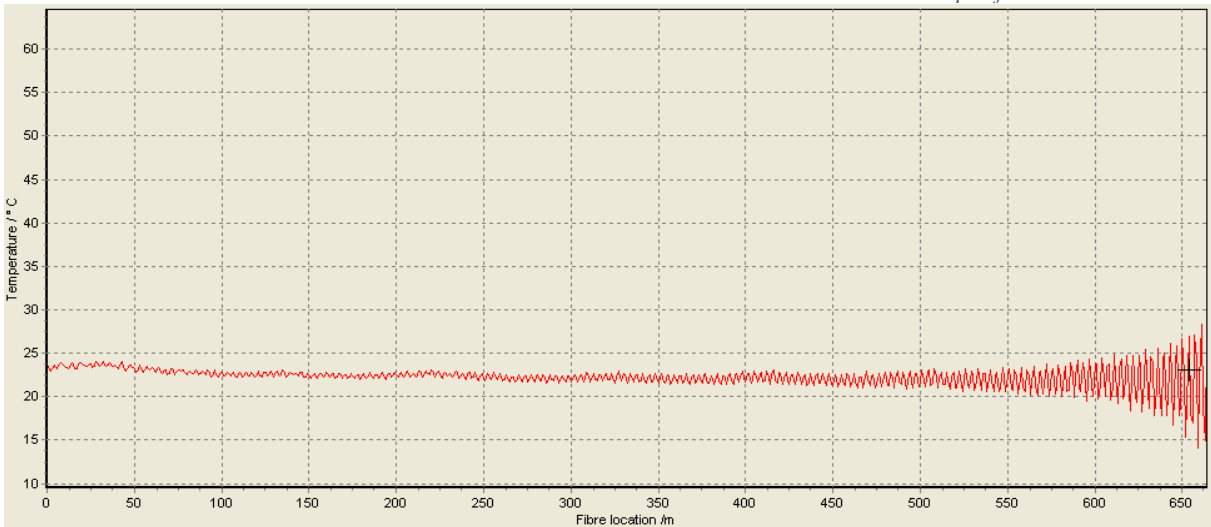
Figure B. 6: Temperature distribution along fiber for spatial resolution=1 m.

Spatial resolution (m)	2
Averages (time domain)	2
Conditions	Ambient

Table B. 4: Measurement specification Test 3.
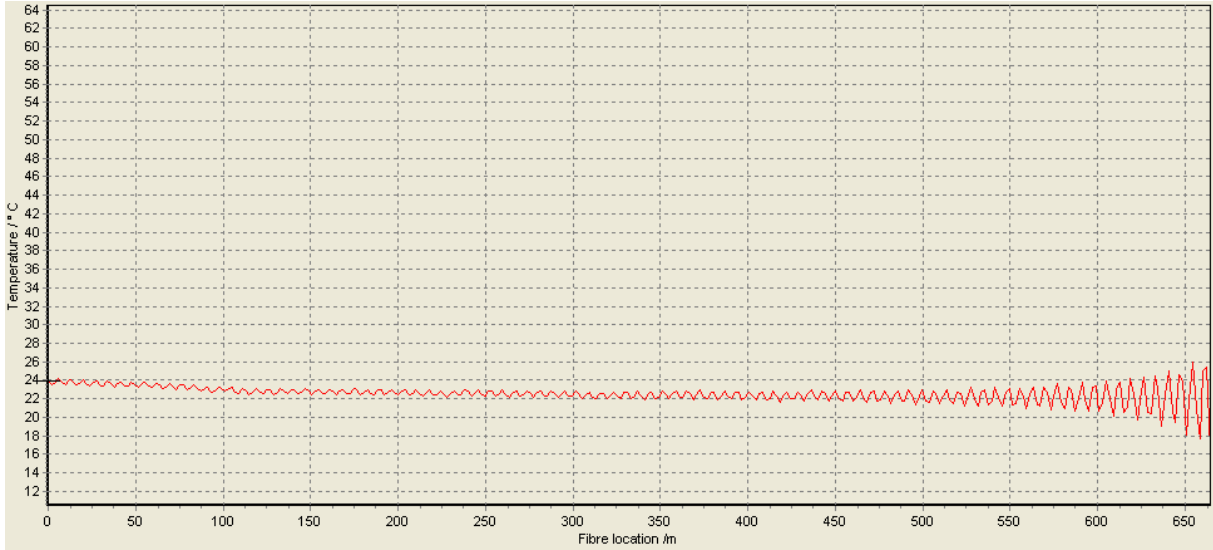
Figure B. 7: Temperature distribution along fiber for spatial resolution=2 m.

Spatial resolution (m)	3
Averages (time domain)	2
Conditions	Ambient

Table B. 5: Measurement specification Test 4.
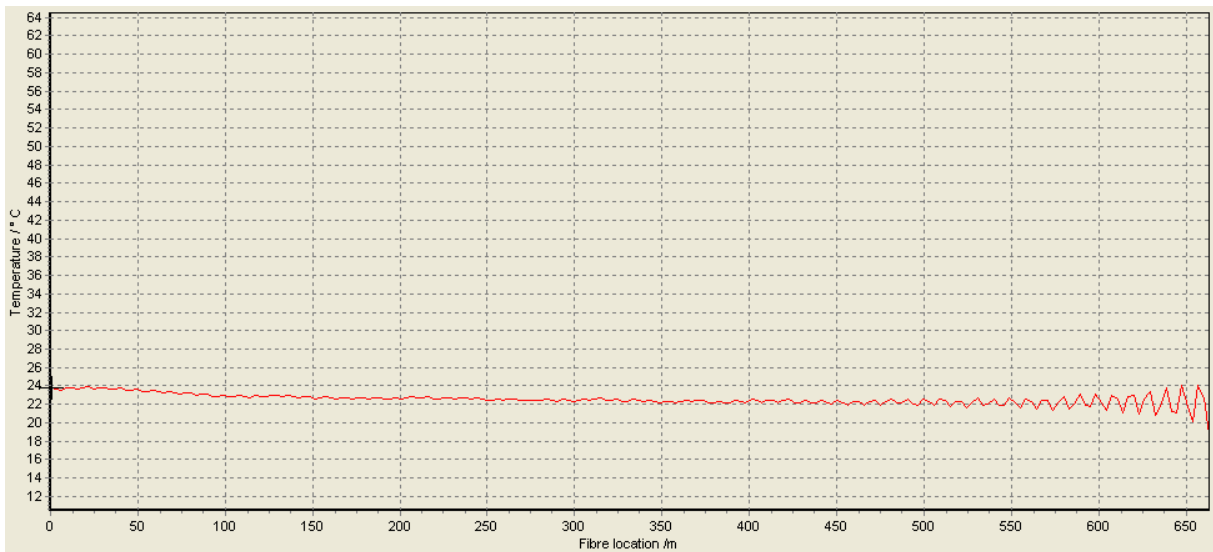
Figure B. 8: Temperature distribution along fiber for spatial resolution=3 m.

TEST 5: Accuracy for a long measurement time

Figure B.9 illustrates the temperature (°C) profile along various fiber lengths (m), for a measurement time of 50 s.

Spatial resolution (m)	1
Averages (time domain)	2
Conditions	Ambient

Table B. 6: Measurement specification Test 5.
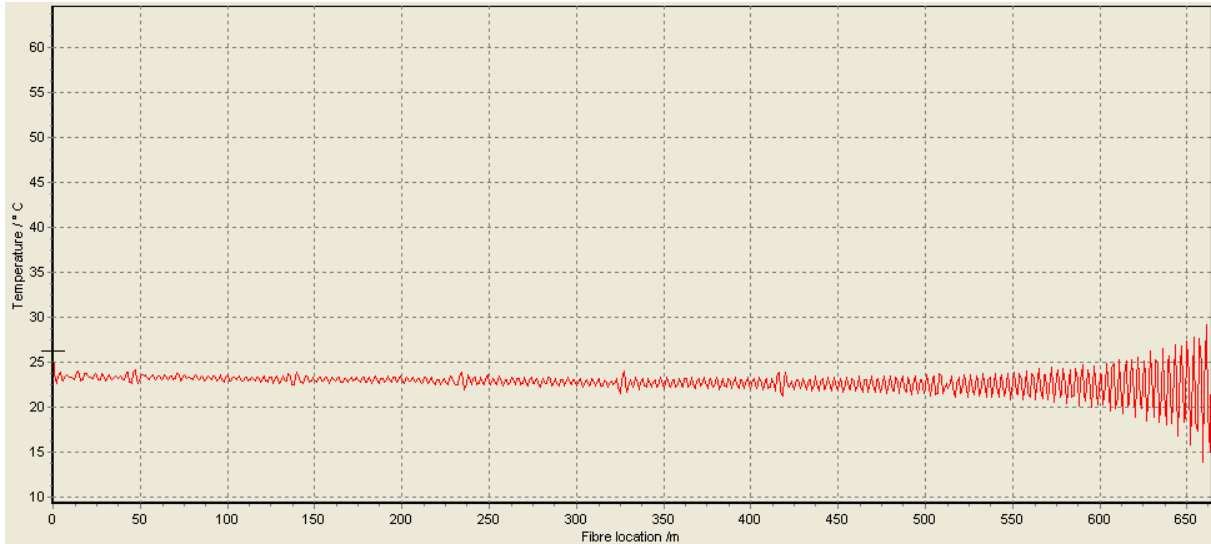
Figure B. 9: Temperature profile for measurement time=50 s.

TEST 6-8: Accuracy vs. fiber length

The following graphs show the temperature (°C) profile along various fiber lengths (m). The measurement specifications given in Table B.7 are constant for all tested fiber lengths.

Spatial resolution (m)	1
Averages (time domain)	2
Conditions	Ambient

Table B. 7: Measurement specification Test 6-8.
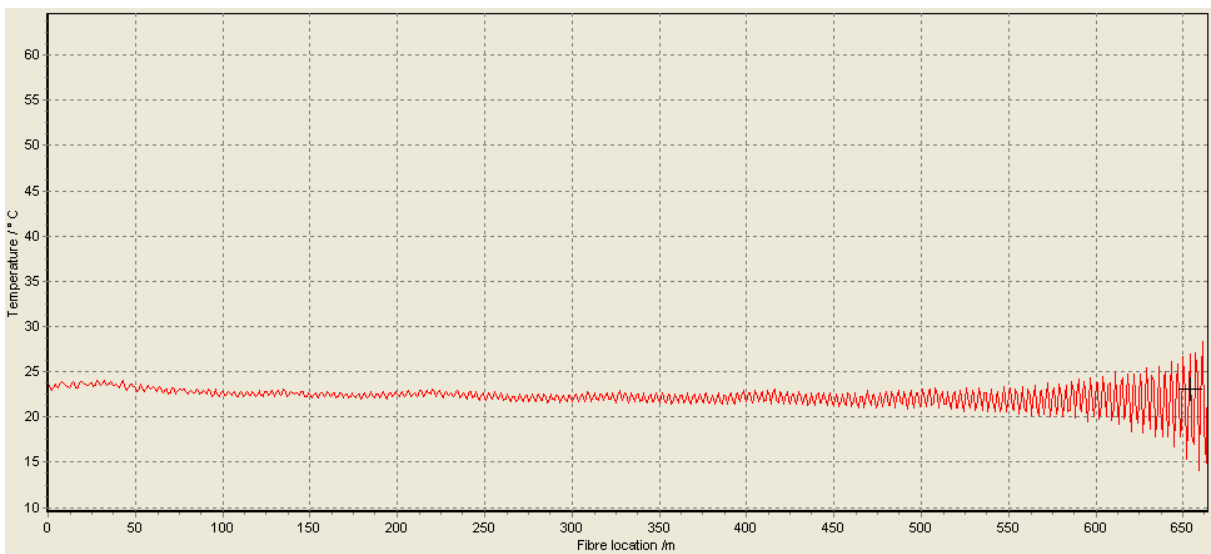
Figure B. 10: Temperature profile along a 670 m long fiber.
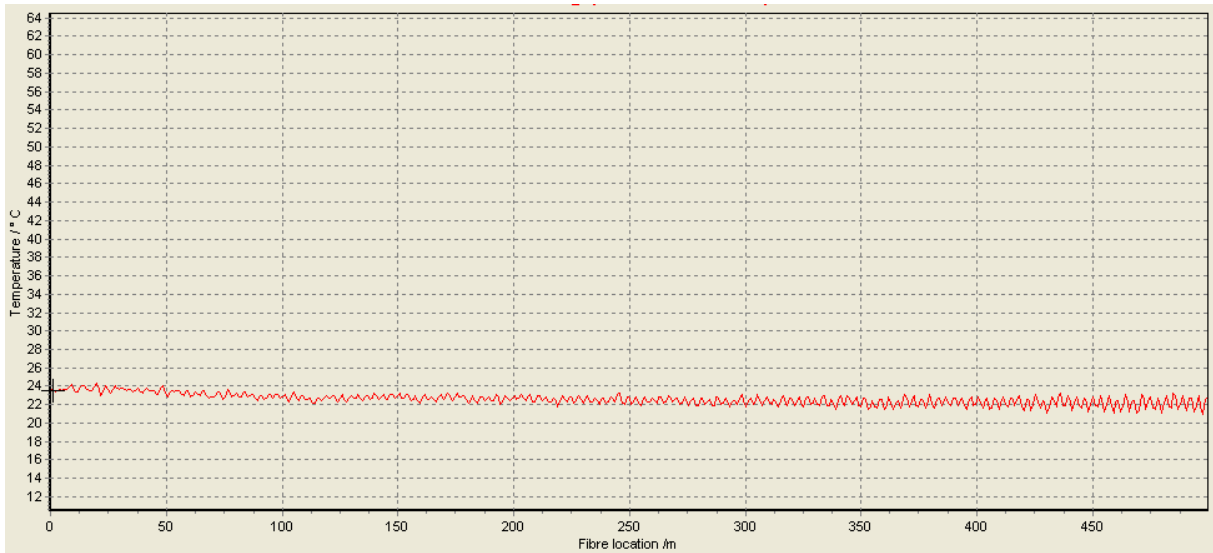
Figure B. 11: Temperature profile along a 500 m long fiber.
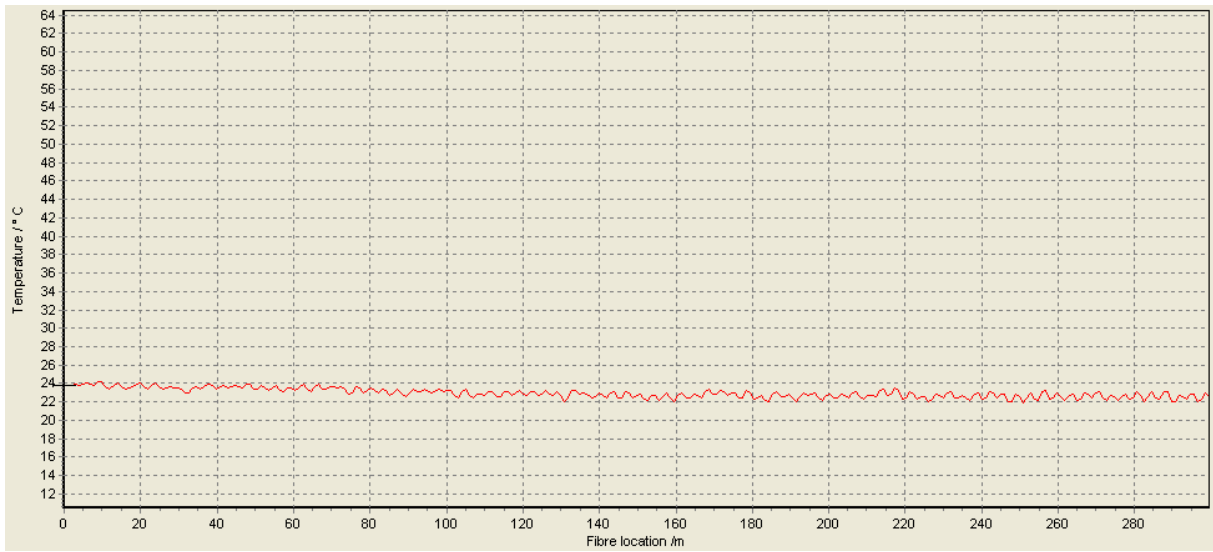
Figure B. 12: Temperature profile along a 300 m long fiber.
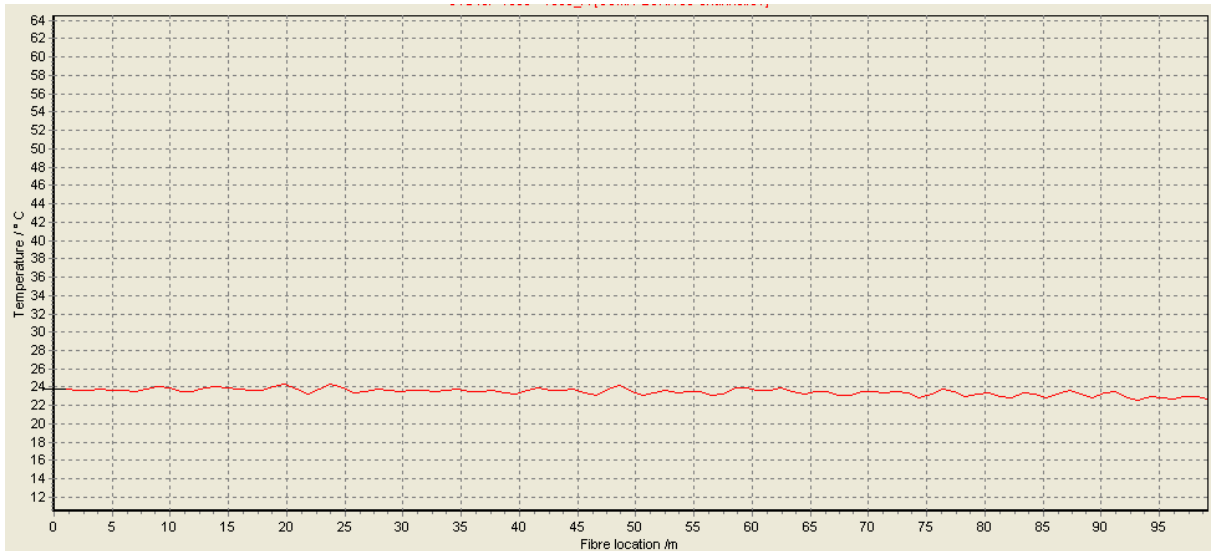
Figure B. 13: Temperature profile along a 100 m long fiber.

TEST 9-12: Accuracy vs. averages

The following graphs presents the temperature (°C) profile along the fiber length (m) for various number of averages.

Spatial resolution (m)	1
Averages (time domain)	1
Conditions	Ambient

Table B. 8: Measurement specifications Test 9.
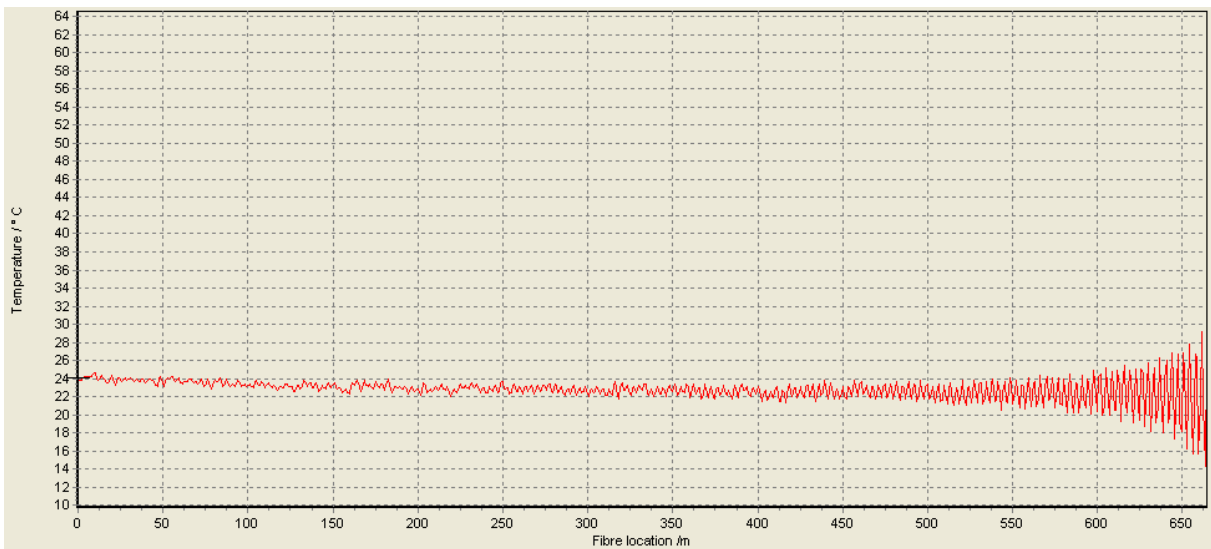
Figure B. 14: Temperature profile for averages=1.

Spatial resolution (m)	1
Averages (time domain)	3
Conditions	Ambient

Table B. 9: Measurement specifications Test 10.
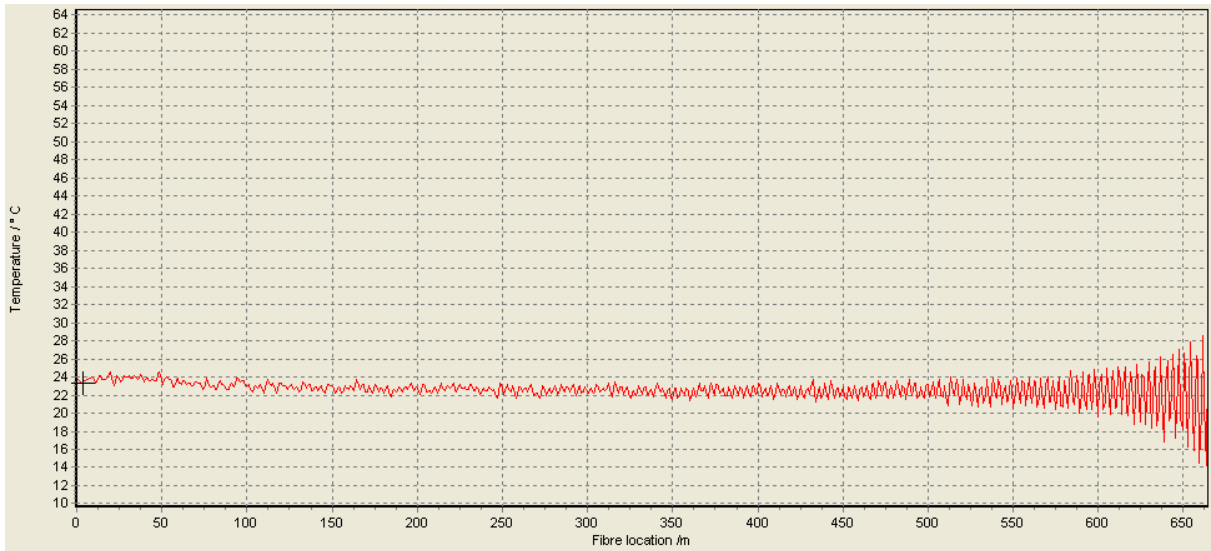
Figure B. 15: Temperature profile for averages=3.

Spatial resolution (m)	1
Averages (time domain)	5
Conditions	Ambient

Table B. 10: Measurement specifications Test 11.
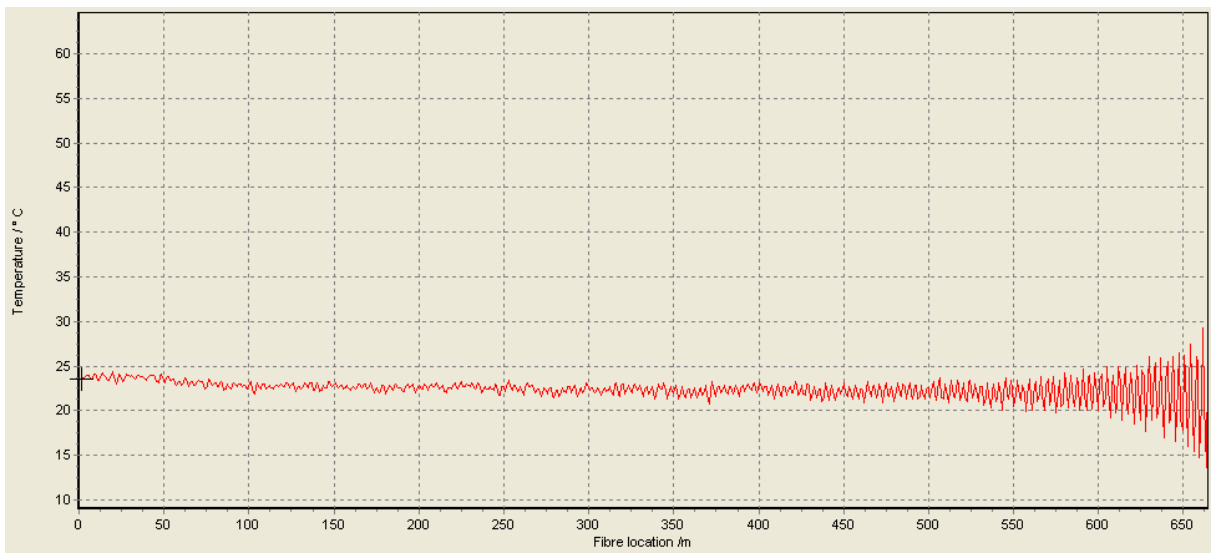
Figure B. 16: Temperature profile for averages=5.

Spatial resolution (m)	1
Averages (time domain)	10
Conditions	Ambient

Table B. 11: Measurement specifications Test 12.
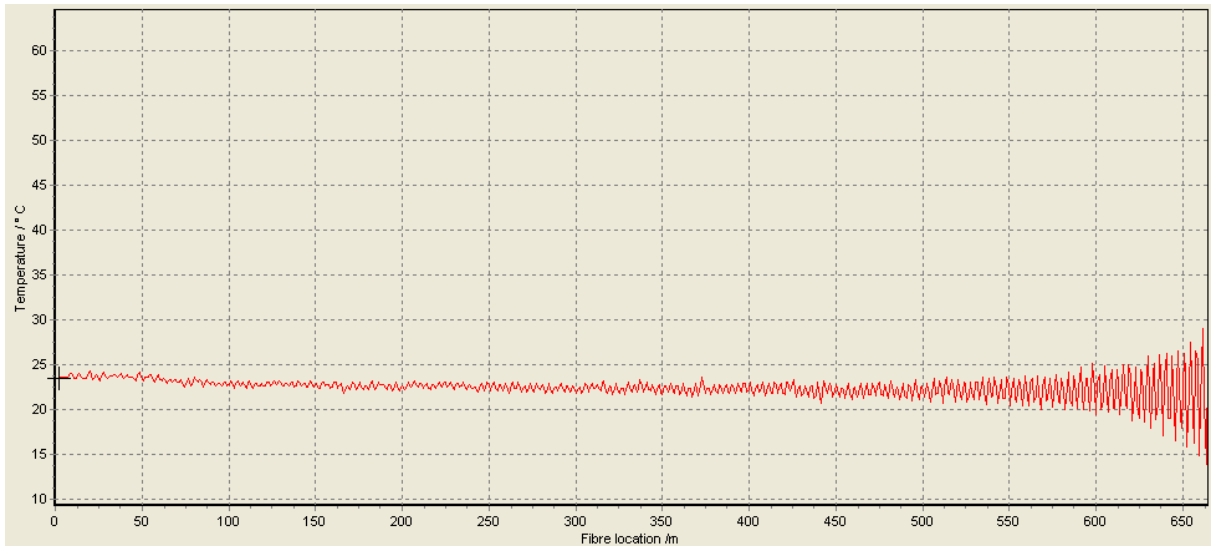
Figure B. 17: Temperature profile for averages=10.

TEST 13-16: Hot-spot detection

The graphs in this section show how spatial resolution effects the ability to detect hot-spots. The y-axis is temperature (°C) and the x-axis is fiber length (m).

Spatial resolution (m)	1
Averages (time domain)	2
Conditions	Ambient

Table B. 12: Measurement specifications Test 13a.
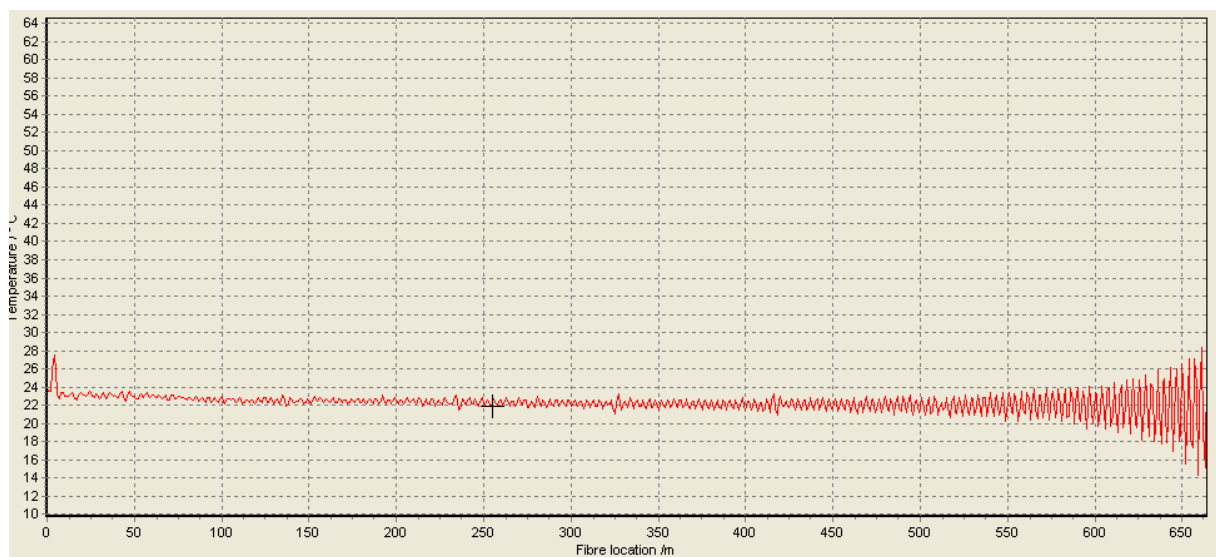
Figure B. 18: Hot-spot detection for spatial resolution=1 m.

Spatial resolution (m)	1.5
Averages (time domain)	2
Conditions	Ambient

Table B. 13: Measurement specifications Test 14.
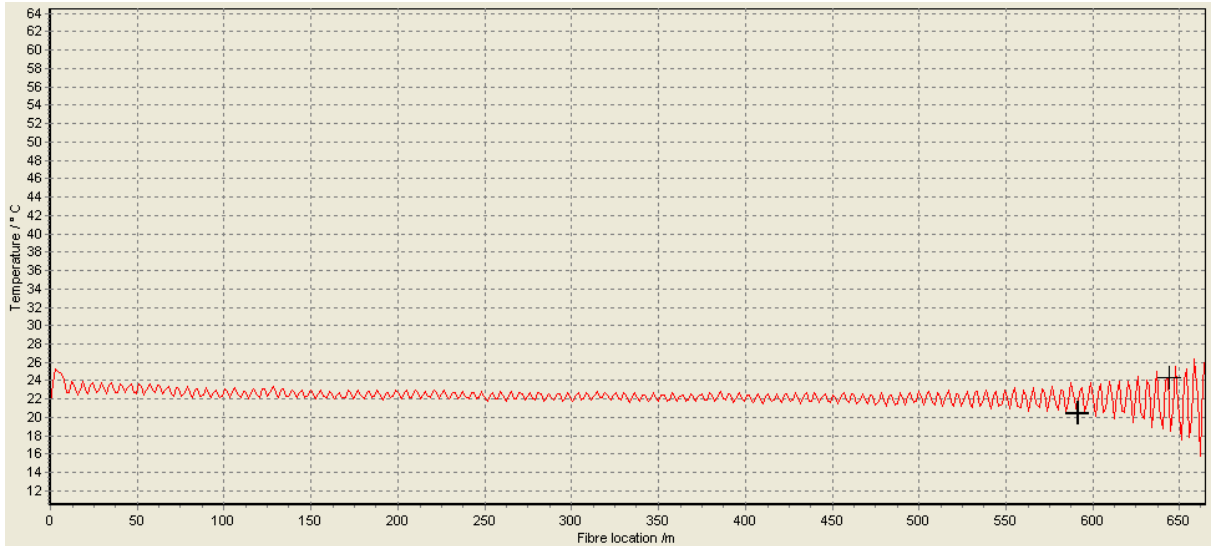
Figure B. 19: Hot-spot detection for spatial resolution=1.5 m.

Spatial resolution (m)	2
Averages (time domain)	2
Conditions	Ambient

Table B. 14: Measurement specifications Test 15a.
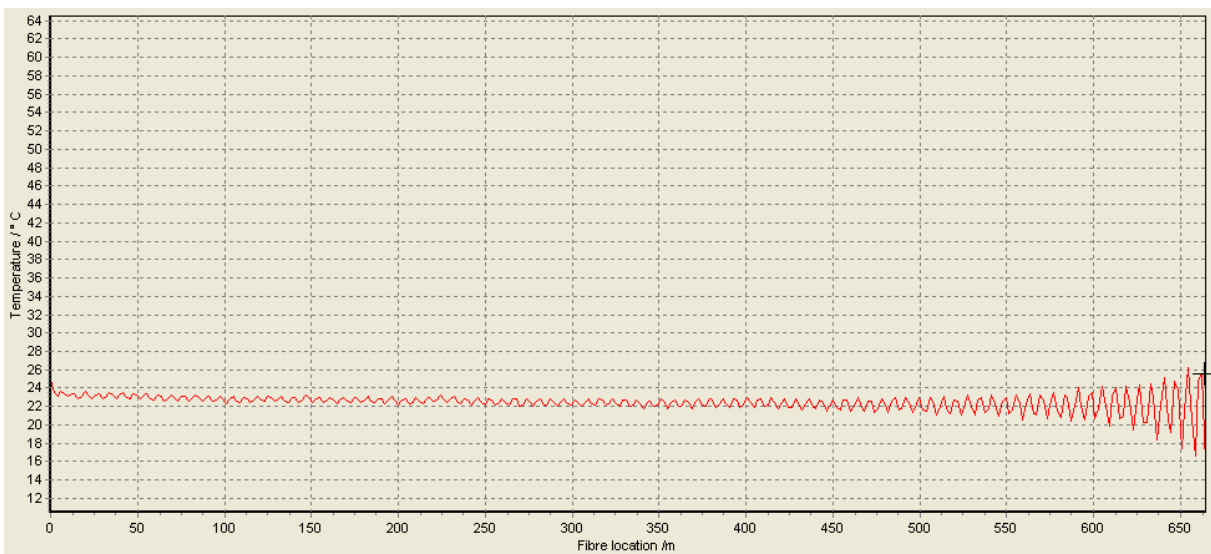
Figure B. 20: Hot-spot detection for spatial resolution=2 m.

Spatial resolution (m)	3
Averages (time domain)	2
Conditions	Ambient

Table B. 15: Measurement specifications Test 16.
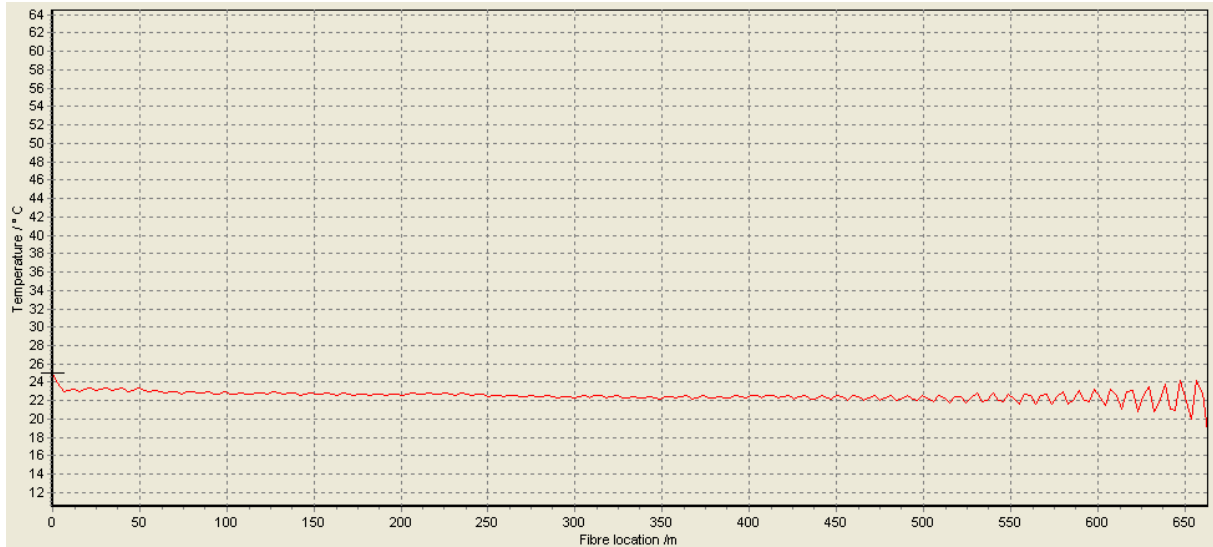
Figure B. 21: Hot-spot detection for spatial resolution=3 m.

Spatial resolution (m)	1
Averages (time domain)	2
Conditions	Ambient

Table B. 16: Measurement specifications Test 13b.
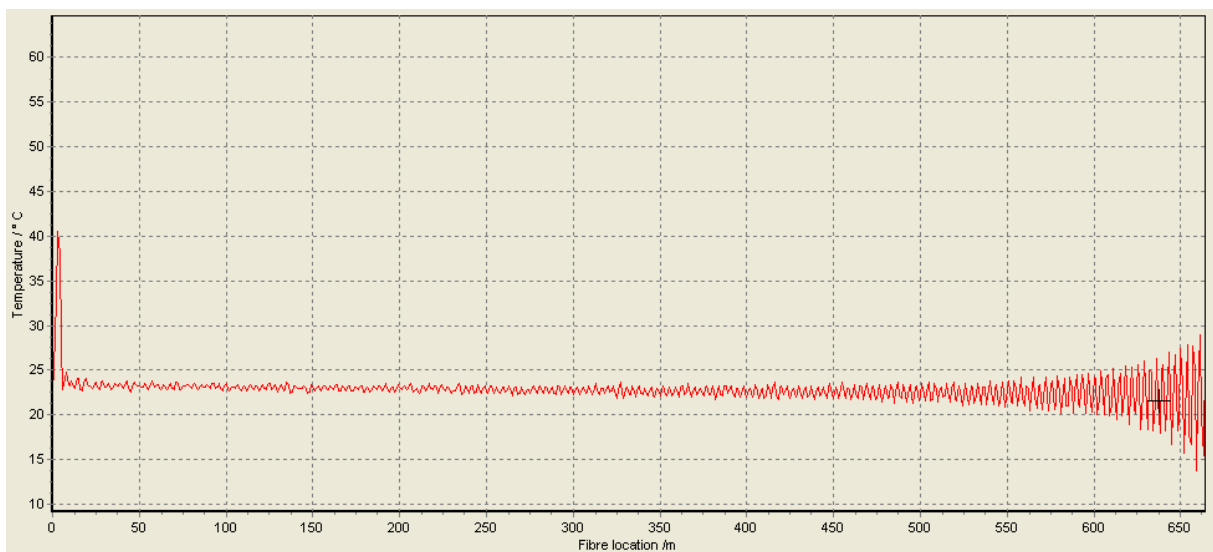
Figure B. 22: Hot-spot detection when heat was applied to a larger fiber area, sp.res=1 m.

78

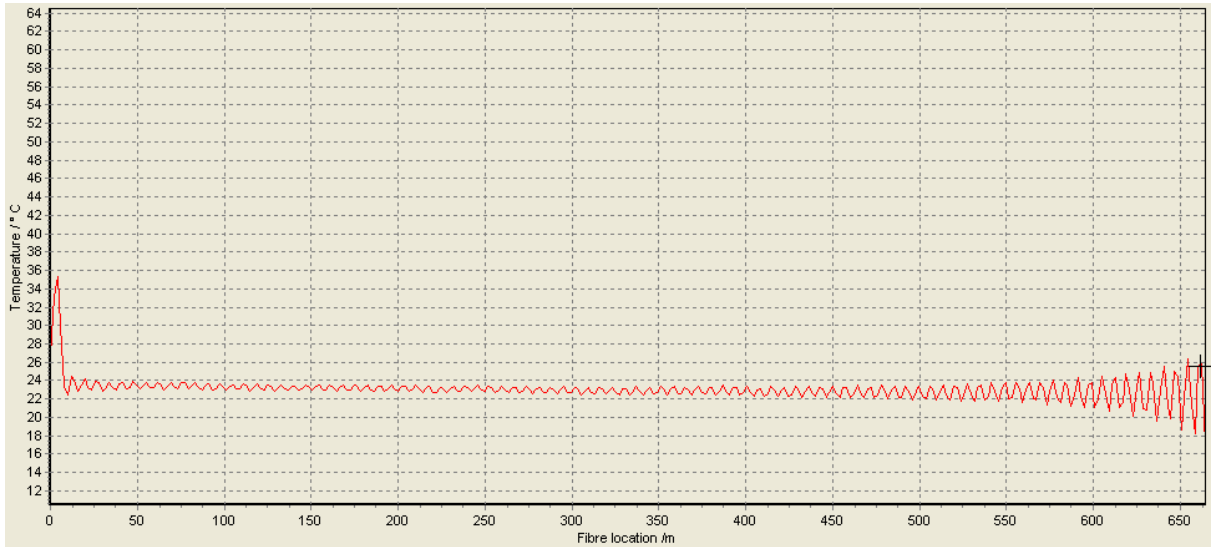| Spatial resolution (m)	2
Averages (time domain)	2
Conditions	Ambient

Figure B. 23: Hot-spot detection when heat was applied to a larger fiber area, sp.res=2 m.

TEST 17: Fiber break evaluation

The following information was provided when measurements were tried continued after a complete fiber break.
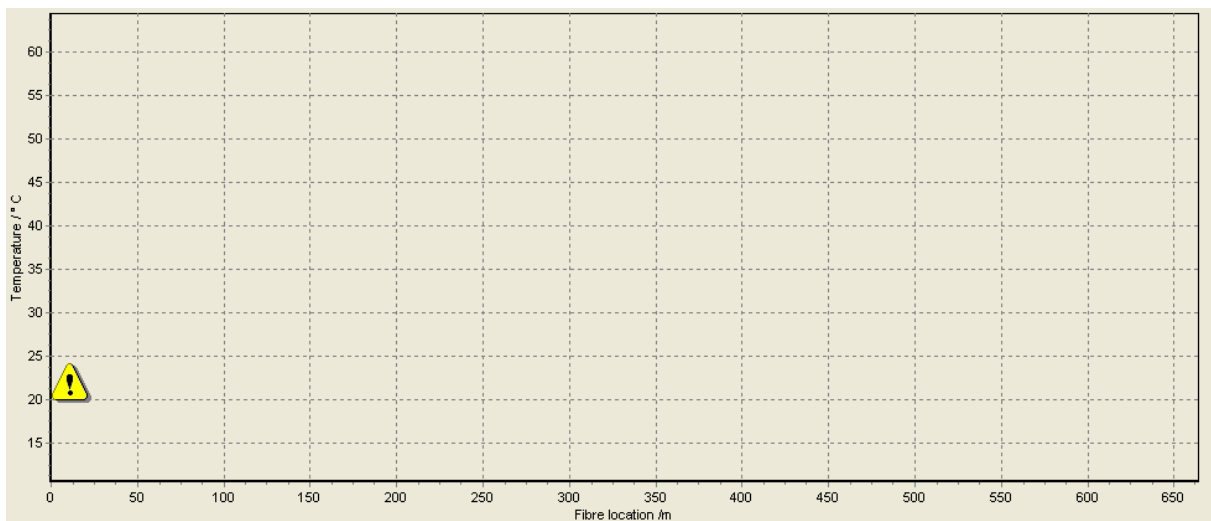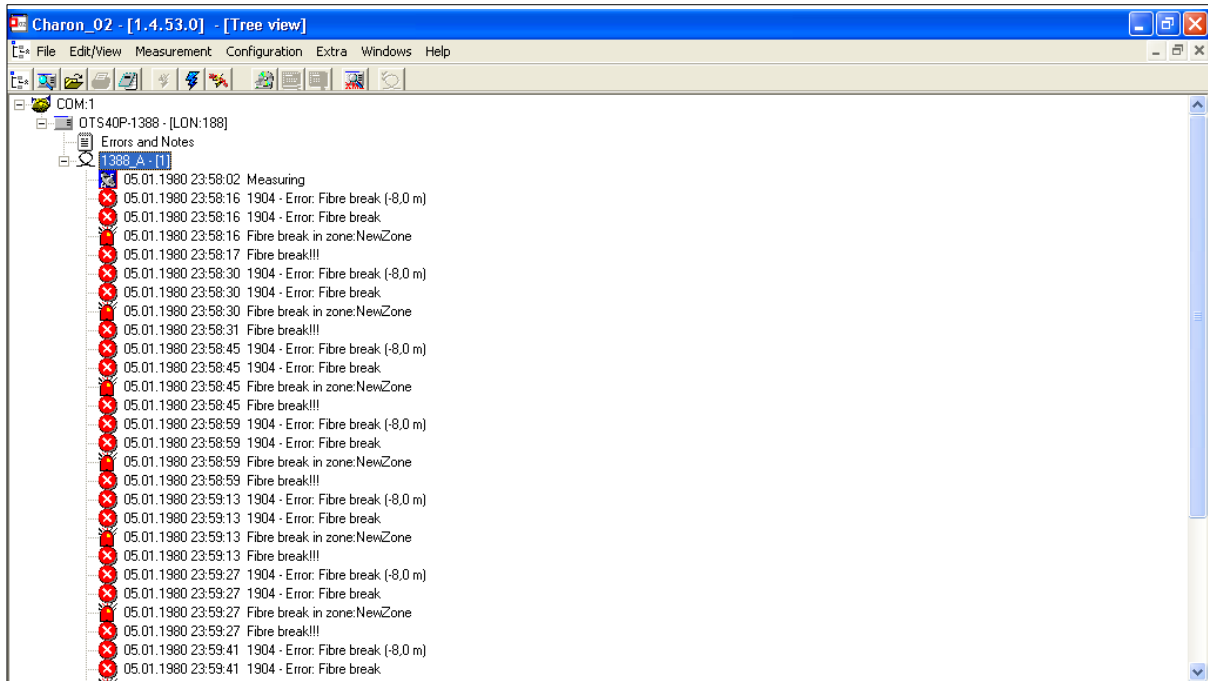

Figure B. 24: Fiber break.

Figure B. 25: Fiber break error messages